ISTANBUL TECHNICAL UNIVERSITY ★ GRADUATE SCHOOL

SYNTHESIS, CHARACTERIZATION, AND APPLICATIONS OF DYES EMITTING IN THE UV-VIS AND NEAR INFRARED REGIONS

M.Sc. THESIS

Emre Can UYSAL

Department of Chemistry

Chemistry Programme

MAY 2025

ISTANBUL TECHNICAL UNIVERSITY ★ GRADUATE SCHOOL

SYNTHESIS, CHARACTERIZATION, AND APPLICATIONS OF DYES EMITTING IN THE UV-VIS AND NEAR INFRARED REGIONS

M.Sc. THESIS

Emre Can UYSAL
(509221255)

Department of Chemistry

Chemistry Programme

Thesis Advisor: Assoc. Prof. Dr. Ayşe DAUT ÖZDEMİR

MAY 2025

ISTANBUL TEKNİK ÜNİVERSİTESİ ★ LİSANSÜSTÜ EĞİTİM ENSTİTÜSÜ

UV-GÖRÜNÜR VE YAKIN KIZILÖTESİ BÖLGELERDE IŞIMA YAPAN BOYALARIN SENTEZİ, KARAKTERİZASYONU VE UYGULAMALARI

YÜKSEK LİSANS TEZİ

Emre Can UYSAL
(509221255)

Kimya Anabilim Dalı

Kimya Programı

Tez Danışmanı: Doç. Dr. Ayşe DAUT ÖZDEMİR

MAYIS 2025

Emre Can UYSAL, a M.Sc. student of İTU Graduate School student ID 509221255 successfully defended the thesis/dissertation entitled "SYNTHESIS, CHARACTERIZATION, AND APPLICATIONS OF DYES EMITTING IN THE UV-VIS AND NEAR INFRARED REGIONS", which he prepared after fulfilling the requirements specified in the associated legislations, before the jury whose signatures are below.

Thesis Advisor :	**Assoc. Prof. Dr. Ayşe DAUT ÖZDEMİR** İstanbul Technical University	.....
Jury Members :	**Prof. Dr. Bünyamin KARAGÖZ** Istanbul Technical University	.....
	Prof. Dr. Aydan DAĞ Bezmialem Vakıf University	.....

Date of Submission : 13 May 2025
Date of Defense : 23 May 2025

To my beloved family and friends,

FOREWORD

I would like to thank many of my friends and family throughout this challenging master's degree. Their support and assistance throughout this journey have played a significant role in shaping my future personality.

First of all, I would like to express my deep gratitude to Assoc. Prof. Dr. Ayşe DAUT ÖZDEMİR, who has undertaken my advisorship in this journey. Her understanding attitude, academic consultancy and guidance on my academic career are very important to me. I also would like to thank Bleda Can SADIKOĞULLARI for his helpful support, thorough guidance, great friendship, and committedness during the experiments along with his valuable and optimistic comments.

I would also like to thank the valuable members of the L-305 laboratory, Assoc. Prof. Dr. Demet GÖEN ÇOLAK, Sibel KAYA and Zehra Gül ÇOBAN AYAZTEKİN, for their valuable support.

I would like to express my endless gratitude to Oğuzhan ASLANTÜRK, Gürkan BOZKURT and Gülşah İlayda TEZCAN for their constant support at every moment and I would also like to thank them for turning their friendship into memories that will be engraved in our memories for a lifetime.

I would like to express my gratitude to my family, who supported me with the hardships and goodness of these four years I spent to graduate from university. I would not have been able to complete this journey without my family, who see their happiness as their own and rejoice with me and support me in my hard times. First of all, I would like to thank my parents Ayşe UYSAL and Abdullah UYSAL for their endless support and helping me find my way in this world. I wouldn't be able to see this day without their endless sacrifices. Later, I would like to express my endless thanks to Emircan UYSAL, my brother, friend and mentor, and I wish him to achieve great success in his academic life. Additionally, I would like to thank Research Assistant Halide Nur DURSUN for her support and remind her how important her constructive comments are to me.

I would also like to thank my colleagues, Research Assistant Dr. Ceyda ŞİMŞEK İNCE and Research Assistant Alican TOPALOĞLU, who guided me in academic life.

I would like to take this opportunity to thank the individuals who have made significant contributions to the process of this study.

May 2025

Emre Can UYSAL
(Chemist)

TABLE OF CONTENTS

Page

ABBREVIATIONS

ACN : Acetonitrile
AIBN : Azobis(isobutyronitrile)
BODIPY : Boron – dipyrromethene
C4P : Calix[4]pyrrole
CPADB : 4-Cyanopentanoic Acid Dithiobenzoate
DCE : Dichloroethane
DCM : Dichloromethane
DMSO : Dimethyl sulfoxide
EDG : Electron Donor Group
EWG : Electron Withdrawing Group
EtOAc : Ethyl Acetate
EtOH : Ethanol
FT-IR : Fourier Transform Infrared Spectroscopy
GMA : Glycidyl Methacrylate
GPC : Gel Permeation Chromatography
IDA : Indicator Displacement Assay
LOD : Limit of Detection
Macro-CTA : Macro Chain Transfer Agent
MeOH : Methanol
NIR : Near – Infrared (region)
NMR : Nuclear Magnetic Resonance Spectroscopy
OEGMA : Oligo (ethyleneglycol) methacrylate
PET : Photoinduced Electron Transfer
PGMA : Poly(glycidyl methacrylate)
POEGMA : Poly(oligo (ethyleneglycol) methacrylate)
RAFT : Reversible Addition Chain Fragmentation Transfer Polymerization
TLC : Thin Layer Chromatography
RT : Room temperature
UV-Vis : Ultraviolet – Visible Spectroscopy
QE : Quenching Efficiency

SYMBOLS

%	**:** Percentage
λ	**:** Wavelength
λabs	**:** Absorption wavelength
λems	**:** Emission wavelength
°C	**:** Degree Celcius
δ	**:** Chemical shift
ϕ	**:** Quantum Yield
g	**:** Gram
h	**:** Hour
L	**:** Liter
M	**:** Molarity
mg	**:** Miligram
ml	**:** Mililiter
MHz	**:** Megahertz
nm	**:** Nanometer
K_{sv}	**:** Stern-Volmer Constant

LIST OF TABLES

Page

LIST OF FIGURES

Page

SYNTHESIS, CHARACTERIZATION, AND APPLICATIONS OF DYES EMITTING IN THE UV-VIS AND NEAR INFRARED REGIONS

SUMMARY

In this thesis, synthesis, characterization and applications of synthetic organic dyes, especially Aza-BODIPY derivatives, which can absorb and emit light in a wide wavelength range are discussed. Aza-BODIPY dyes have remarkable applications in various fields such as biological imaging, photodynamic therapy and sensor technologies due to their light emitting properties in the near infrared (NIR) region (700–1700 nm). In this study, two different Aza-BODIPY derivatives were synthesized using the O'Shea method: one was unsubstituted and the other had a structure containing para-hydroxyl (*p*-OH) group. Then, the unsubstituted Aza-BODIPY compound was converted to new derivatives containing bromine and formyl groups by bromination and formylation processes. These three different dye molecules were used in the detection of nitroaromatic compounds and the effects of different electron donating (EDG) and electron withdrawing (EWG) groups on the sensor performance were investigated.

In the second application, a selective IDA (Indicator Displacement Assay) sensor system against halogen ions (especially fluoride ion) was designed by combining Aza-BODIPY and calix[4]pyrrole molecules. There is no study in the literature where these two molecules are used together as sensors. In the third and last application, the Aza-BODIPY derivative was integrated into the PGMA-*b*-OEGMA polymeric system synthesized by RAFT polymerization. This system was made compatible with biological environments and a potential structure was created for intracellular imaging applications.

The results obtained revealed that different functional groups attached to the Aza-BODIPY center directly affect the electronic structure of the system and determine the sensor performance. EDG groups increased the electron density of Aza-BODIPY and provided stronger interaction with nitro compounds, while EWG groups weakened the PET mechanism and decreased the sensitivity. However, exceptional cases such as the resonance effect of the formyl group showed that this limitation can be overcome.

The Aza-BODIPY dye was incorporated into a polymeric framework and rendered suitable for biological environments in the second use. Studies using intracellular imaging may be possible with this structure. The third use was the creation of an IDA sensor system that was selective for halogen ions, particularly fluoride ions, by conjugating the Aza-BODIPY molecule with the calix[4]pyrrole structure.

The study generally emphasized the advantages of Aza-BODIPY dyes such as high photostability, wide wavelength tunability and structural flexibility, while also evaluating some limitations such as selectivity and solubility. This thesis sheds light on the future applications by revealing the versatile usage potential of Aza-BODIPY based systems.

UV-GÖRÜNÜR VE YAKIN KIZILÖTESİ BÖLGELERDE IŞIMA YAPAN BOYALARIN SENTEZİ, KARAKTERİZASYONU VE UYGULAMALARI

ÖZET

Rodamin, siyanin, ftalosiyanin, BODIPY ve Aza-BODIPY gibi çeşitli sentetik organik boyalar, benzersiz fotofiziksel özellikleri nedeniyle son yıllarda önemli ilgi görmüştür. Bu özellikler, çok çeşitli dalga boylarında ışık emisyonlarına ve yaymalarına olanak tanır ve bu da çok çeşitli uygulamalarda kullanılmalarını sağlar. Örneğin, geniş spektrumlu fotofiziksel özellikleri nedeniyle, fotodinamik terapi ve fototermal terapi gibi çeşitli hastalık tedavilerinde ve hücre içi görüntüleme ve biyolojik görüntüleme gibi sağlık teşhisi için kritik öneme sahip teknolojilerde yaygın olarak kullanılmaktadırlar. Bu tür moleküller, tıbbi uygulamalardaki kullanımlarına ek olarak, uygun fotofiziksel özellikleri ve enerji transferine izin veren moleküler yapıları sayesinde güneş hücreleri, kemosensörler gibi enerji malzemeleri olarak da literatürde yer bulmuştur.

Aza-BODIPY molekülleri, Rogers tarafından 1943'te keşfedildiklerinden beri biyoloji, malzeme bilimi ve sensörler gibi alanlarda geniş bir uygulama yelpazesi bulmuştur. Bu kadar çeşitli uygulama yelpazesinin nedeni, 700-1700 nm aralığında NIR emisyonuna sahip olmaları, BODIPY moleküllerinin ise sadece 520-600 nm aralığında olması ve bu nedenle BODPIY'nin Stokes kaymalarının 10-25 nm arasında kalmasına ve zayıf penetrasyon derinliğine yol açmasıdır. Aza-BODIPY'ler, mezo pozisyona bir azot molekülünün eklenmesiyle aromatik konjugasyonu artırdıkça batokromatik bir kayma sergiler. BODIPY moleküllerinin analogları olmalarının yanı sıra, artan aromatik konjugasyon genellikle 90-100 nm arasında λ_{max} değerine sahip Aza-BODIPY molekülleri ile sonuçlanır ve kullanım alanına bağlı olarak üstün özellikler sağlar. Aza-BODIPY sentezi için literatürde O'shea yöntemi, Carreria yöntemi ve Lukyantes yöntemi olmak üzere üç farklı yöntem önerilmektedir.

Bu çalışma kapsamında iki ana Aza-BODIPY molekülü sentezlendi. Bu sentezler, *E*-kalkon bileşiğinden başlanarak O'shea yöntemi ile sentezlendi. Sentezlenen boyalar, sübstitüye bir grup içermeyen bir Aza-BODIPY molekülü ve *p*-OH grubu içeren bir Aza-BODIPY molekülüdür. Daha sonra, sübstitüye bir grup içermeyen bir Aza-BODIPY molekülü, brominasyon ve formilleme işlemi ile brom ve formil grubu içeren moleküllere dönüştürüldü. Burada elde edilen üç farklı boya, bu farklı EDG (Elektron Veren Grup) ve EWG (Elektron Çeken Grup) gruplarının halka üzerindeki etkisini incelemek için nitroaromatik sensörler olarak kullanıldı. Böylece, bu grupların etkisi literatürde yapılan çalışma ile karşılaştırıldı.

İkinci uygulama çalışmasında, kalix[4]pirol molekülünün hidrojen bağları aracılığıyla çeşitli anyonları (özellikle halojenleri) yüksek seçicilikle tanıma özelliğinden ve Aza-BODIPY'nin sunduğu floresan avantajlarından yararlanılarak bir flor sensörü sentezlenmiştir ve flor anyonlarına tepkisi incelenmiştir. Literatürde iki molekülün sensör görevi gördüğü bir çalışma bulunmamaktadır.

Son bölümde, sentezlenen Aza-BODIPY türevi polimerik sistemlere entegre edildi. RAFT polimerizasyonu ile sentezlenen polimerik sistemler kullanıldı: PGMA-*b*-OEGMA. Bu polimerik sistemler, hücre içi görüntüleme uygulamalarında kullanılmak üzere Aza-BODIPY molekülü ile modifiye edildi. Fonksiyonelleştirilmiş Aza-BODIPY türevi, floresan özellikleri sayesinde polimerlerin hücre içi etkileşimlerinin görüntülenmesine olanak tanır.

Sonuç olarak, Aza-BODIPY çekirdeğine bağlı farklı elektron verici (EDG) ve elektron çeken (EWG) gruplarının sistemin genel elektronik yapısı üzerindeki etkisi araştırılmıştır. *p*-OH Aza-BODIPY, beş farklı nitroaromatik bileşiğe karşı test edildi. Sonuçlara göre, ticari olarak temin edilebilen nitroaromatik moleküller (TNT, DNT ve MNT) incelendiğinde, 1×10^5 civarında benzer K_{sv} sonuçları elde edildi. Bu benzerlik, *p*-OH Aza-BODIPY'ün hidroksil gruplarının varlığı nedeniyle oldukça elektron açısından zengin olmasına ve elektron eksikliği olan nitroaromatik bileşiklerle güçlü etkileşimlere olanak sağlamasına bağlanabilir, böylece bu nitroaromatikler arasındaki elektron eksikliği derecesi, etkileşim kuvvetini belirlemede ihmal edilebilir hale gelmiştir. İlginç bir şekilde, nitroalifatiklere yönelik bağlanma sabitinin, hidrojen bağı ile rasyonalize edilebilen herhangi bir nitroaromatik bileşikten daha yüksek olduğu gözlemlendi. *p*-OH Aza-BODIPY'teki fenolik hidroksil grupları, nitroalifatik molekülün asidik protonuyla hidrojen bağı kurulmasını sağlayarak potansiyel olarak floresan söndürmeyi kolaylaştırmıştır. Tüm sonuçlar göz önüne alındığında, hidroksi grubunun eklenmesi nitroaromatik bileşiklere olan afiniteyi artırırken, aynı zamanda nitroaromatiklere yönelik seçiciliği azaltır. Yukarıda verilen birkaç nedene atfedilebilecek şekilde, *p*-OH Aza-BODIPY'ün suda çözünmüş TNP'ye en yüksek K_{sv} değerini verdiği gözlenmiştir. TNP, fenolik hidroksil grubu nedeniyle diğer nitroaromatiklere göre daha asidik bir yapıya sahiptir. Bu durum, özellikle elektronca zengin bir yapıya sahip olan *p*-OH Aza-BODIPY 'in güçlü π–π istiflenmesi ve asit-baz etkileşimi göstermesine neden olmuştur. TNP'nin –OH grubu bir hidrojen bağı donörü olarak hareket edebilir ve *p*-OH Aza-BODIPY'in hidroksil grupları bağlanma sabitini artırmıştır. Söndürme verimleri dikkate alındığında, tüm test edilen nitro bileşiklerinde %60-80 oranında söndürme gözlenmiştir ve bu, suda hazırlandığında toplam söndürme gösteren TNP hariç, düşük seçiciliği göstermektedir. Bu durumun, Aza-BODIPY moleküllerinin düşük suda çözünürlüğünden kaynaklandığı ve bunun sulu söndürme verimini etkilemiş olabileceği düşünülmektedir; ancak bu fark önemli görülmemiştir.

Brom atomu içeren Aza-BODPIY bileşiği ilk olarak beş ayrı nitroaromatik kimyasalla karşılaştırılarak değerlendirildi. Sonuçlar, ticari olarak erişilebilen nitroaromatik bileşikler (TNP, TNT, DNT ve MNT) incelendiğinde yaklaşık 1×10^4 M^{-1}'lik özdeş K_{sv} değerlerinin elde edildiğini gösterdi. *p*-OH Aza-BODIPY"in aksine, Brom atomu içeren Aza-BODIPY de farklı nitro bileşikleri ile yapılan titrasyonların sonuçlarının benzer K_{sv} değerleri vermesinin nedenlerinden biri, bu bileşiğin hidrojen bağı yapabilen hidroksi gibi bir grup içermemesidir. Öte yandan, K_{sv} değerleri Brom atomu içeren Aza-BODIPY ile yapılan titrasyonlara kıyasla daha düşüktür. *p*-OH Aza-BODIPY 'in hidroksil grupları, halkanın elektron zenginliğini artıran ve elektron-zayıf nitro bileşikleri ile yüksek K_{sv} ile floresan söndürmeye sahip olan elektron veren gruplardır. Brom grupları elektron çeken gruplardır ve Aza-BODPIY halkasının elektron yoğunluğunu azaltarak düşük K_{sv} değerlerinin gözlenmesine neden olmuşlardır. İlginçtir ki, Formil grubu içeren Aza-BODIPY bileşiği nitroaromatiklere ve nitroalifatiklere benzer bir yanıt göstermiştir. Aza-BODIPY genellikle nitro gruplarının neden olduğu PET (fotoindüklenmiş elektron transferi) mekanizmasını

tetikleyen elektron açısından zengin bir π-sistemi içerir ve Aldehit grubu içeren Aza-BODPIY bileşiği ve nitro bileşikleri benzer elektron alıcı kapasitelerine sahip olduğundan, K_{sv}'ler yaklaşık 1×10^4 M^{-1}'lik benzer değerlerde gözlenmiştir. Brom atomu, hem elektron çeken (endüktif) hem de ağır atom etkisi nedeniyle sistemler arası geçişi (ISC) artırarak fosforesans veya üçlü durum transferi yoluyla söndürmeyi etkilemiştir. Söndürme verimlilikleri düşünüldüğünde, test edilen tüm nitro bileşiklerinde %8-20 söndürme gözlemlenmiştir, bu da Aza-BODIPY molekülüne brom grubunun eklenmesinin sistemin elektron zenginliğini azalttığını göstermektedir. Bu durum, brom grubu içeren Aza-BODIPY bielşiğinin elektron açısından fakir nitro bileşikleriyle etkileşimini azaltmasına neden olmuştur.

Formil grubu içeren Aza-BODIPY bileşiğini değerlendirmek için beş ayrı nitroaromatik bileşik kullanıldı. Sonuçlar, ticari olarak erişilebilen nitroaromatik bileşikler (TNP, TNT, DNT ve MNT) analiz edildiğinde yaklaşık 1×10^5 M^{-1}'lik özdeş K_{sv} değerlerinin bulunduğunu gösterdi. K_{sv} değerleri incelendiğinde, Elektron veren grup eklenmiş bir *p*-OH Aza-BODPIY molekülüne kıyasla benzer değerler elde edildi. Formil grubunun elektron çeken gruplar olduğu bilinmesine rağmen, bu grup ışıkla uyarıldığında rezonans etkisine sahiptir, bağlı olduğu florofor grubu yüksek enerjili bir elektronik duruma girer. Böylece, elektron-zayıf nitro bileşiklerine karşı 1×10^5 düzeyinde K_{sv} değerleri elde edimiştir. İlginç bir şekilde, nitroalifatiklere yönelik bağlanma sabitinin nitroaromatik bileşikler kadar yüksek olduğu gözlendi. Formil grubu, sensörü elektron-zayıf yapar. Bu durum Aza-BODIPY'nin uyarılmış halde PET (fotoindüklenmiş elektron transferi) mekanizmasına karşı daha hassas olmasına neden olur. PET için gerekli enerji farkı sadece aromatik değil aynı zamanda alifatik nitro bileşikleri tarafından da sağlanabilir. Çünkü nitroalifatikler de güçlü elektron alıcılarıdır. Formil grubu genellikle Aza-BODIPY bileşiğini elektrofilik türlere karşı hassas hale getirir, ancak seçicilik sağlamaz. Başka bir deyişle, Aldehit grubu içeren Aza-BODIPY, nitroaromatik veya nitroalifatik olmalarına bakılmaksızın her iki tür elektron alıcısına da söndürme tepkisi göstermiştir. Söndürme verimliliklerine bakıldığında, Bileşik 10'un nitro bileşiklerine karşı %52-79 arasında değerlere sahip olduğu görülmektedir. Bu, formil grubunun QE (Sönümleyici Verimliliği) değerini bir elektron veren grup kadar artırmadığını, ancak rezonans etkisi nedeniyle Brom'a kıyasla daha yüksek sönümleyici verimlili değerlerine sahip olduğunu göstermektedir.

Elektron veren gruplara sahip bileşiklerin Aza-BODIPY yapısının elektron zenginliğini artırarak nitro bileşikleri ile daha güçlü etkileşimler gösterdiği gözlemlenmiştir. Öte yandan, Elektron çeken gruplar genellikle halkadaki elektron yoğunluğunu azaltır ve PET (fotoindüklenmiş elektron transferi) mekanizmasının etkinliğini sınırlayarak sensör performansını düşürür. Ancak, formil grubunun rezonans etkisi gibi bazı istisnalar, bu tür bileşiklerin beklenmedik şekilde etkili sensör davranışı sergilemesine neden olmuştur. Bu bulgular, Aza-BODIPY tabanlı sensörlerin seçici algılama yeteneğinin doğrudan fonksiyonel grup yapısıyla ilişkili olduğunu ortaya koymaktadır.

Bu tezde yürütülen çalışmalar kapsamında, Aza-BODIPY boyalarının diğer geleneksel organik boyalara kıyasla avantajları (yüksek fotostabilite, geniş dalga boyu ayarlanabilirliği, yapısal esneklik, vb.) ve bazı sınırlamaları (seçicilik sorunları, çözünürlük sınırlamaları, vb.) değerlendirilmiştir. Elde edilen sonuçlar, Aza-BODIPY tabanlı sistemlerin çok yönlü kullanılabilirliğini açıkça göstermekte ve farklı alanlara kolayca entegre edilebilen bir platform sağlamaktadır.

1. INTRODUCTION

Various synthetic organic dyes, such as rhodamine, cyanine, phthalocyanine, BODIPY, and Aza-BODIPY, have attracted considerable attention in recent years due to their unique photophysical properties. These properties allow them to absorb and emit light over a wide range of wavelengths, which enables them to be used in a wide variety of applications. For example, due to their broad-spectrum photophysical properties, they are widely used in various disease treatments such as photodynamic therapy and photothermal therapy, as well as in technologies that are critical to health diagnosis such as intracellular imaging and bioimaging (Celli et al., 2010) (Kowada et al., 2015). In addition to their use in the medical applications, such molecules have also found a place in the literature as energy materials such as solar cells, chemosensors thanks to their suitable photophysical properties and their molecular structures that allow energy transfer (Klfout et al., 2017).

Organic dye research, which began with the discovery of aniline dye in the 19th century, has diversified and increased until today (Johnston, 2008). Over time, each new organic dye molecule discovered has offered certain advantages and disadvantages compared to existing systems; this has caused the dyes to be preferred in different application areas according to their properties. In particular, the ability of these dyes to absorb and emit at different wavelengths has contributed significantly to the expansion and diversification of their areas of use. Phthalocyanine is one of the most researched organic dyes and is an important molecule used in photodynamic therapy and optoelectronics. These dyes generally gain these properties due to their aromatic ring structure and their ability to coordinate metal ions (Lever, 1965). On the other hand, BODIPY compounds are preferred as fluorescent probes due to their superior photostability. Aza-BODIPYs are formed by adding a nitrogen atom to the meso position of BODIPY molecules; this modification gives them the ability to work in the near-IR region. This feature creates an ideal situation especially for intracellular imaging applications (Sonkaya et al., 2022).

In the literature, in current studies, especially in the bioimaging applications, studies on molecules that emit light in the near-IR region have begun to increase, and many organic dyes have been synthesized in this context, examples of which are phthalocyanines, BODIPYs, Aza-BODIPYs and porphyrins (Escobedo et al., 2010) (Figure 1.1).

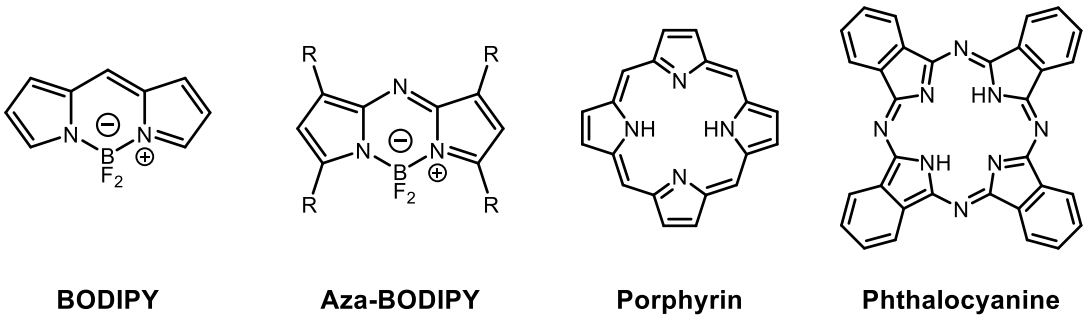

Figure 1.1 : General molecular formulas of phthalocyanines, BODIPYs, Aza-BODIPYs and porphyrins.

Despite the abundance of various organic dyes that emit and absorb in the near-IR region, these molecules often present two main disadvantages: poor thermal stability and photostability. However, the Aza-BODIPY dyes, which were introduced to the literature by Rogers in 1943 (Figure 1.2), were formed by adding nitrogen to the meso position of the BODPIY molecules, and have managed to overcome these two disadvantages and have increased in popularity in recent years because they can emit light at different wavelengths, allowing for various modifications based on the starting molecules (Rogers, 1943). Accordingly, Aza-BODIPY molecules offer a wide range of applications thanks to their structural and photophysical properties, and form the basis of this thesis (Kaur et al., 2024)(Zhao et al., 2023) (Shi et al., 2020). Within the scope of the thesis, various Aza-BODIPY derivatives were synthesized and structurally modified. These molecules were evaluated as sensors for the detection of nitroaromatic compounds, in IDA (Indicator Displacement Assay) systems and in intracellular imaging applications. As a result of the studies, it was observed that these molecules gave promising successful results in the mentioned application areas.

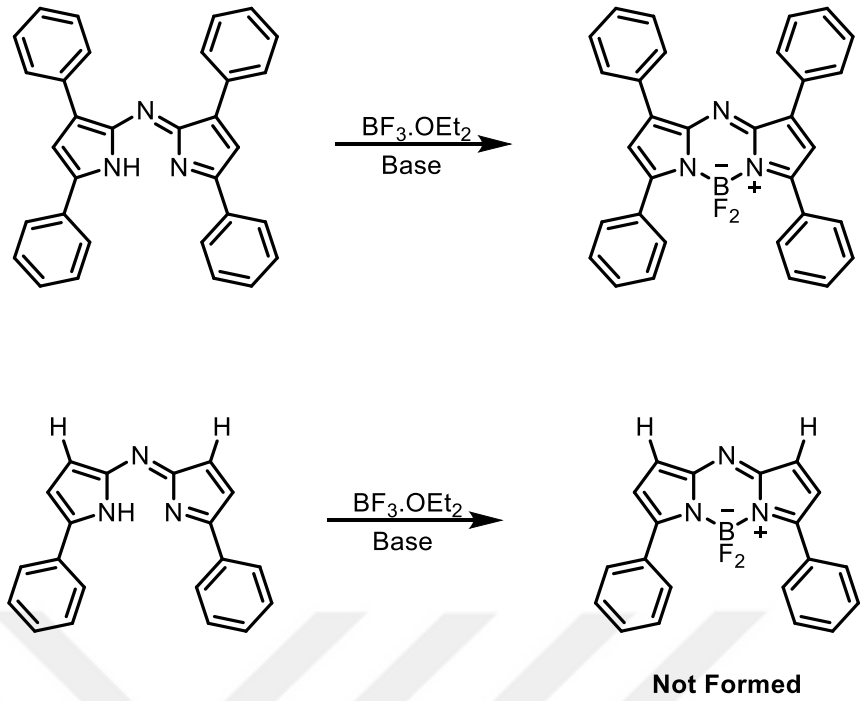

Figure 1.2 : The first Aza-BODIPY molecules synthesized in the literature (Rogers, 1943).

2. THEORETICAL PART

2.1. Aza-Boron-Dipyrromethene (Aza-BODIPY) Molecules

BODIPYs are known as a fluorescent dye core and are formed by the complexation of two pyrrole rings with BF_2 (boron difluoride). Aza-BODIY molecules are usually obtained by replacing a carbon atom with a nitrogen atom, thus taking the suffix *Aza-*. The structure of the Aza-BODIPY molecules restricts the rotation of the double bonds and this ensures that the resulting molecule is planar and rigid which is showing increased fluorescence yield and luminescence (ϕ/brightness). This causes the molecule to generally resort to emission as a relaxation mechanism after absorption, and this restriction of rotation in the double bonds generally shifts the emission wavelength to the near-IR region (L. Zhang et al., 2023). This change generally causes them to have a higher quantum yield, photo and thermal stability and narrow emission bands compared to BODIPY molecules (Figure 2.1). Aza-BODIPY molecules generally exhibit increased π electron delocalization, which results in their fluorescence properties. In addition, the core structure of the resulting Aza-BODIPY molecule generally exhibits electron-withdrawing properties and contains reactive regions around this core. This allows the addition of electron-donating groups or various functional groups to the Aza-BODIPY derivatives (Lu et al., 2014).

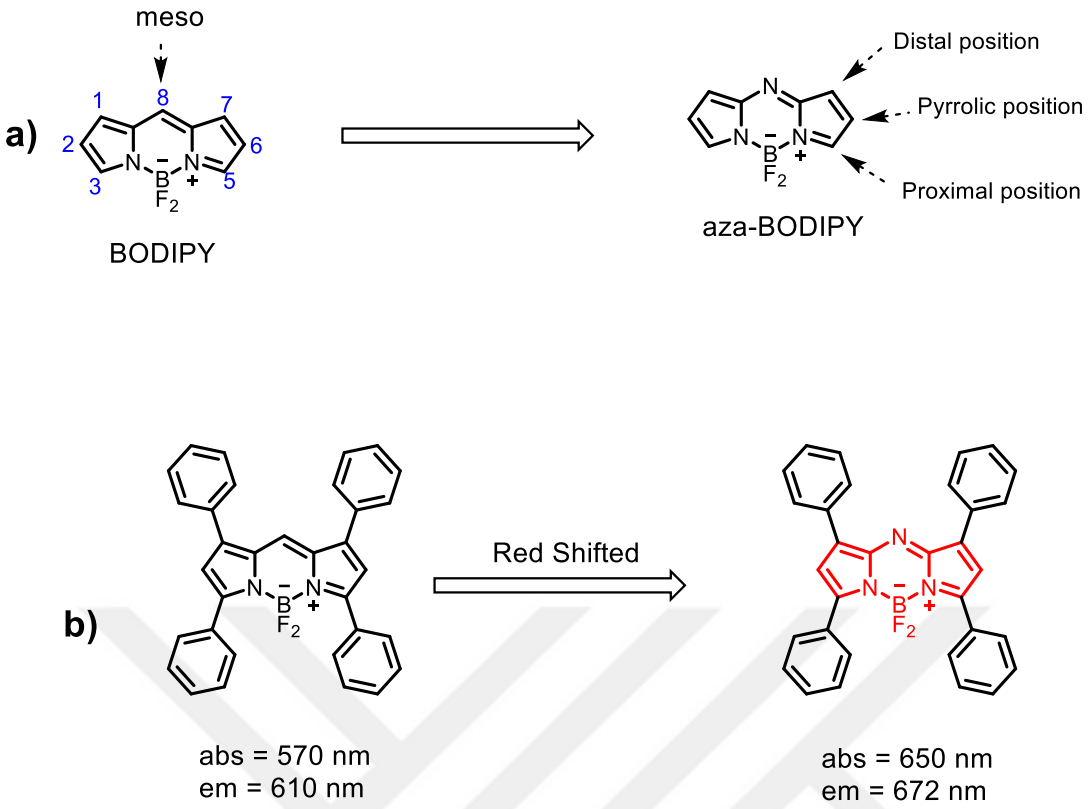

Figure 2.1 : General molecular structures of BODIPY and Aza-BODIPY molecules (a) and λ_{abs} and λ_{em} values (b) (Zhao et al., 2023).

Since their discovery by Rogers in 1943, Aza-BODIPY molecules have found a wide range of applications in biology, materials science, and sensors. The reason for such a diverse range of applications is that they have NIR emission in the range of 700–1700 nm, while BODIPY molecules have only 520–600 nm, which causes the Stokes shifts of BODPIY to remain between 10–25 nm, leading to poor penetration depth (Kaur et al., 2024). Aza-BODIPYs exhibit a bathochromatic shift as the addition of a nitrogen molecule to the meso position increasing aromatic conjugation. In addition to being analogs of BODIPY molecules, increased aromatic conjugation generally results in Aza-BODIPY molecules with λ_{max} between 90-100 nm and provide superior properties depending on the field of use (Schäfer et al., 2022).

There are three different methods proposed in the literature for the synthesis of Aza-BODIPY, namely O'shea's method, Carreria's method and Lukyantes' method (Killoran et al., 2002)(Zhao and Carreira, 2005)(Donyagina et al., 2008). (Figure 2.2)

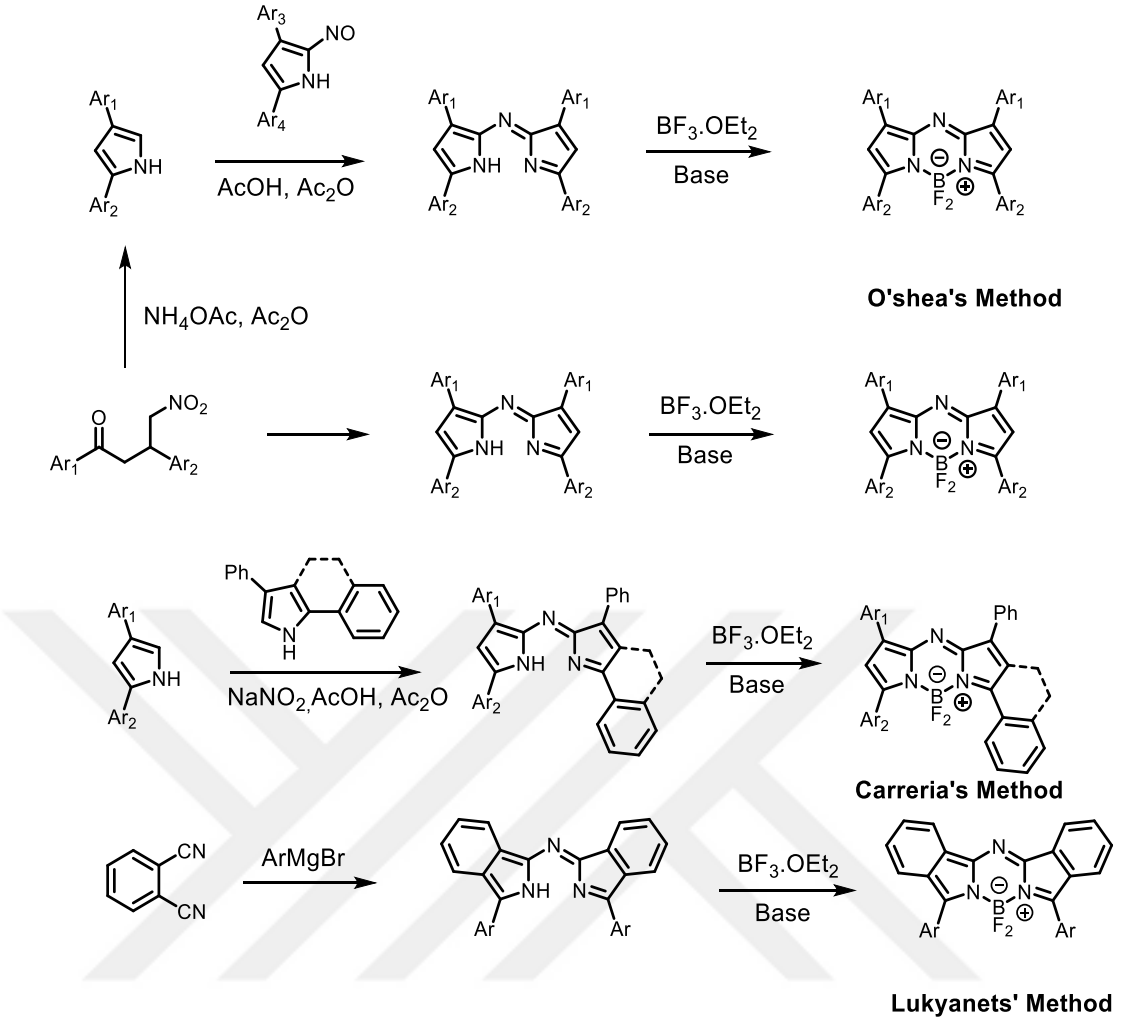

Figure 2.2 : Synthesis of Aza-BODIPY, namely O'shea's method, Carreria's method and Lukyantes' method (Kaur et al., 2024).

In the synthesis method presented by O'shea et al., Michael addition was made to symmetric or asymmetric E-chalcone compounds and then they were fused with NH_4OAc and in the last step BF_2 chelate was formed with $BF_3.OEt_2$. The advantage of this synthesis method is that it includes mild reaction conditions and various functionalized Aza-BODIPY compounds can be obtained from the starting materials. The disadvantage is that the yield of all reactions is low (Killoran et al., 2002). On the other hand, while the Carreira method can synthesize Aza-BODIPY compounds in high yields, the disadvantage of this method is that the reaction conditions used are more hazardous. In this method, substituted pyrroles are directly cyclized and then converted into BF_2 chelate (Zhao and Carreira, 2005). The method proposed by Lukyanets et al. leads to the synthesis of only symmetric Aza-BODIPY compounds and has low yields (Donyagina et al., 2008).

Tetra-aryl systems are one of the generally preferred methods for red shifting in Aza-BODIPY molecules. In this case, four aromatic rings are attached to the core Aza-BODIPY molecule. This generally shifts the absorption and emission properties to the near-IR region. In addition, conformational restriction of these molecules allows the absorption and emission maxima to be increased. By this method, intramolecular free movements are restricted and directed to energy discharge by emission during relaxation, which causes a significant extension of the emission wavelength. Two widely used methods for this purpose are B–O chelation and carbocyclic fusion (Chibani et al., 2012). (Figure 2.3)

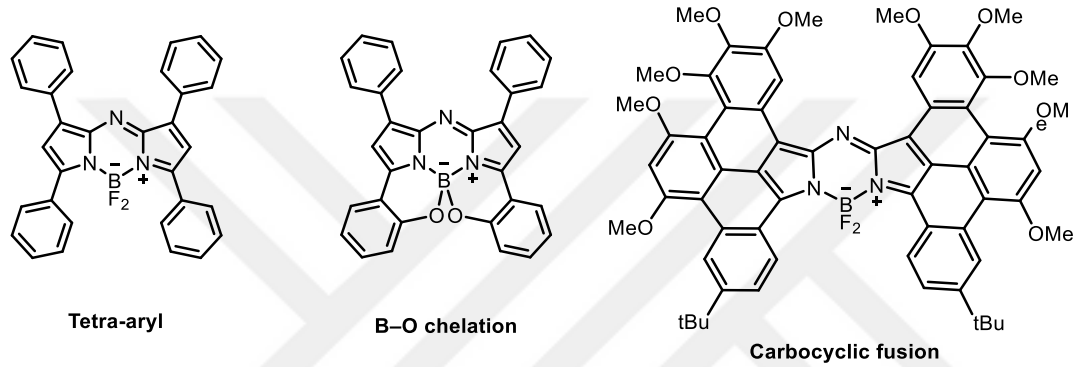

Figure 2.3 : Tetra-aryl, B–O chelation and carbocyclic fusion systems in Aza-BODIPY molecules (Chibani et al., 2012).

The addition of different substituents, i.e. electron donating (EDG) and withdrawing groups (EWG), to the Aza-BODIPYs affects their photophysical properties and can generally lead to their use in different application areas. EDG can cause a redshift in the emission wavelength, reducing the quantum yield. On the other hand, EWG increases the redshift, increases the absorbed wavelength and also offers high molar absorptivity (Shukla et al., 2023). (Table 2.1)

Table 2.1: Effects of EDG and EWG on Aza-BODIPY molecules (Killoran et al., 2002)(Murtagh et al., 2009)(Koch and Ravikanth, 2019)(Gorman et al., 2004).

Structure	Solvent	λ_{abs} (nm)	λ_{ems} (nm)	EDG or EWG	Reference
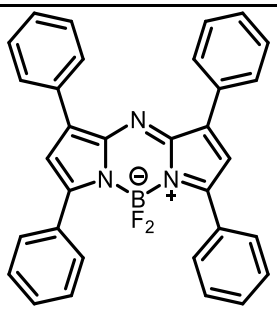	$CHCl_3$	650	672	None	Killoran et al., 2002

Table 2.1 (continued): Effects of EDG and EWG on Aza-BODIPY molecules (Killoran et al., 2002)(Murtagh et al., 2009)(Koch and Ravikanth, 2019)(Gorman et al., 2004).

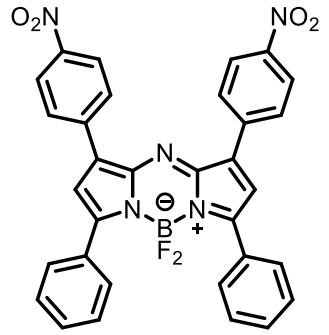	ACN	662	696	EWG	Murtagh et al., 2009
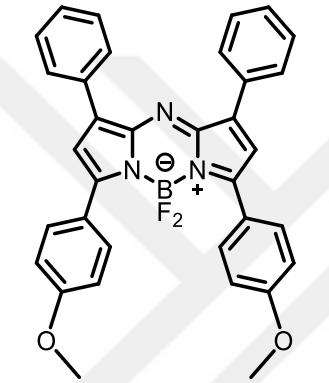	MeOH	688	716	EDG	Koch and Ravikanth, 2019
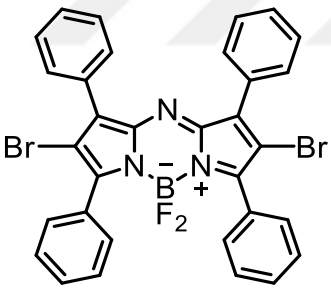	EtOH	645	666	EWG	Gorman et al., 2004

Different functionalization methods of Aza-BODIPY dyes are also available. Especially for biological applications, it is of great importance that Aza-BODIPY molecules are water soluble. Such modifications, unlike those mentioned above, usually involve additional chemical reactions after the synthesis of the molecules. The planar and rigid structures of the Aza-BODIPY molecules and their large aromatic ring systems cause aggregation via π–π interactions. This aggregation occurs particularly as a result of the overlapping of p-orbitals and the stacking of molecules. This significantly reduces their water solubility and limits their use in biological applications. Although conventional Aza-BODIPY dyes are hydrophobic, hydrophilicity is often possible by modifying their structure, encapsulating them in

nanoparticles, or integrating them into polymeric systems. Due to the all these characteristics given, Aza-BODIPYs have variety of applications in different areas such as: probes for the detection of metal ions and biological analytes, pH sensors, photodynamic therapy (PDT), photothermal therapy (PTT), photoacoustic (PA) imaging, optoelectronics (Kaur et al., 2024)(Xu et al., 2020).

2.2. Aza-BODIPY Based Fluorescent Sensor Systems for Detection of Nitro Aromatic Compounds

Nitroaromatic compounds (NACs) have high potential energy due to the simultaneous presence of high oxidizing and reducing groups in their structures and are widely used in many areas such as plastic explosive fillers, military ammunition and industrial explosives (Bener et al., 2022)(Albert et al., 1999)(Meaney and McGuffin, 2008). These compounds pose great risks in terms of security, as they are highly sensitive to external factors such as heat, friction or impact. At this point, the detection of NACs is of great importance in many critical areas from military security to environmental and public health. NACs such as TNT (trinitrotoluene), DNT (dinitrotoluene) and TNP (trinitrophenol) and aliphatic nitro compounds such as RDX (cyclotrimethylenetrinitramine) and NG (nitroglycerin) are widely used as explosives, but also cause serious health and environmental problems due to their high toxicity and carcinogenic effects (Saxena et al., 2005)(Behera et al., 2020)(Kovacic and Somanathan, 2014). (Figure 2.4) These compounds have a high risk of spreading into the environment during production, storage and disposal processes. Especially if they mix with drinking water and soil, they can cause long-term permanent damage to living organisms; they can lead to liver damage, nervous system disorders, muscle diseases and cancer (United States Enviromental Protection Agency, 2014). In addition, NACs pose a great threat in terms of illegal use and can be used in terrorist acts and illegal explosive production. Therefore, rapid, sensitive and reliable detection of NACs is necessary not only to ensure national security, but also to prevent environmental pollution and protect public health (Jiao et al., 2022)(Santiwat et al., 2023).

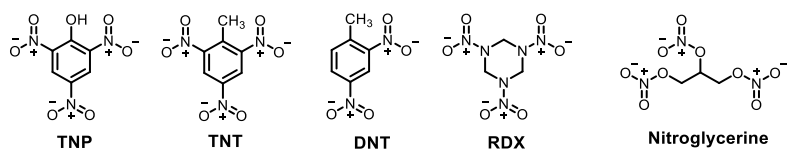

Figure 2.4 : Chemical structures of the most common examples of nitro compounds.

At this point, while traditional detection methods (GC-MS, LC-MS, X-ray Imaging, etc.) offer an expensive and laborious method that is not suitable for field use, fluorescence chemosensors offer lower cost, fast and portable solutions. Fluorescence chemosensors are inherently realized using optically active compounds such as organic fluorophore materials, quantum dots and metal-organic cages and conjugated/unconjugated polymeric systems containing them. Consequently, they provide high sensitivity and selectivity and have an important place in environmental, health and safety areas by enabling the detection of target components at lower concentrations. Although organic fluorophore materials have been tried as explosive sensors in the literature due to their π-π interactions, the majority of studies focus on pyrene, rhodamine, coumarin, triphenylamine, tetraphenyl ethene and porphyrin (Gunturkun et al., 2023)(Lv et al., 2023)(Selatnia et al., 2018)(Jing et al., 2019)(Sun et al., 2017)(Xue et al., 2023).

For example, He et al. (2011) developed fluorescent polymeric films for the purpose of nitroaromatic sensing in water (He et al., 2011). For this purpose, poly(pyrene-co-phenyleneethylene) was synthesized and coated on the surface of glass plates. This study demonstrated not only the selective response to TNT but also the ease of applicability of the sensor by film formation. Another study based on pyrene is the study of polyethersulfone-based nanofiber by Lei et al (Sun et al., 2015). Similarly, a polystyrene-based, pyrene-covalently bonded nanofiber membrane that can operate both in aqueous media and in the vapor phase was studied by Uyar et al (Senthamizhan et al., 2015). Both studies highlight the durability of the high fluorescence intensity of pyrene groups in flexible electrospun nanofibers and the ease of use and reproducibility of the nanofibers in the detection of NACs. (Figure 2.5)

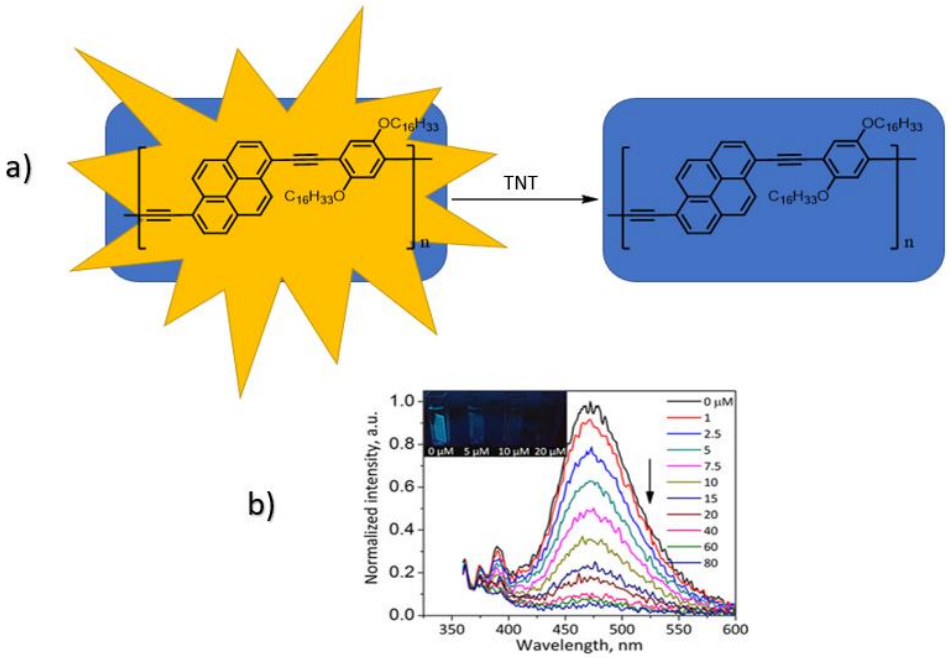

Figure 2.5 : Schematic representation of the polymeric films developed by He et al. (2011) for nitroaromatic detection in water (a) and analysis results against TNT molecule (b) (He et al., 2011).

Qayyum et al. (2021) evaluated AIEgens (aggregation-triggered emission) as explosive sensors using TPE-based thiophene system (Qayyum et al., 2021). The importance of the water dependence of the emission capabilities of AIEs in terms of determination of aqueous media was emphasized in the study, and in which there was a significant response capability for nitrophenol ($K_{sv} = 2 \times 10^5$ M^{-1}). In addition, the study, in which various nitroaromatic compounds were tested, showed the damping effect colorimetrically with strip probes. This study, which is distinguished from other examples in terms of being an AIE study, is a common situation for TPA and TPE based explosive sensors. In the study conducted by Ece Akkoç and Bünyamin Karagöz in 2022, uniform pyrene-based microspheres with a diameter of 1 μm were synthesized by dispersion polymerization using EGDMA (ethylene glycol dimethacrylate) and PySt (4-pyrenylstyrene) monomers and used as explosive sensors (Akkoc and Karagoz, 2022). (Figure 2.6)

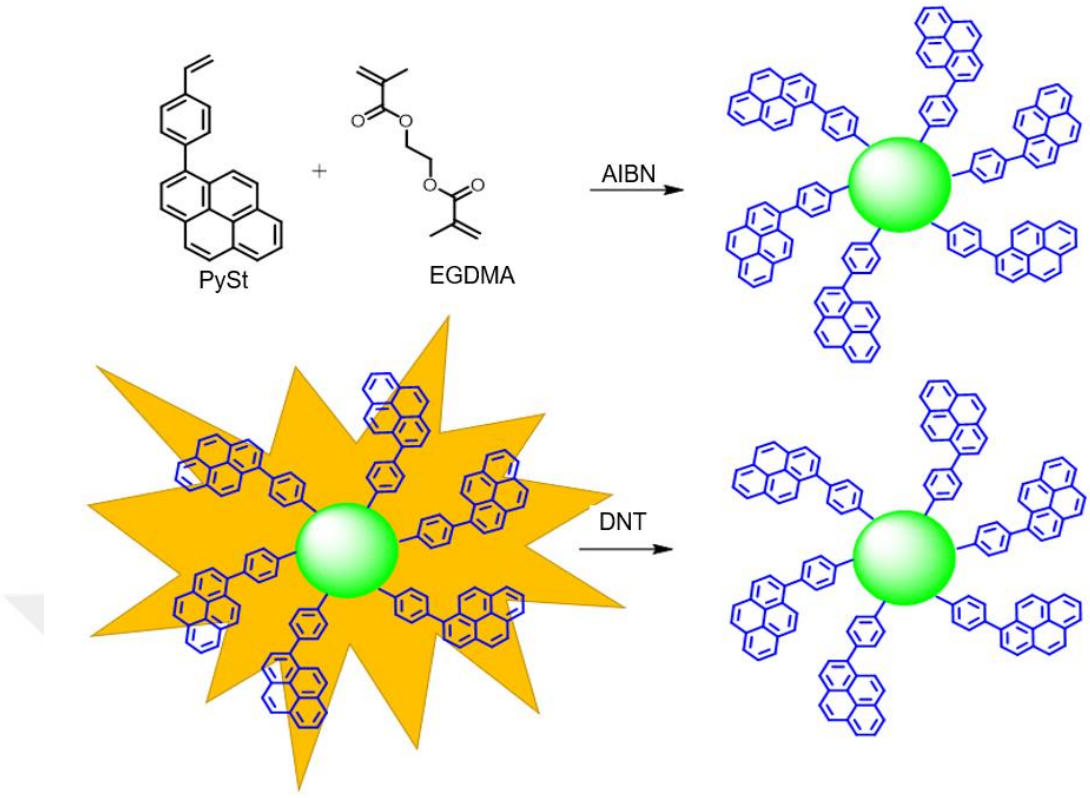

Figure 2.6 : Schematic representation of the use of the cross-linked molecularly imprinted fluorescent conjugated polymer (MICP) system as a nitroaromatic sensor, developed by Ece Akkoç and Bünyamin Karagöz in 2022 (Akkoc and Karagoz, 2022).

In another study conducted by Şen et al. in 2021, a TNT-sensitive and selective optical sensor was designed that works with the FRET (fluorescence quenching amplification resonance energy transfer) mechanism of the rhodamine 110 dye (Şen et al., 2021). Rhodamine, which provides a strong donor with the presence of amine groups, interacts with electron-deficient -NO_2 in TNT species and offers an effective method for the determination of TNT with a detection limit at ppm level, which is not affected by potential external analytes that may come from camouflage materials (Akkoc and Karagoz, 2022). The obtained microspheres were tested with TNP, TNT and DNT in various solvent environments and it was stated that they showed very strong fluorescence activity even at very low concentrations (6.67 µg/mL solvent). In the study, it was emphasized that the detection limit was reached at the nanomolar level (LOD 1.39 ppb for DNT) and P(PySt-EGDMA) microspheres showed high selectivity and sensitivity against DNT.

In a study conducted by Isci et al. (2025), an explosive sensor system based on TPA and TPE compounds TT (thienothiophene) based AIE (aggregation induced emission)

was tested. In the study, the effect of the electron density of TPA and TPE on selectivity was explained and it was emphasized that it was a system sensitive to TNP (K_{sv} = 29000 M^{-1}). This study, which differs from other examples in terms of being an AIE study, is a common situation for TPA and TPE based explosive sensors (Isci et al., 2025).

However, Aza-BODIPY compounds (4,4′-difluoro-4-bora-3a,4a,8-triaza-s-indacenes) have properties that can compete with known fluorophore compounds with their high absorption coefficients, chemical and photostability, high quantum yield and sharp fluorescence peaks and stand out as a very promising group of dyes for the detection of NACs (Hall et al., 2005)(Li et al., 2020). The Aza-BODIPY compound, unlike many other fluorophore compounds commonly used in the literature, stands out with its ability to absorb and emit in the near infrared (NIR) and infrared (IR) regions. In this way, it has great potential, especially in terms of environmental health and biological monitoring. Dyes that can emit in the NIR region minimize their effects on living organisms. Therefore, Aza-BODIPYs could become an important research tool in areas such as environmental monitoring and health security. Moreover, their high quantum yield and stability make them ideal for long-term and reliable detection applications.

In the literature, the first and only explosive sensor made with Aza-BODIPYs was realized by Sadikogullari et al. in 2023 via tetraphenyl conjugated Aza-BODIPY and was shown to be suitable for the detection of NACs. This sensor can be easily applied on solid surfaces or in solution and its use as strip probes was convenient. In the study, it was also emphasized that Aza-BODIPY has advantages over other dyes frequently encountered in the literature in the field of bioaccumulation due to its low toxicity and high lipophilicity (Sadikogullari et al., 2023). (Figure 2.7)

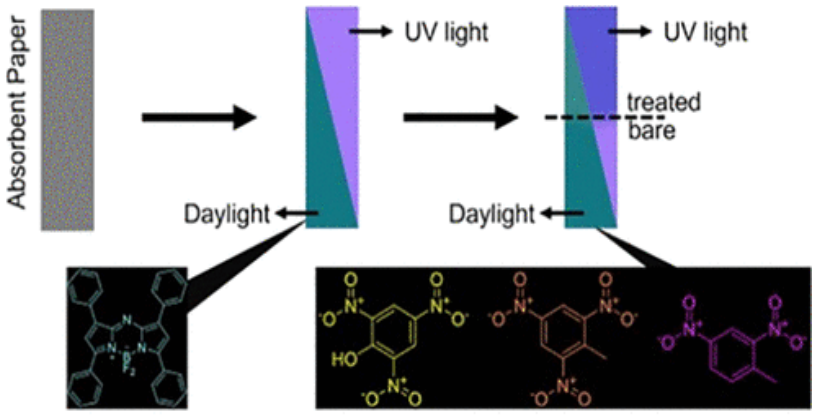

Figure 2.7 : Schematic representation of the Aza-BODIPY compound from the nitroaromatic sensor study conducted in the literature (Sadikogullari et al., 2023).

2.3. Aza-BODIPY Based Fluorescent IDA Sensor Systems

Since 1867, when optical-based sensors were discovered, molecular sensors have gained an important place in the identification of specific analytes in the biological, environmental and agricultural fields (Wu et al., 2017). In the development of molecular sensors, some limitations have created some guidelines that guide researchers; these limitations are complex reaction steps and reusability of sensors (Sedgwick et al., 2021). In the design of sensors, researchers generally studied host-guest interactions in nature and designed their molecular structures accordingly increase the reusability of sensors. This interaction also paved the way for IDA (indicator displacement assays) sensors, called supramolecular-based molecular sensors. IDA sensor systems consist of two important parts, which are the molecules that form the host-guest system that is tried to be imitated in nature. Here, the guest molecule is an optical molecule that is generally an indicator, and the host is a synthetic sensor (Sedgwick et al., 2021) (Figure 2.8).

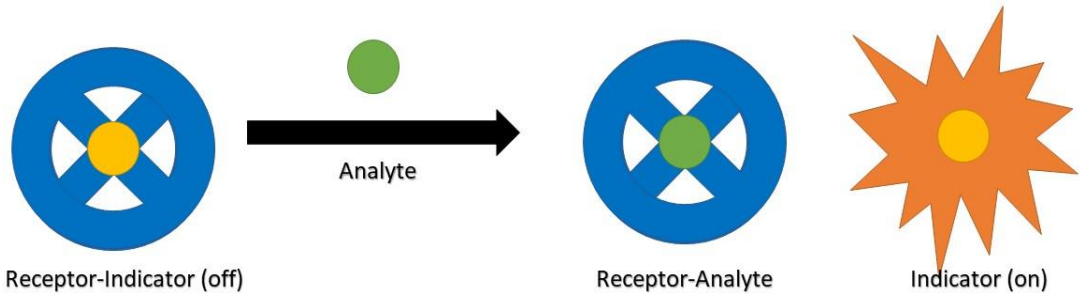

Figure 2.8 : Schematic representation of the traditional IDA sensors (Sedgwick et al., 2021).

Designed IDA (Indicator Displacement Assay) molecules must be designed appropriately according to some properties of the analyte. These properties can generally be classified as the size, charge or hydrophobicity of the analyte. In addition, the affinity of the host molecule to be used for the analyte must be higher than other similar molecules. When the analyte binds to the host molecule, an indicator molecule must be released in the environment; thus, a colorimetric or optical signal can be obtained. The fact that this signal is directly proportional to the analyte concentration forms the basis of the working principle of a sensor (Nguyen and Anslyn, 2006). IDA sensors can be constructed using a variety of supramolecular structures such as calix[4]arene, resorcin[4]arene or calix[4]pyrrole (Lo and Wong, 2008)(Gropp et al., 2018)(Amharar and Aydogan, 2022).

Calix[4]pyrrole molecules are molecules that find their place in sensor and biology applications in the literature, especially due to their ion recognition and ion transport properties (Kim and Sessler, 2015). These molecules can recognize various anions (especially halogens) with high selectivity through hydrogen bonds, thanks to the four pyrrole rings in their structures (Figure 2.9).

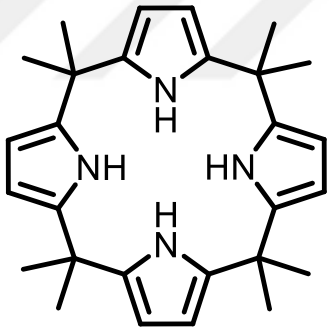

Figure 2.9 : Structure of calix[4]pyrrole.

One of the most important features of calix[4]pyrrole molecules is their ability to undergo structural changes during sensor applications. This feature allows them to react to the analyte, increasing their turn-on sensor properties, i.e. their ability to react in the analyte environment. Calix[4]pyrrole has been used extensively in the literature for the detection of anions. In this thesis, Aza-BODIPY and calix[4]pyrrole molecules will be brought together and made into a sensor for the fluoride ion.

Fluoride is often found in medicines, underground water sources and chemical warfare agents (Sakai et al., 2005)(Ayoob and and Gupta, 2006). Therefore, it is important that its detection is done quickly and with high accuracy. Boron-dipyrromethane and

dipyrromethene have generally been used as fluoride sensors, but these sensors operate with the indicator-spacer-receptor (ISR) approach (Chen et al., 2021)(You et al., 2010). The use of IDA sensors for this purpose will generally solve the problems of the above approach and there are examples in the literature (Amharar and Aydogan, 2022). Within the scope of this thesis, the advantages offered by IDA sensors will be used and the high ϕ/brightness features of Aza-BODIPY will be integrated into these systems.

In their study, Amharar and Aydogan (2022) developed a low-cost and high-sensitivity turn-on IDA sensor to detect fluoride ion using the octamethylcalix[4]pyrrole molecule (Amharar and Aydogan, 2022). Here, 4-methylumbelliferone and fluorescein molecules and their tetrabutylammonium (TBA) salts were used together to impart fluorescence properties to the sensor, i.e. to produce a fluorescent chemosensor. The schematic representation of the study is given in Figure 2.10.

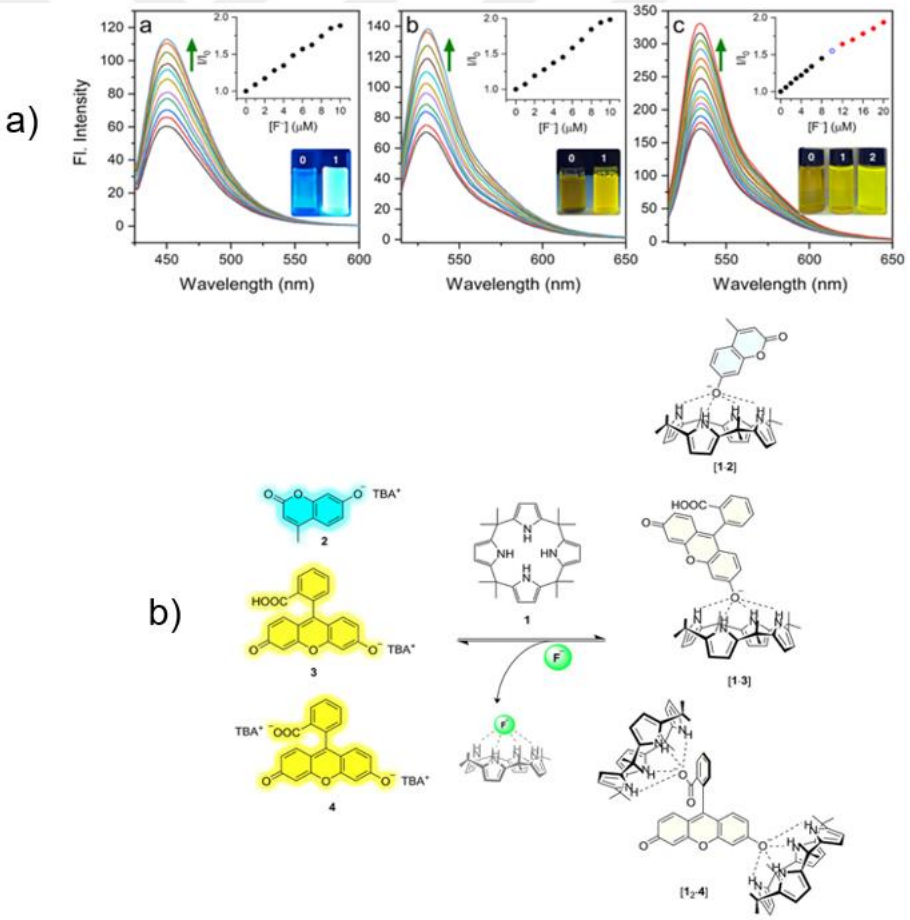

Figure 2.10 : Fluoresence responses towards fluoride anion by the molecules synthesized by Amharar and Aydogan (2022) (a) and schematic representation of the turn-on IDA sensor system for fluoride detection in the literature (b) (Amharar and Aydogan, 2022).

In this study, the researchers reported that they developed a cheap system for fluoride anion detection, and the system they developed worked well in ACN and THF. They also observed that the sensor system was selective for fluoride anion in the presence of other anions, but they mentioned that the system they developed had a low detection limit for fluoride anion detection.

As mentioned, Aza-BODIPY molecules have recently attracted attention in the literature and have been used as fluorine anion sensors. Zou et al. (2014) developed an Aza-BODIPY sensor in a turn-off mechanism, i.e. by losing its fluorescence property, both in solution and in living HeLa cells (Zou et al., 2014). Aza-BODIPY was synthesized by researchers by combining 4-bromophenol and magnesium, then reacted with phthalonitrile. Then a silicon group was added to the Aza-BODIPY molecule, which reacted with the fluorine anion in the medium, destroying the fluorescence property of the dye and forming a turn-off sensor. The schematic representation of the study is given in Figure 2.11.

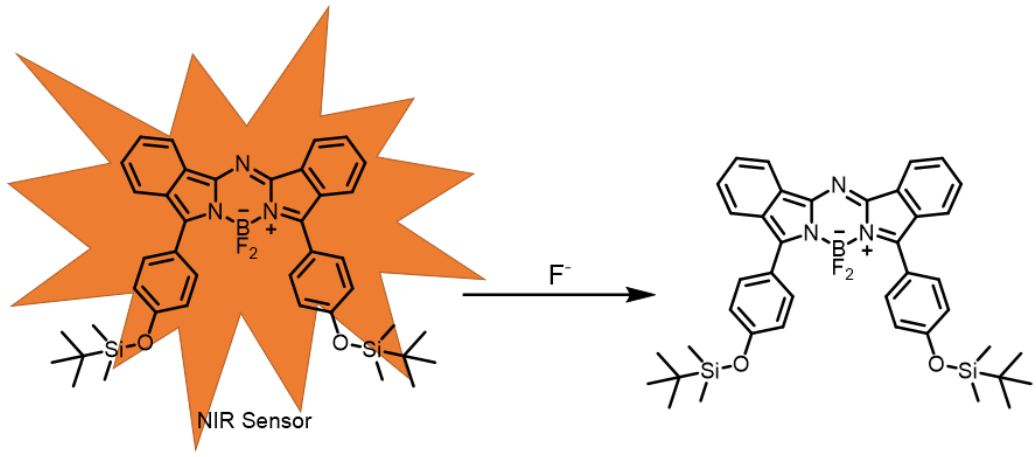

Figure 2.11 : Schematic representation of the turn-off fluoride sensor system containing Aza-BODIPY core in the literature (Zou et al., 2014).

Swamy P. et al. (2015) synthesized triarylborane–Aza-BODIPY conjugate in a study and applied it as a sensor for fluorine anion. In this study, the synthesized molecule contains two triarylborane groups that emit light in the visible region and one Aza-BODIPY molecule that emits light in the near-IR region (Swamy P et al., 2015). The absorption range of the final product synthesized was reported to be 300–800 nm. It was emphasized that the interaction between the groups emitting light in the visible

region and the Aza-BODIPY core was weak and in this case, it was determined that there was energy transfer to the core part. This explains the wide absorption range. Later, when this molecule was used as a counter-sensor for fluorine anion, quenching was observed in both regions and it was emphasized that the molecule showed turn-off sensor properties against anions. Figure 2.12 emphasizes the synthesized molecule and its wide spectrum range.

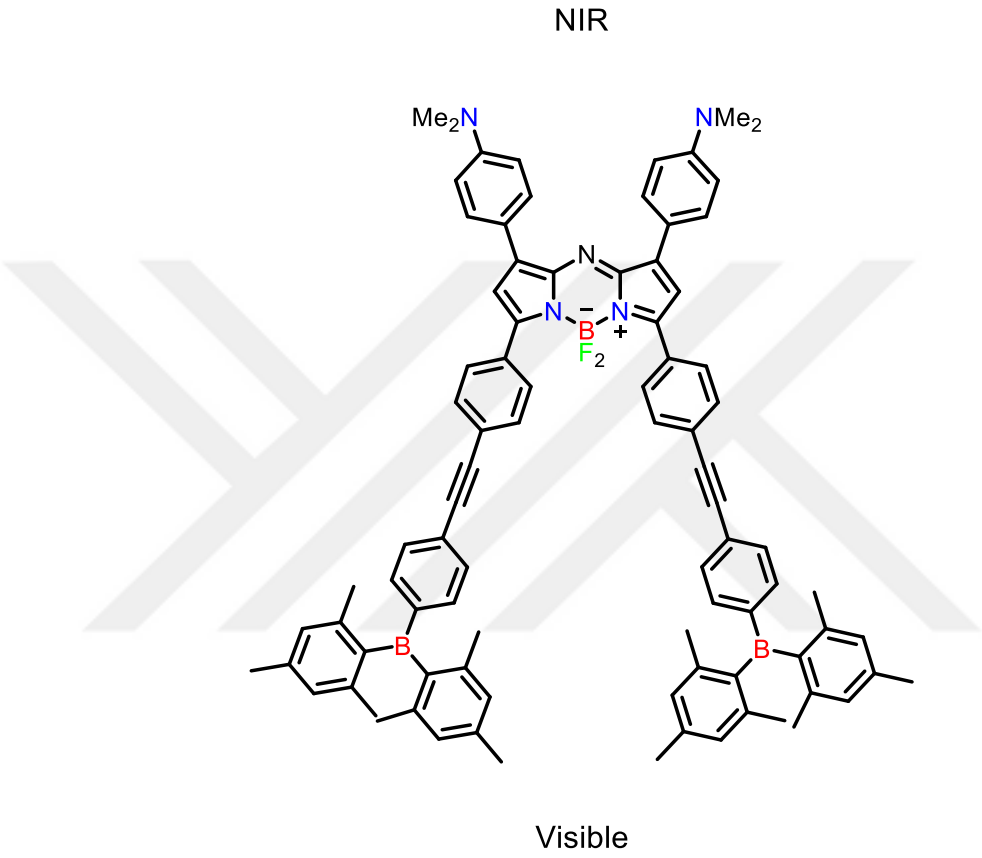

Figure 2.12 : Triarylborane–Aza-BODIPY conjugate synthesized by Swamy P. et al. (2015) and its wide range spectrum (Swamy P et al., 2015)

2.4. Aza-BODIPY Molecules for Cell Imaging Agents

Fluorescence imaging is a technique that has gained popularity and has been studied more recently due to its advantages over similar imaging studies in the literature as a highly sensitive, less harmful and less costly (Xu et al., 2020). Due to these advantages, this method has potential in physiological studies and pathological imaging. This method generally requires a fluorescent molecule such as an organic dye. In the selection of probes to be used in these studies, molecules that emit light especially in the near-IR region (700–1700 nm) have attracted the attention of researchers and have

begun to be used. Here, there are various advantages offered by such emitting sizes. To give a brief example; these molecules have high light uptake and low photon scattering. In addition, their low autofluorescence properties provide an example for obtaining high-resolution images (Tian et al., 2019). Today, studies have shifted from traditional Near-IR-I region fluorescent molecules to Near-IR-II region fluorescent molecules. In this case, Aza-BODIPY molecules that exhibit fluorescence in both regions have gained popularity, and modified Aza-BODIPY molecules or these molecules integrated into polymeric systems have been used as intracellular imaging agents in the literature. Electromagnetic spectrum has been given in Figure 2.13.

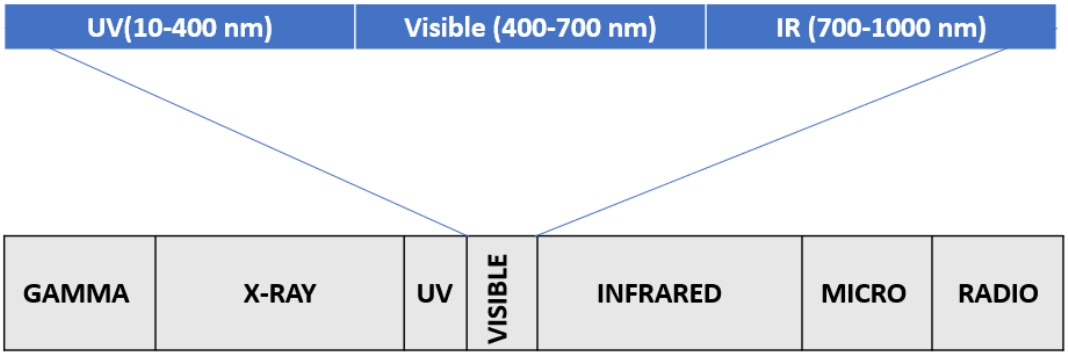

Figure 2.13 : Electromagnetic spectrum (Austin et al., 2021).

Zhu et al. (2017) used the Aza-BODIPY molecule for intracellular imaging in a study (Zhu et al., 2017). Here, the researchers used the dye molecule functionalized with tetraphenylethylene and fluorene on MCF-7 cells and observed that the molecules effectively entered the cell and gave strong red fluorescence in the cytoplasm. They observed that the groups they added also improved the fluorescence properties, shifted the emission wavelength to longer waves and increased the fluorescence efficiency. This study also shows that the properties of these molecules can be improved by adding groups and that such applications are more suitable. Fluorescence images of cells stained with Aza-BODIPY and DAPI (4′,6-diamidino-2-phenylindole) dyes are given in Figure 2.14.

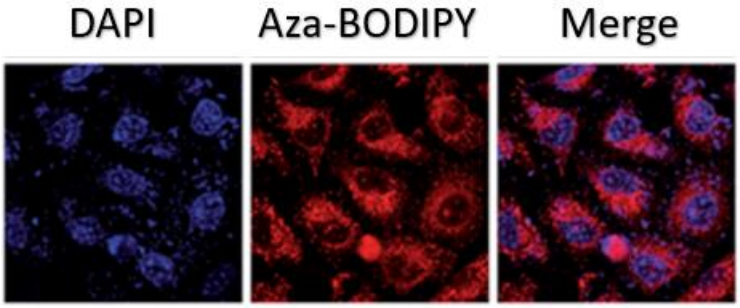

Figure 2.14 : Fluorescence images of cells stained with Aza-BODIPY and DAPI dyes from study demonstrated by Zhu et al. (2017) (Zhu et al., 2017).

Chansaenpak et al. (2018) encapsulated Aza-BODIPY molecules in biodegradable polymeric nanoparticles (AZB-NO2@PCL) for intracellular imaging, thus increasing the water solubility of these molecules (Chansaenpak et al., 2018). They then used the resulting polymeric system as an imaging tool on human glioblastoma cells, and the results were promising. It was observed that the resulting nanoparticles were taken into the cells within 3 hours, and the fluorescence signal increased over time, and also showed high biocompatibility. Fluorescence images of cells stained with Aza-BODIPY and DAPI dyes are given in Figure 2.15.

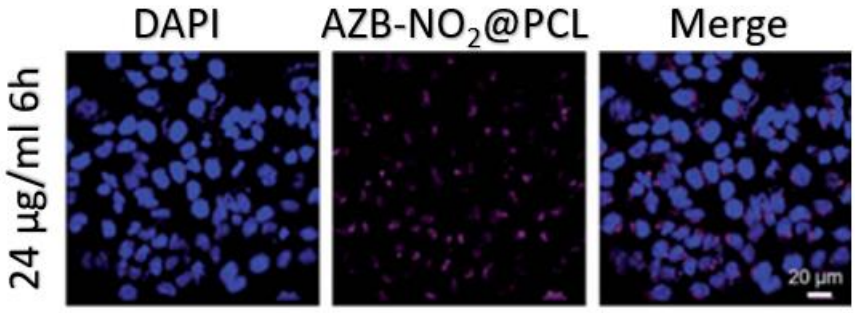

Figure 2.15 : Fluorescence images of cells stained with Aza-BODPIY and DAPI dyes from study demonstrated by Chansaenpak et al. (2018) (Chansaenpak et al., 2018).

In the study conducted by A. Li et al. (2025), new photosensitizers that target the plasma membrane of cancer cells and have strong properties for photodynamic therapy (PDT) were developed by fluorinating the Aza-BODIPY molecule with perfluoro-tert-butoxymethyl (PFBM) groups (Li et al., 2025). It was reported in this study that the developed dye molecules target the plasma membrane of cancer cells and are activated by light and kill cancer cells. The fluorination in this study transforms Aza-BODIPY

from an ordinary dye into a smart therapeutic agent that both finds and kills cancer cells and can perform dual imaging. (Figure 2.16)

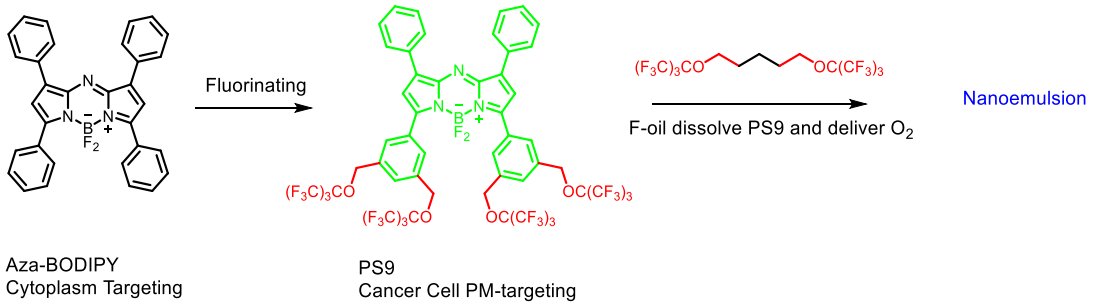

Figure 2.16 : Schematic representation of the study of the Aza-BODIPY molecule, which was developed by Li et al. (2025) and used as both a visualization and therapeutic agent (A. Li et al., 2025).

2.5. Aim of the Thesis

Aza-BODPIY molecules are one of the organic dyes that have become popular in the literature as mentioned above. This popularity is due to their various properties and some advantages compared to other dyes mentioned in the literature. Because the structure of the Aza-BODIPY molecules prevents the double bonds from rotating, the resultant molecule is rigid and planar, exhibiting higher luminescence (ϕ/brightness) and fluorescence yield. Due to the constraint of rotation in the double bonds, the molecule often turns to emission as a relaxation mechanism after absorption, which typically causes the emission wavelength to move to the near-IR region. This situation generally makes them a potential candidate for biological applications in biological systems, both because the wavelength is less dangerous for living cell samples compared to other dyes and because they have less autofluorescence. Their ability to absorb and emit in the near-IR region has also paved the way for sensor applications and various studies have been done in this area. The thesis will focus on the synthesis, effects of different substituent on molecules, characterization and various application areas of these potentially promising Aza-BODIPY molecules.

Within the scope of this study, two main Aza-BODIPY molecules were synthesized. These molecules were synthesized by O'shea method, namely starting from *E*-chalcone compound. The synthesized dyes are an Aza-BODIPY molecule without a substituted group and an Aza-BODIPY molecule with a *p*-OH group. Then, an Aza-BODIPY molecule without a substituted substance was converted into molecules containing bromine and aldehyde in pyrrolitic positions by bromination and formylation

processes respectively. The three different dyes obtained here were used as nitroaromatic sensors to examine the effect of these different EDG and EWG groups on the ring. Thus, the effect of these groups was compared with the study done in the literature (Sadikogullari et al., 2023).

In the second application study, a fluorine sensor will be synthesized by taking advantage of the property of calix[4]pyrrole molecule to recognize various anions (especially halogens) with high selectivity through hydrogen bonds and the fluorescence advantages offered by Aza-BODIPY, and its response to fluoride anion will be investigated. There is no study in the literature where these two molecules act as a sensor.

In the last part, synthesized aza-BODIPY derivative is integrated into polymeric systems. Polymeric systems synthesized by RAFT polymerization were used: PGMA-*b*-OEGMA. That polymeric systems were modified with Aza-BODIPY molecule for their use in intracellular imaging applications. The functionalized Aza-BODIPY derivative allows the visualization of intracellular interactions of polymers thanks to its fluorescence properties.

3. EXPERIMENTAL PART

3.1. Materials

All solvents used in the syntheses and purifications were provided by LabKim. The reagents used in the syntheses were provided by Aldrich Chemicals. Deuterated solvents required for characterization (NMR spectroscopy) and silica/Alumina solid phases used in column chromatography for purification after synthesis processes were provided by Merck Millipore.

3.2. Instrumentation

NMR analysis have been performed using an Agilent VNMRS 500 MHz Nuclear Magnetic Resonance Spectrometer at ITU Department of Chemistry, whereas spectrophotometric analysis have been performed using a PG Instruments T80+ UV-Vis spectrophotometer. An Agilent Cary Eclipse fluorescence spectrophotometer equipment was used to detect fluorescence at room temperature using a quartz cell with a 10 mm path length. Thermo LCQ-Deca ion trap mass instruments (HR-MS) were used to record the mass spectra. Measurements using gel permeation chromatography (GPC) were performed using an Agilent device (model 1100). A Cary 630 FT-IR instrument (Agilent Technologies) was used to capture Fourier transform infrared (FT-IR) spectra in the 4000–400 cm^{-1} range. Time-resolved fluorescence data were recorded using a Horiba Jobin Yvon SPEX Fluorolog 3-2iHR (France) instrument.

3.3. Synthetic Procedures

3.3.1. Synthesis of *p*-OH substituted Aza-BODIPY compound

3.3.1.1. Synthesis of 4′ – hydroxy – *E* – chalcone (1)

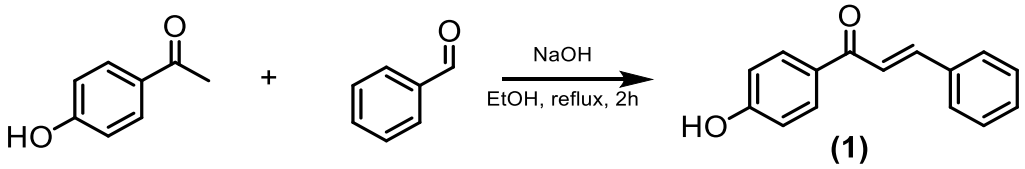

Figure 3.1 : Synthesis of 4′ – hydroxy – *E* – chalcone (1).

5 mL benzaldehyde (0.049 mol) and 6.672 g *p*-hydroxyacetophenone (0.049 mol) were dissolved in 39 mL of ethanol. In a different flask, the basic solution was prepared by dissolving 4.9 g of NaOH (0.123 mol) in 49 mL of water and allowed to reach room temperature. The prepared NaOH solution was added dropwise to the solution containing benzaldehyde and *p*-hydroxyacetophenone. The reaction mixture was stirred under reflux for 2 hours. After the completion of the reaction which was observed by TLC, the mixture was cooled to room temperature. 1N HCl solution was added to the cooled reaction mixture under ice bath and precipitation was observed. After the precipitation was complete, the mixture was kept in the refrigerator (~4 °C) overnight. Then, the precipitate was filtered, washed with cold MeOH and recrystallized in EtOH/Water mixture. The resulting solid was observed as pale yellow. The reaction scheme of synthesis of 4′ – hydroxy – *E* – chalcone is given in Figure 3.1.

Yield observed: 82% (9 g product)

^{1}H – NMR(500 MHz, $CDCl_3$): δ = 8.05 – 7.99 (m, 2H, Aromatic H); δ = 7.82 (d, *J* = 15.6, 1H, CH = CH); δ = 7.68 – 7.63 (m, 2H, Aromatic H); δ = 7.55 (d, *J* = 15.7, 1H, CH = CH); δ = 7.47 – 7.38 (m, 3H, Aromatic H); δ = 6.99 – 6.92 (m, 2H, Aromatic H); δ = 5.91 (s, 1H, –OH). (Figure 3.2)

^{13}C – NMR(125 MHz, $CDCl_3$): δ = 188.95 (1C, Carbonyl); δ = 160.10 (1C, H – C – C – OH); δ = 149.37 (1C, H – C = C – H); δ = 144.27 (1C, Aromatic); δ = 131.18 (3C, Aromatic); δ = 130.42 (2C, Aromatic); δ = 128.95 (2C, Aromatic); δ = 128.40 (1C, Aromatic); δ = 128.40 (1C, H – C = C – H); δ = 121.84 (2C, Aromatic) (Figure 3.4)

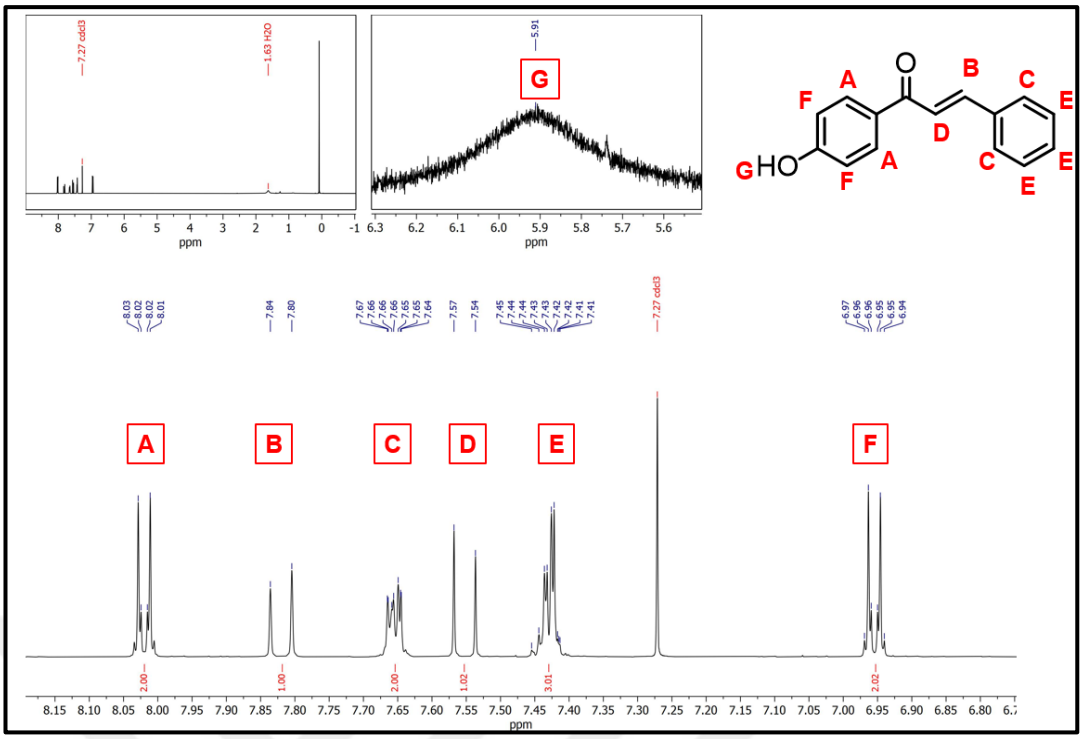

Figure 3.2 : (500 MHz, $CDCl_3$) ^1H – NMR of Compound 1.

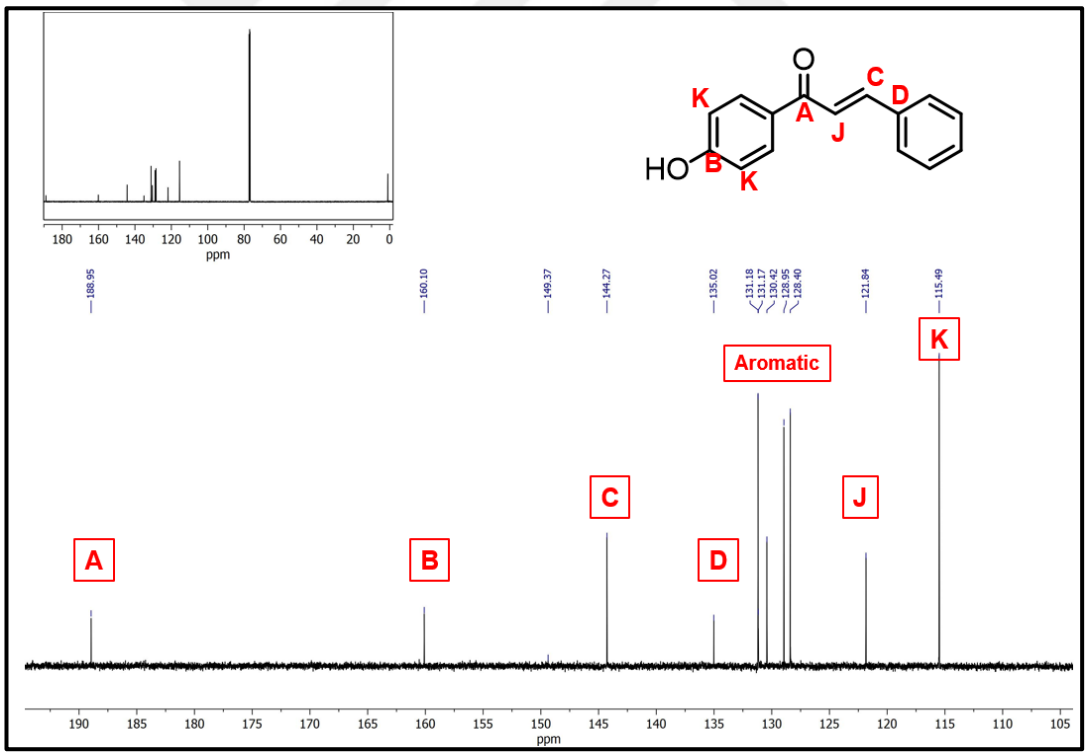

Figure 3.3 : (125 MHz, $CDCl_3$) ^{13}C – NMR of Compound 1.

3.3.1.2. Micheal addition of nitromethane to 4′ – hydroxy – *E* – chalcone (2)

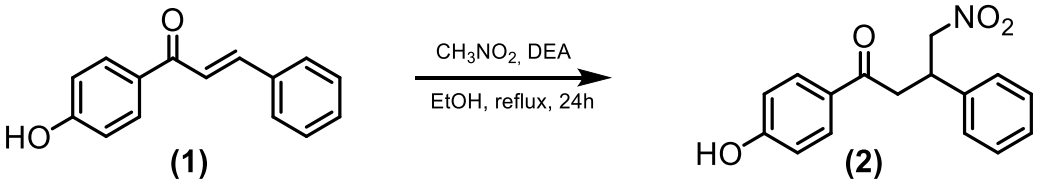

Figure 3.4 : Micheal addition of nitromethane to 4′ – hydroxy – *E* – chalcone (2).

0.0045 mol Compound 1 (1 g) was dissolved in 15 mL of methanol to prepare a solution in a 2 necked round bottom flask. To this solution, a mixture containing 2.3 mL of diethylamine (0.022 mol) and 2.4 mL of nitromethane (0.045 mol), prepared in a different flask, was added dropwise. The reaction mixture was refluxed for 24 hours. After the progress of the reaction monitored by TLC, the mixture was cooled and acidification was performed by adding 1N HCl dropwise under an ice bath. The reaction mixture was kept in the refrigerator (~4 °C) overnight, and the reaction mixture was used in the next step for the synthesis of *p* – OH substituted Aza-dipyrromethene compound. The reaction scheme of Michael addition of nitromethane to 4′ – hydroxy – *E* – chalcone is given in Figure 3.4.

3.3.1.3. Synthesis of *p* – OH substituted Aza-dipyrromethene (3)

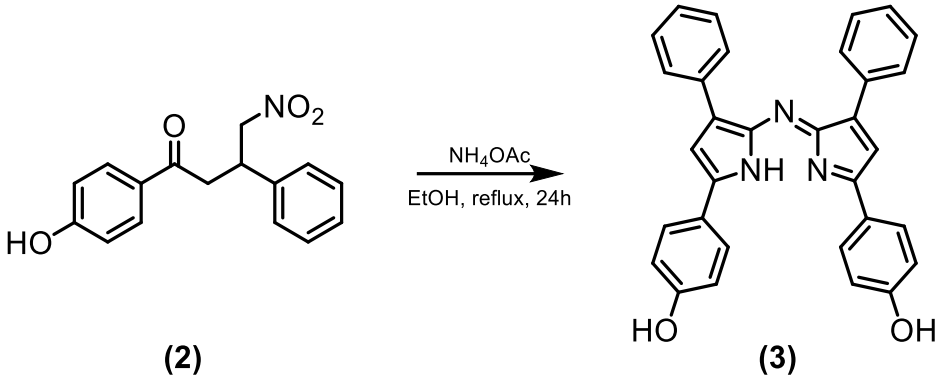

Figure 3.5 : Synthesis of *p* – OH substituted Aza-dipyrromethene (3).

2.5 g (0.009 mol) of Compound 2 was taken and dissolved in 65 mL of EtOH. 24.25 g (0.315 mol) of ammonium acetate was added to the resulting solution. The reaction mixture was refluxed for 24 h. After the reaction period, EtOH was evaporated, and the precipitated materials were washed with distilled water. The precipitate was then dried, yielding blue-black solids **(3)** (Murtagh et al., 2009). The reaction scheme of synthesis of *p* – OH substituted Aza-dipyyromethene is given in Figure 3.5.

Yield observed: 45% (1 g product)

^{1}H – NMR (500 MHz, DMSO-d_6): δ = 10.26 (s, 1H, –OH); δ = 8.11 – 8.06 (m, 4H, Aromatic H); δ = 7.96 – 7.89 (m, 4H, Aromatic H); δ = 7.53 (s, 2H, dipyrromethene); δ = 7.46 (t, *J* = 7.6, 4H, Aromatic H); δ = 7.37 (t, *J* = 7.3, 2H, Aromatic H); δ = 7.04 – 6.98 (m, 2H, Aromatic H). (Figure 3.6)

^{13}C – NMR (125 MHz, DMSO-d_6): δ = 161.41 (2C, dipyrromethene); δ = 157.76 (1C, dipyrromethene); δ = 144.77 (1C, dipyrromethene); δ = 141.97 (1C, dipyrromethene); δ = 132.55 (2C, Aromatic); δ = 132.41 (2C, Aromatic); δ = 129.86 (6C, Aromatic); δ = 129.49 (2C, Aromatic); δ = 129.14 (6C, Aromatic); δ = 122.17 (2C, Aromatic); δ = 119.97 (4C, Aromatic); δ = 126.55 (2C, dipyrromethene); δ = 116.36 (1C, dipyrromethene). (Figure 3.7)

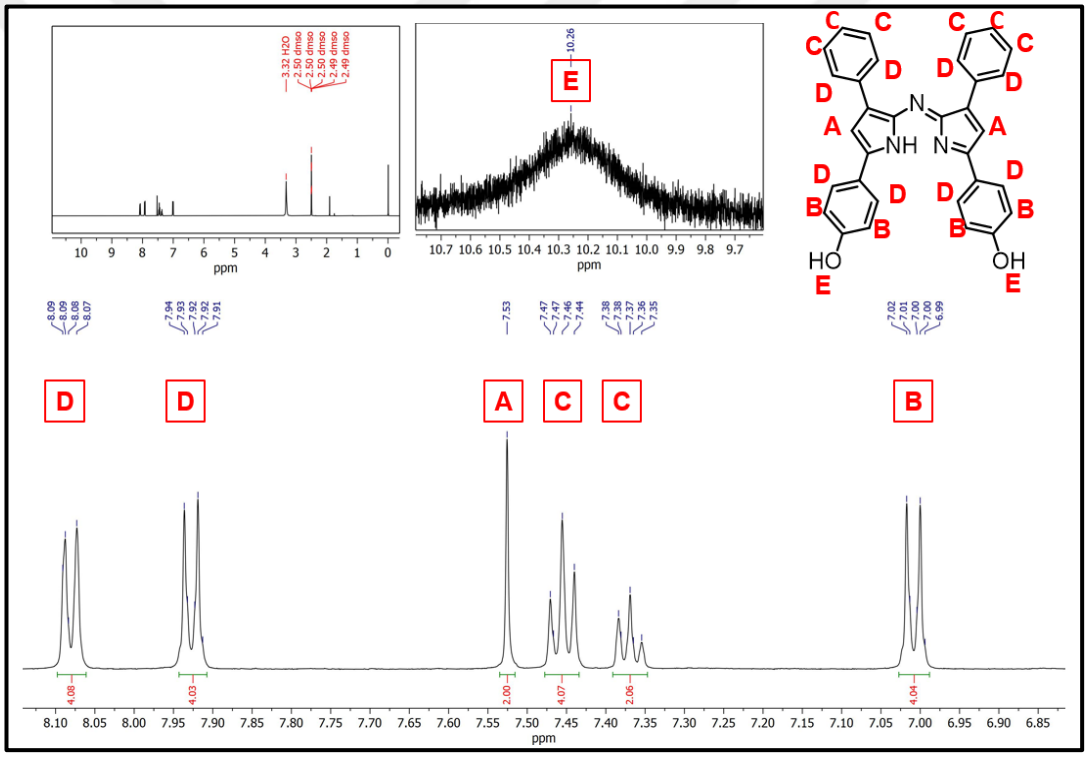

Figure 3.6 : (500 MHz, DMSO-d_6) ^{1}H – NMR of Compound 3.

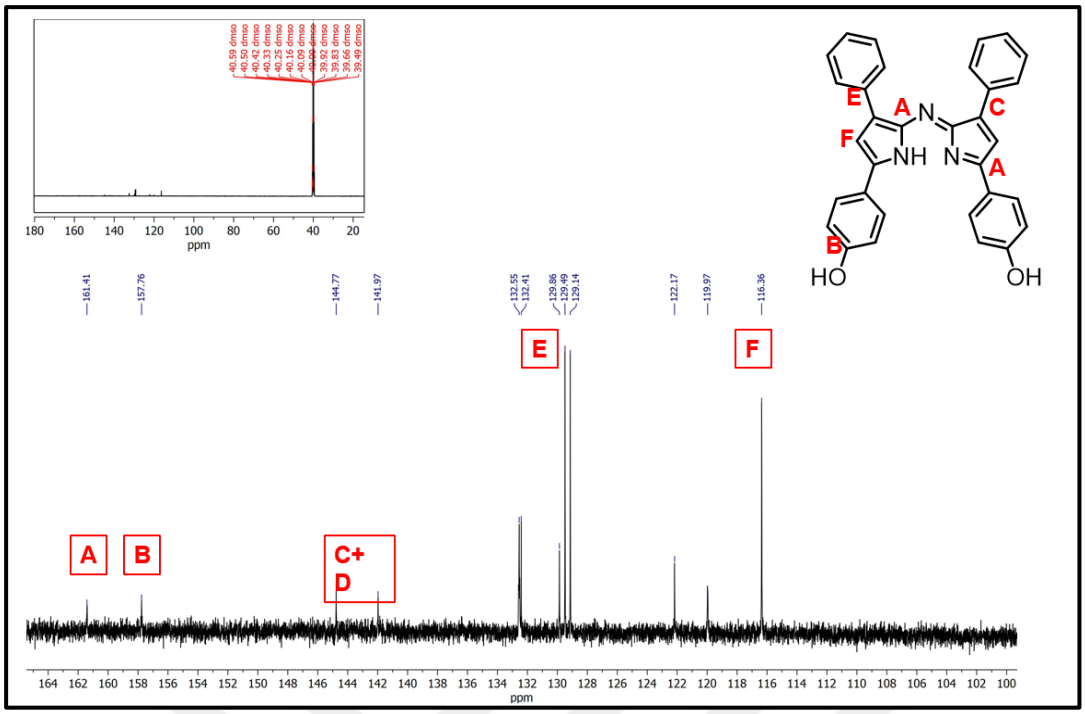

Figure 3.7 : (125 MHz, DMSO-d_6) ^{13}C – NMR of Compound 3.

3.3.1.4. Synthesis of *p*-OH substituted-Aza-BODIPY (4)

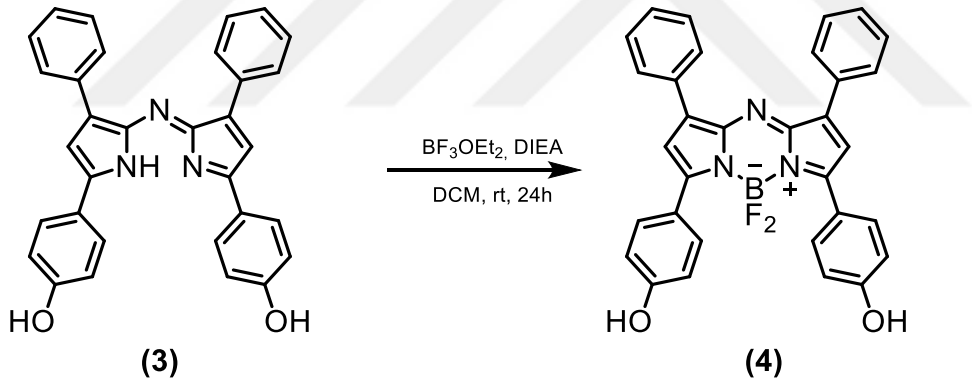

Figure 3.8 : Synthesis of *p*-OH substituted-Aza-BODIPY (4).

0.3 g (0.00062 mol) of Compound 3 was taken and dissolved in 30 mL DCM in a 2 necked round bottom flask. 1.08 mL (0.0062 mol) of diisopropylethylamine was added to the resulting solution and the mixture was stirred for 10 min. Then, 1.1 mL (0.0086 mol) of BF_3 Et_2O was added to the solution. The reaction mixture was stirred under N_2 atmosphere for 24 h. At the end of the reaction period, 30 mL of EtOH was added to the mixture and DCM and EtOH were removed in a rotavapor. The resulting solid was washed with distilled water and purified by column chromatography using DCM/EtOAc (4:1). As a result, the formation of a red metallic solid was observed

(Murtagh et al., 2009). The reaction scheme of synthesis of *p* – OH substituted Aza-BODIPY is given in Figure 3.8.

Yield observed: 50% (0.15 g product)

^{1}H – NMR(500 MHz, DMSO-d_6): δ = 10.45 (s, 1H, –OH); δ = 8.12 (dd, *J* = 30.9, 8.2 Hz, 8H, Aromatic H); δ = 7.54 (dd, *J* = 15.6, 8.3 Hz, 6H, Aromatic H); δ = 7.46 (t, 2H, dipyrromethene); δ = 6.94 (d, *J* = 8.9 Hz, 4H, Aromatic H). (Figure 3.9)

^{13}C – NMR(125 MHz, DMSO-d_6): δ = 161.41 (2C, dipyrromethene); δ = 157.76 (1C, dipyrromethene); δ = 144.77 (1C, dipyrromethene); δ = 141.97 (1C, dipyrromethene); δ = 132.55 (2C, Aromatic); δ = 132.41 (2C, Aromatic); δ = 129.86 (6C, Aromatic); δ = 129.49 (2C, Aromatic); δ = 129.14 (6C, Aromatic); δ = 122.17 (2C, Aromatic); δ = 119.97 (4C, Aromatic); δ = 126.55 (2C, dipyrromethene); δ = 116.36 (1C, dipyrromethene). (Figure 3.10)

^{19}F – NMR(470 MHz, DMSO-d_6): δ = -130.52 (q, J = 65.5, 32.3 Hz, BF_2). (Figure 3.11)

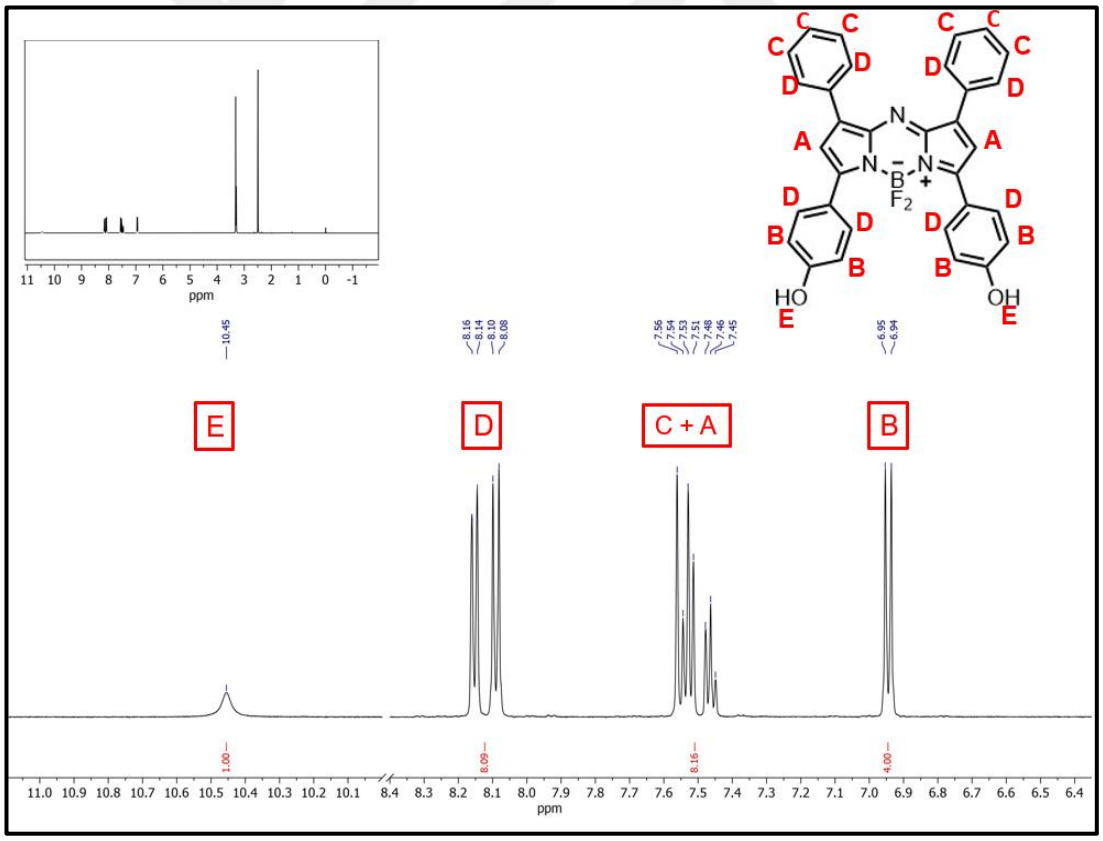

Figure 3.9 : (500 MHz, DMSO-d_6) ^{1}H – NMR of Compound 4.

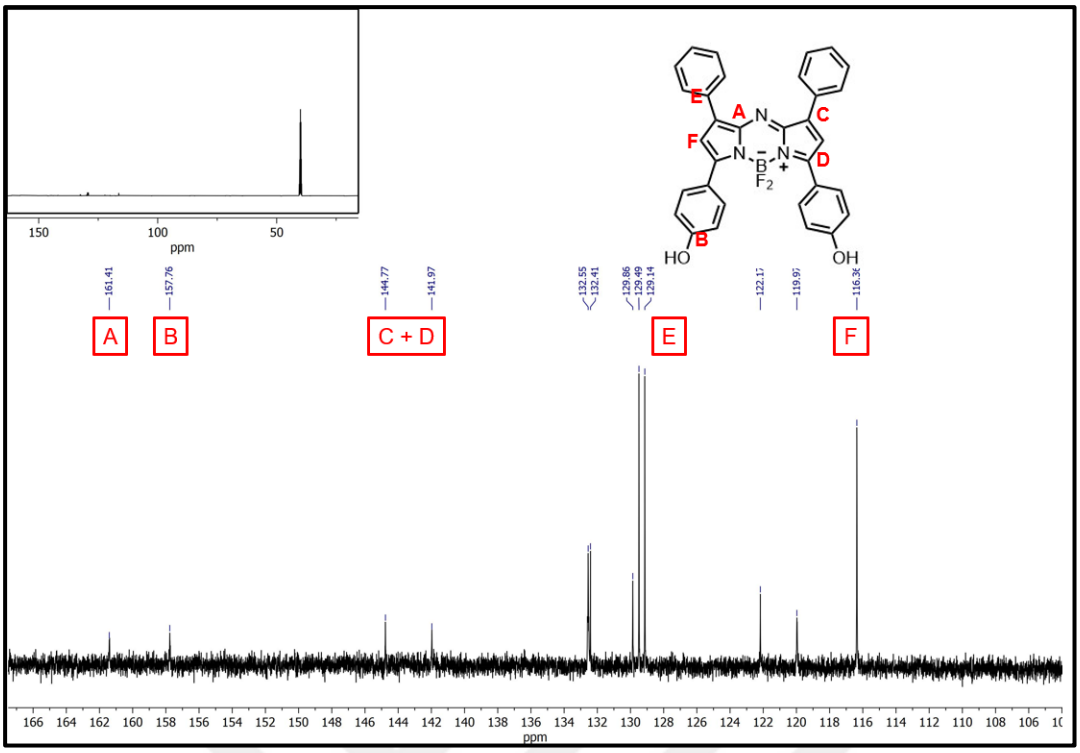

Figure 3.10 : (125 MHz, DMSO-d_6) ^{13}C – NMR of Compound 4.

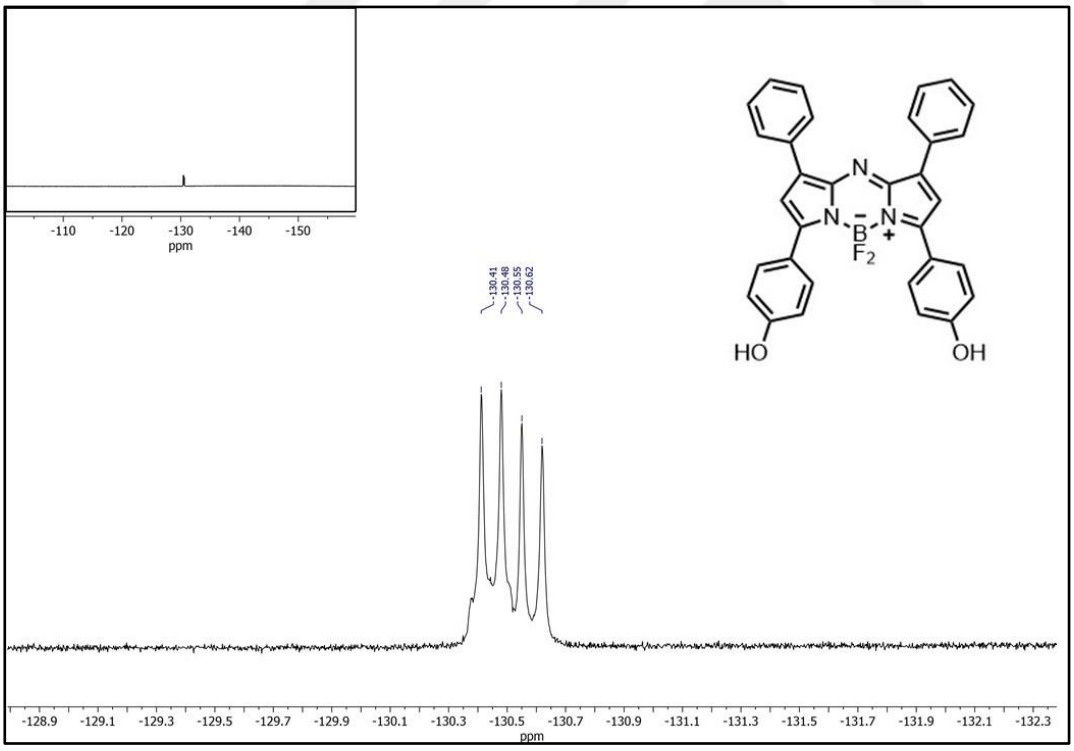

Figure 3.11 : (470 MHz, DMSO-d_6) ^{19}F – NMR of Compound 4.

3.3.2. Synthesis of tetra phenyl Aza-BODIPY compound

3.3.2.1. Synthesis of *E* – chalcone (5)

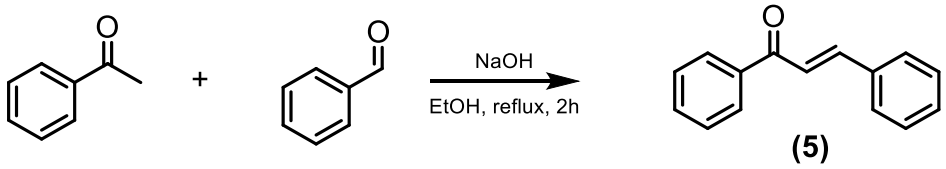

Figure 3.12 : Synthesis of *E* – chalcone (5).

2.95 mL benzaldehyde (0.029 mol) and 3.39 ml acetophenone (0.029 mol) were dissolved in 12 mL of ethanol. In a different flask, the basic solution was prepared by dissolving 2.960 g of NaOH (0.074 mol) in 29.5 mL of water and allowed to reach room temperature. The prepared NaOH solution was added dropwise to the solution containing benzaldehyde and acetophenone. The reaction mixture was stirred under reflux for 2 hours. After the completion of the reaction observed by TLC, the mixture was cooled to room temperature. 1N HCl solution was added to the cooled reaction mixture under ice bath and precipitation was observed. After the precipitation was complete, the mixture was kept in the refrigerator (~4 °C) overnight. Then, the precipitate was filtered, washed with cold MeOH and recrystallized in EtOH/Water mixture. The resulting solid was observed as pale yellow. The reaction scheme of synthesis of *E*-chalcone is given in Figure 3.12.

Yield observed: 89% (5.5 g product)

^{1}H – NMR(500 MHz, $CDCl_3$): δ = 8.06 – 8.02 (m, 2H, Aromatic H); δ = 7.83 (d, *J* = 15.7, 1H, CH = CH); δ = 7.66 (dd, *J* = 6.9, 2.8 Hz, 2H, Aromatic H); δ = 7.61 (t, *J* = 7.4 Hz, 1H, CH = CH); δ = 7.57 – 7.50 (m, 3H, Aromatic H); δ = 7.46 – 7.42 (m, 3H, Aromatic H). (Figure 3.13)

^{13}C – NMR(125 MHz, $CDCl_3$): δ = 190.60 (1C, Carbonyl); δ = 144.87 (1C, H – C = C – H; δ = 134.9 (1C, Aromatic); δ = 132.8 (1C, Aromatic); δ = 130.56 (1C, Aromatic); δ = 128.46 (2C, Aromatic); δ = 128.52 (2C, Aromatic); δ = 128.98 (3C, Aromatic); δ = 128.64 (2C, Aromatic); δ = 122.12 (1C, H – C = C – H). (Figure 3.14)

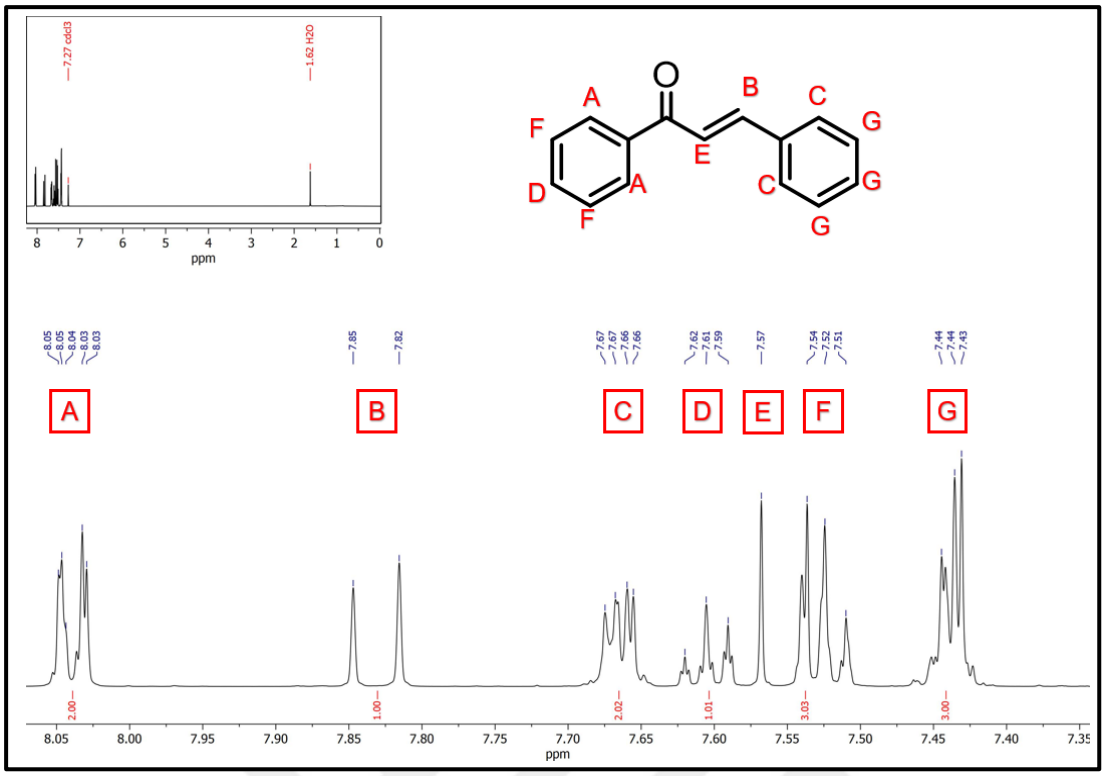

Figure 3.13 : (500 MHz, $CDCl_3$) ^{1}H – NMR of Compound 5.

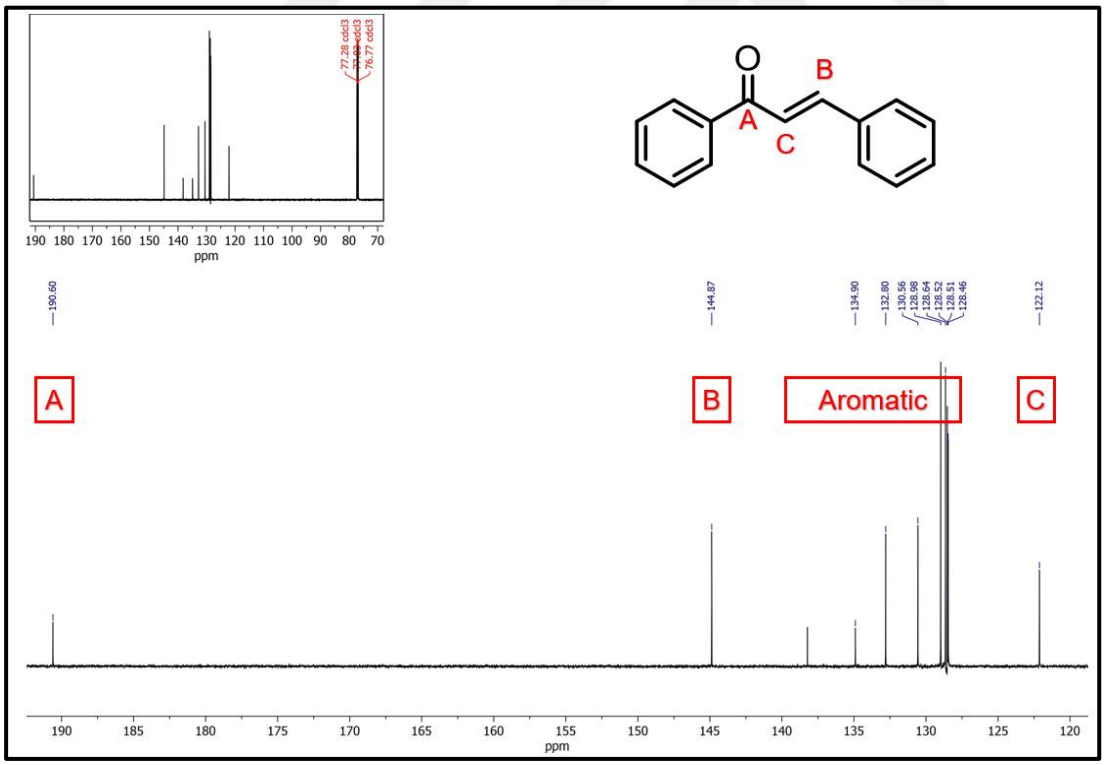

Figure 3.14 : (125 MHz, $CDCl_3$) ^{13}C – NMR of Compound 5.

3.3.2.2. Micheal addition of nitromethane to *E* – chalcone (6)

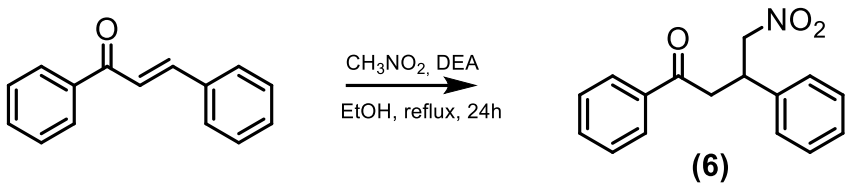

Figure 3.15 : Micheal addition of nitromethane to *E* – chalcone (6).

0.024 mol Compound 6 (5.5 g) was dissolved in 45 mL of ethanol to prepare a solution in a 2 necked round bottom flask. To this solution, a mixture containing 22.98 mL of diethylamine (0.22 mol) and 11.77 mL of nitromethane (0.22 mol), prepared in a different flask, was added dropwise. The reaction mixture was refluxed for 24 hours. After the progress of the reaction was monitored by TLC, the mixture was cooled and acidification was performed by adding 1N HCl dropwise under an ice bath. The reaction mixture was kept in the refrigerator (~4 °C) overnight, and precipitation was observed. The reaction scheme of Michael addition of nitromethane to *E*-chalcone is given in Figure 3.15.

Yield observed: 69% (5 g product)

^{1}H – NMR(500 MHz, $CDCl_3$): δ = 7.93 (dd, J = 8.5, 1.3 Hz, 2H, Aromatic H); δ = 7.61 – 7.56 (m, 1H, Aromatic H); δ = 7.50 – 7.45 (m, 2H, Aromatic H); δ = 7.38 – 7.26 (m, 6H, Aromatic H); δ = 4.85 (dd, *J* = 12.5, 6.6 Hz, 1H, $_2$ON-CH); δ = 4.71 (dd, *J* = 12.5, 8.0 Hz, 1H, $_2$ON-CH); δ = 4.29 – 4.20 (m, 1H, CH-CH); δ = 3.53 – 3.41 (m, 2H, CH-CH). (Figure 3.16)

^{13}C – NMR(125 MHz, $CDCl_3$): δ = 196.83 (1C, Carbonyl); δ = 139.12 (1C, Aromatic); δ = 136.38 (1C, Aromatic); δ = 133.57 (1C, Aromatic); δ = 129.08 (2C, Aromatic); δ = 128.75 (2C, Aromatic); δ = 128.02 (3C, Aromatic); δ = 127.89 (2C, Aromatic); δ = 79.57 (1C, $_2$ON-CH); δ = 41.53 (1C, CH-CH); δ = 29.29 (1C, CH-CH). (Figure 3.17)

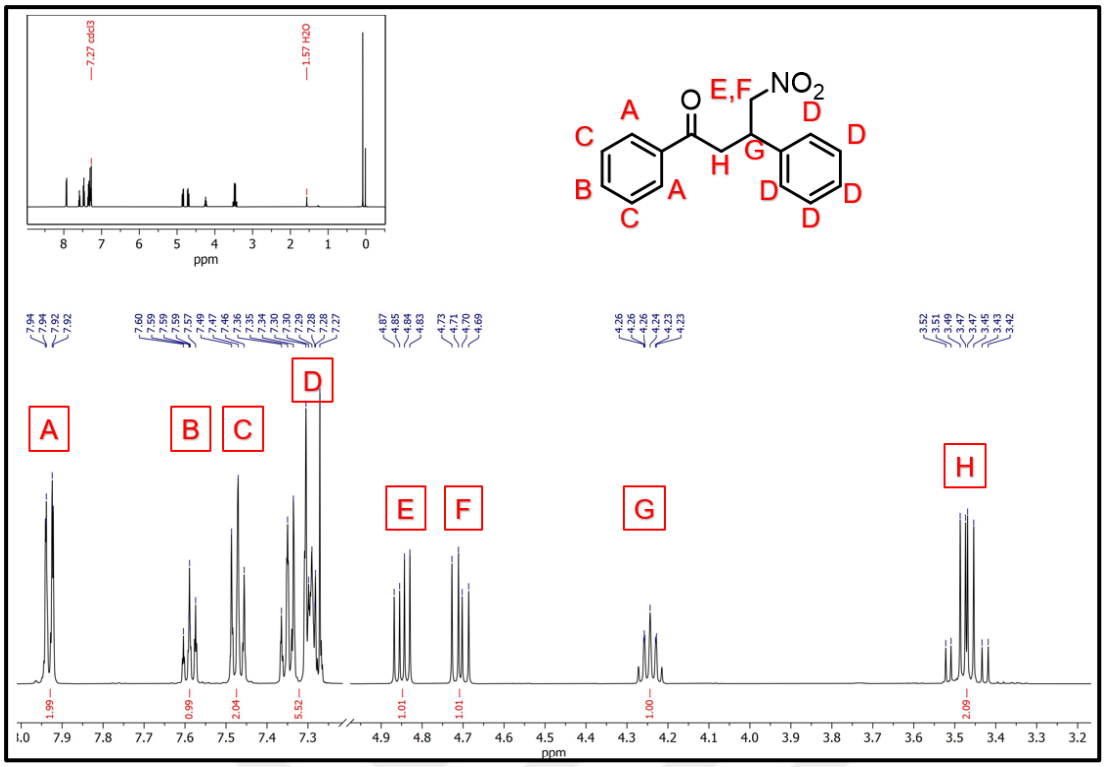

Figure 3.16 : (500 MHz, $CDCl_3$) ^1H – NMR of Compound 6.

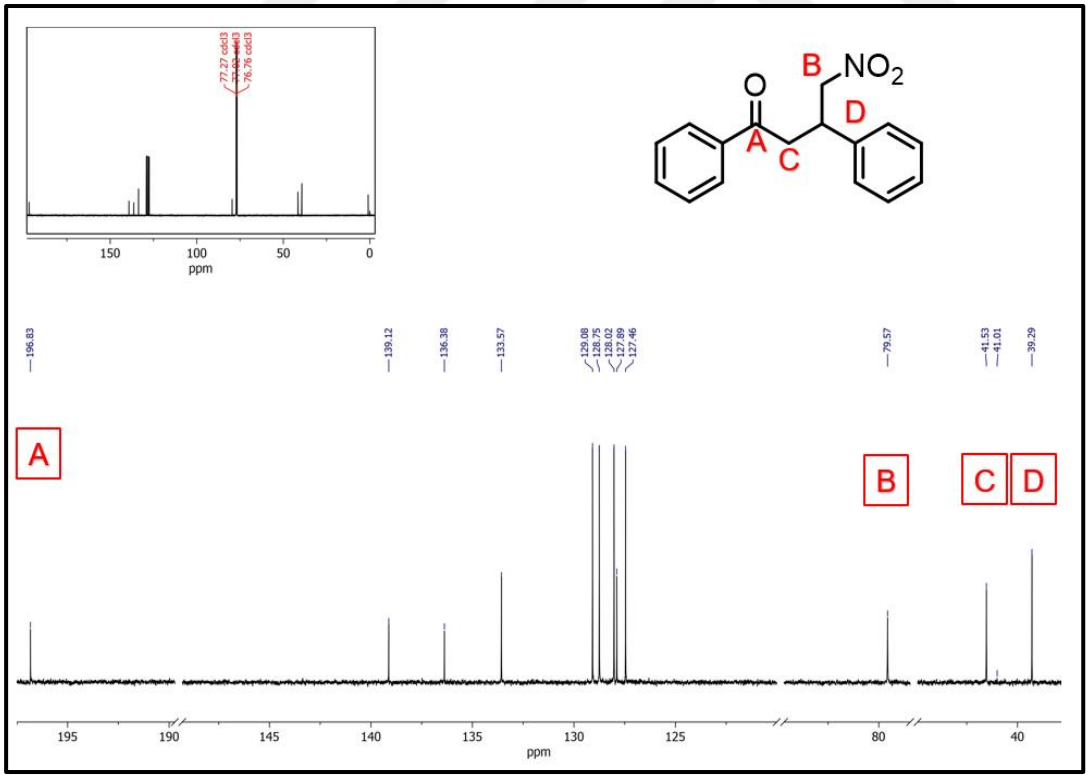

Figure 3.17 : (125 MHz, $CDCl_3$) ^{13}C – NMR of Compound 6.

3.3.2.3. Synthesis of Aza-dipyrromethene (7)

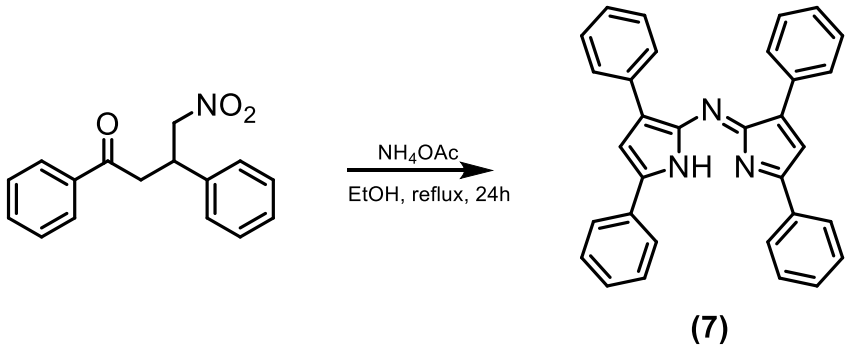

(7)

Figure 3.18 : Synthesis of Aza-dipyrromethene (7).

2.5 g (0.0055 mol) of Compound 6 was taken and dissolved in 65 mL of EtOH. 15.03 g (0.195 mol) of ammonium acetate was added to the resulting solution. The reaction mixture was refluxed for 24 h. After the reaction period, EtOH was evaporated, and the precipitated materials were washed with distilled water. The precipitate was then dried, yielding blue-black solids (Killoran et al., 2008). The reaction scheme of synthesis of Aza-dipyrromethene is given in Figure 3.18.

Yield observed: 94% (3.8 g product)

^{1}H – NMR (500 MHz, $CDCl_3$): δ = 8.08 (d, *J* = 7.1 Hz, 4H, Aromatic H); δ = 7.99 – 7.95 (m, 4H, Aromatic H); δ = 7.55 (t, *J* = 7.5 Hz, 4H, Aromatic H); δ = 7.46 (dt, *J* = 20.8, 7.5 Hz, 6H, Aromatic H); δ = 7.37 (t, *J* = 7.3 Hz, 2H, Aromatic H); δ = 7.22 (s, 2H, dipyrromethene). (Figure 3.19)

^{13}C – NMR (125 MHz, $CDCl_3$): δ = 155.11 (1C, dipyrromethene); δ = 149.60 (1C, dipyrromethene); δ = 142.66 (1C, dipyrromethene); δ = 133.71 (1C, Aromatic); δ = 132.19 (1C, dipyrromethene); δ = 130.06 (2C, Aromatic); δ = 129.15 (6C, Aromatic); δ = 129.08 (2C, Aromatic); δ = 128.01 (6C, Aromatic); δ = 126.56 (2C, Aromatic); δ = 114.92 (2C, Aromatic). (Figure 3.20)

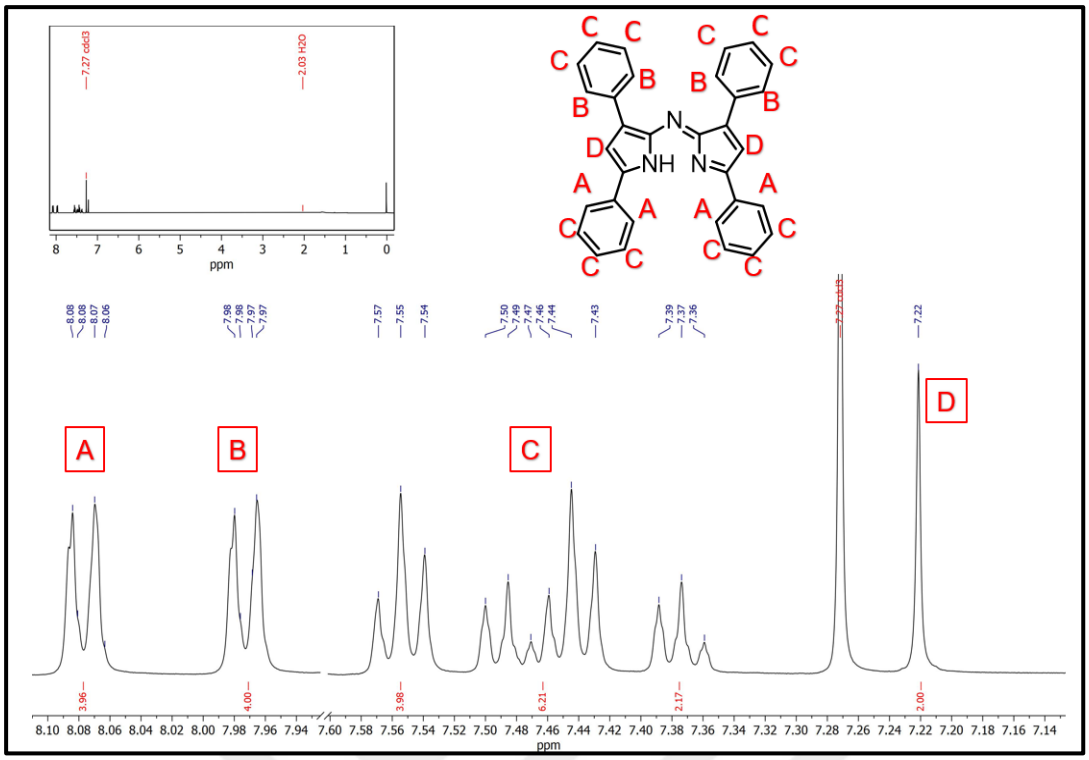

Figure 3.19 : (500 MHz, $CDCl_3$) ^1H – NMR of Compound 7.

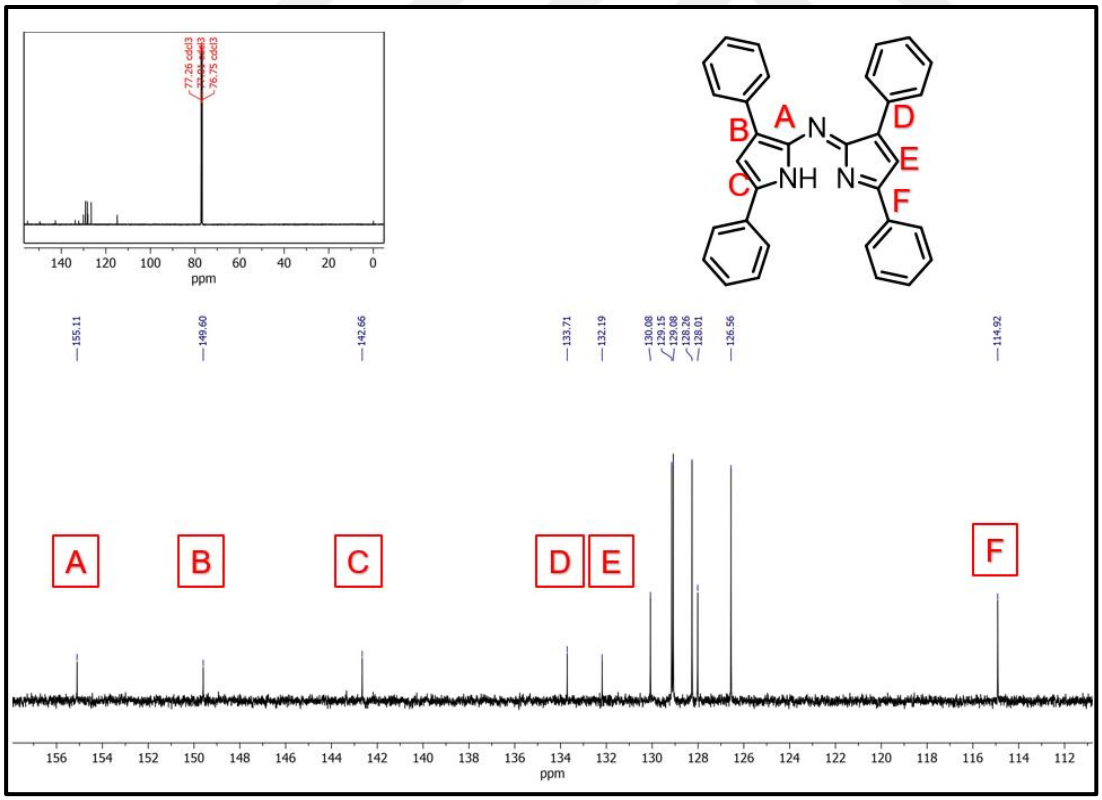

Figure 3.20 : (125 MHz, $CDCl_3$) ^{13}C – NMR of Compound 7.

3.3.2.4. Synthesis tetra phenyl of Aza-BODIPY (8)

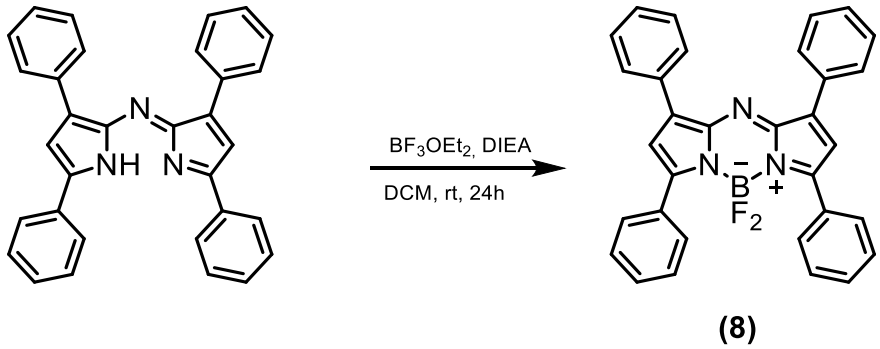

(8)

Figure 3.21 : Synthesis of tetra phenyl Aza-BODIPY (8).

1 g (0.0022 mol) of Compound 7 was taken and dissolved in 30 mL DCM in a 2 necked round bottom flask. 3.4 mL (0.0022 mol) of diisopropylethylamine was added to the resulting solution and the mixture was stirred for 10 min. Then, 3.67 mL (0.0025 mol) of BF_3 Et_2O was added to the solution. The reaction mixture was stirred under N_2 atmosphere for 24 h. At the end of the reaction period, 30 mL of EtOH was added to the mixture and DCM and EtOH were removed in a rotavapor. The resulting solid was washed with distilled water and purified by column chromatography using DCM/HEX (3:2). As a result, the formation of a blue-black solid was observed (Killoran et al., 2008). The reaction scheme of synthesis of Aza-BODIPY is given in Figure 3.21.

Yield observed: 91% (1 g product)

^{1}H – NMR (500 MHz, $CDCl_3$): δ = 8.10-8.04 (m, 8H, Aromatic H); δ = 7.52 – 7.43 (m, 12H, Aromatic H); δ = 7.06 (s, 2H, dipyrromethene). (Figure 3.22)

^{13}C – NMR (125 MHz, $CDCl_3$): δ = 155.57 (1C, dipyrromethene); δ = 145.61 (1C, dipyrromethene); δ = 144.22 (1C, dipyrromethene); δ = 132.31 (1C, Aromatic); δ = 131.60 (1C, dipyrromethene); δ = 130.93 (2C, Aromatic); δ = 129.54 (6C, Aromatic); δ = 129.40 (2C, Aromatic); δ = 128.66 (6C, Aromatic); δ = 128.62 (2C, Aromatic); δ = 119.15 (2C, Aromatic). (Figure 3.23)

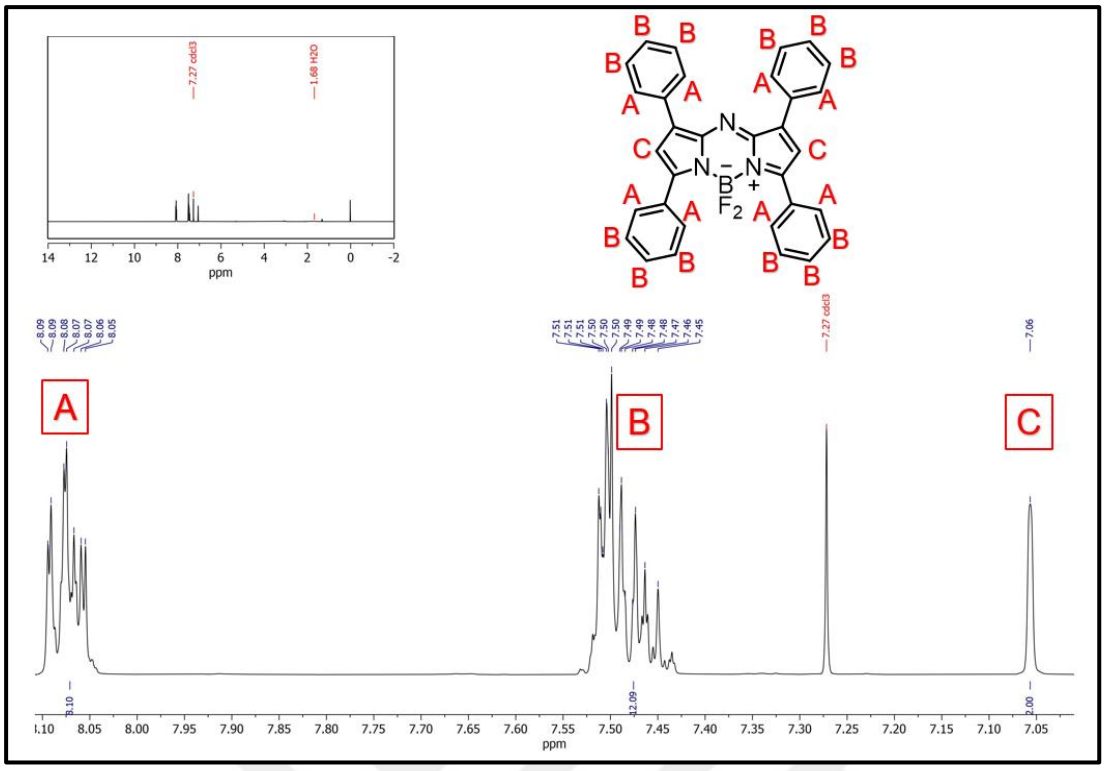

Figure 3.22 : (500 MHz, $CDCl_3$) ^{1}H – NMR of Compound 8.

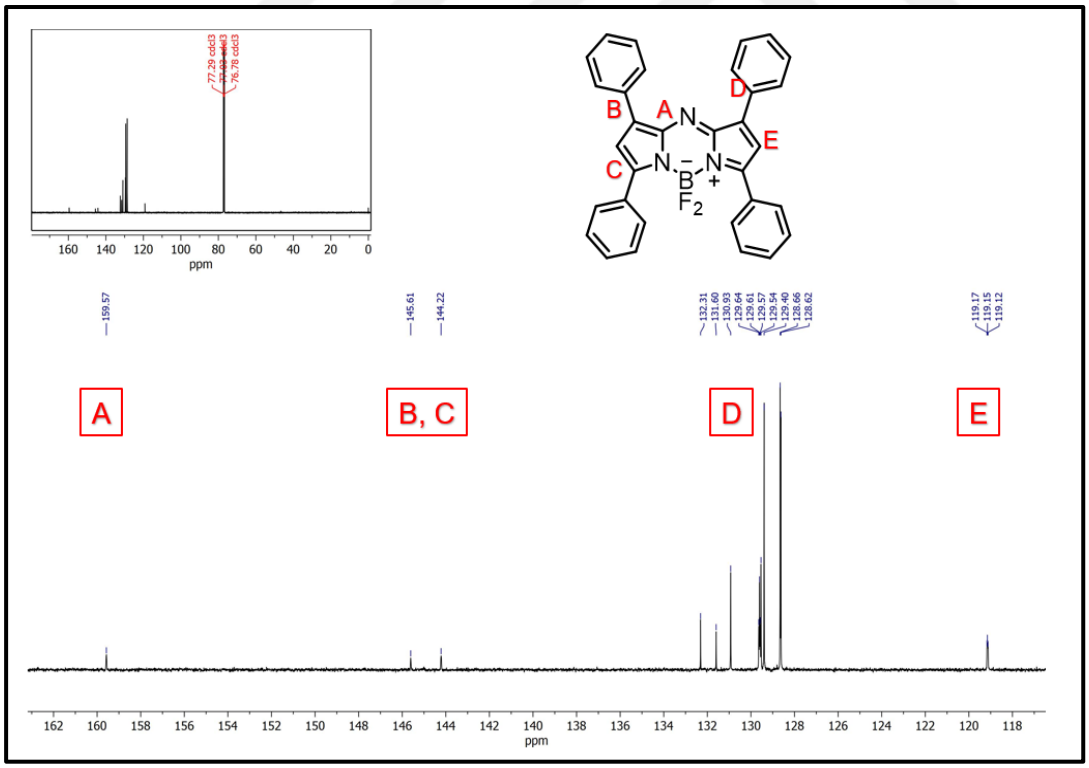

Figure 3.23 : (125 MHz, $CDCl_3$) ^{13}C – NMR of Compound 8.

3.3.3. Bromination of the tetra phenyl Aza-BODIPY (9)

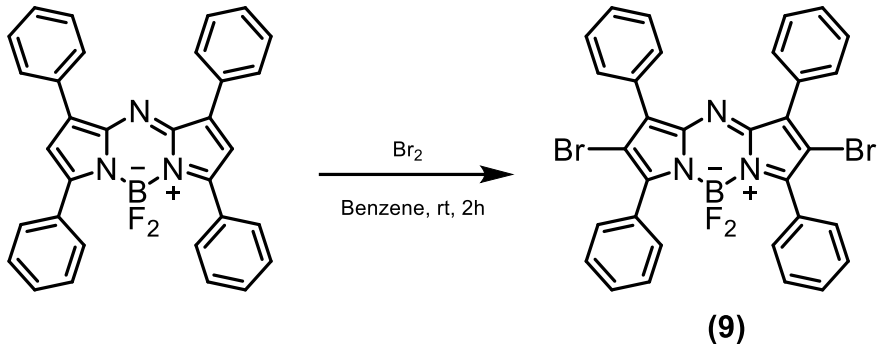

Figure 3.24 : Bromination of the tetra phenyl Aza-BODIPY (9).

0.1 g of Compound 8 (0.0002 mol) was dissolved in 10 mL of benzene in a 2 necked round bottom flask. 0.032 mL of bromine (0.0006 mol) was added to the resulting reaction mixture. The reaction mixture was stirred at room temperature for 2 hours and the completion of the reaction was observed by TLC. Benzene was then removed using a rotary evaporator and Compound 9 was obtained (Gorman et al., 2004). The reaction scheme of bromination of the Aza-BODIPY is given in Figure 3.24.

Yield observed: 92% (0.12 g product)

^{1}H – NMR (500 MHz, $CDCl_3$): δ = 7.91 – 7.86 (m, 4H, Aromatic H); δ = 7.74 (dd, *J* = 7.6, 1.9 Hz, 4H, Aromatic H); δ = 7.51 – 7.43 (m, 12H, Aromatic H). (Figure 3.25)

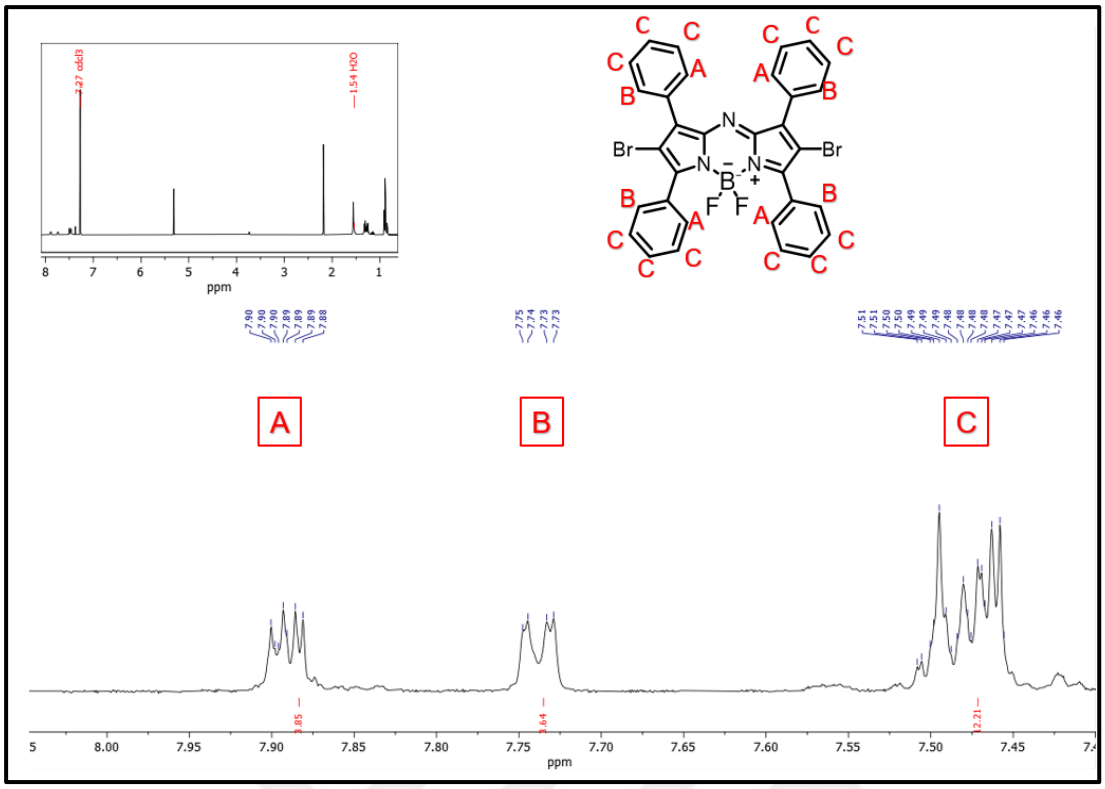

Figure 3.25 : (500 MHz, $CDCl_3$) ^1H – NMR of Compound 9.

3.3.4. Formylation of the tetra phenyl Aza-BODIPY (10)

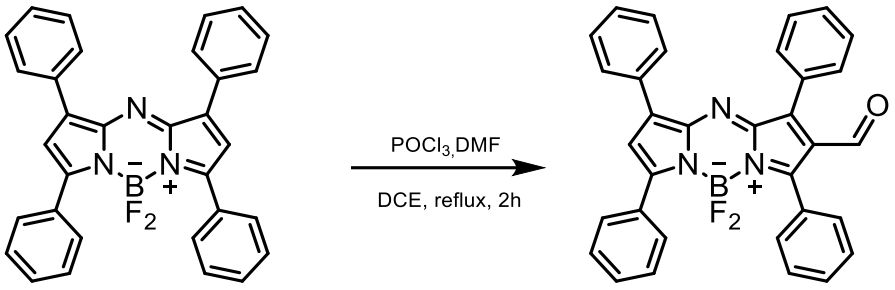

(10)

Figure 3.26 : Formylation of the tetra phenyl Aza-BODIPY (10).

6 mL of DMF (0.077 mol) and 6 mL of $POCl_3$ (0.064 mol) in equal volumes were stirred under nitrogen (N_2) atmosphere at low temperature. After stirring for 30 min, the mixture was brought to room temperature. Then, 0.18 g of Compound 8 (0.0036 mol) dissolved in 15 mL of DCE was added to the reaction medium and the mixture was stirred under N_2 atmosphere for 5 min. The reaction mixture was then stirred at 70 °C for 2 h. After the reaction was completed, the mixture was cooled to room temperature and kept in an ice bath. For neutralization, 250 mL of saturated $NaHCO_3$

solution was added to the mixture and stirred for 1 h. Finally, Compound 10 was purified by column chromatography using Petroleum Ether/EtOAc (1:1) solvent system (Jiao et al., 2009). The reaction scheme of formylation of the Aza-BODIPY is given in Figure 3.26.

Yield observed: 89% (0.16 g product)

^{1}H – NMR (500 MHz, $CDCl_3$): δ = 9.78 (s, 1H, Aldehyde); δ = 8.08 (d, *J* = 7.8 Hz, 4H, Aromatic H); δ = 7.87 (s, 2H, Aromatic H); δ = 7.74 (d, *J* = 7.8 Hz, 2H, Aromatic H); δ = 7.53 (q, *J* = 9.4, 8.4 Hz, 13H, Aromatic H); δ = 7.23 (s, 1H, dipyrromethene). (Figure 3.26)

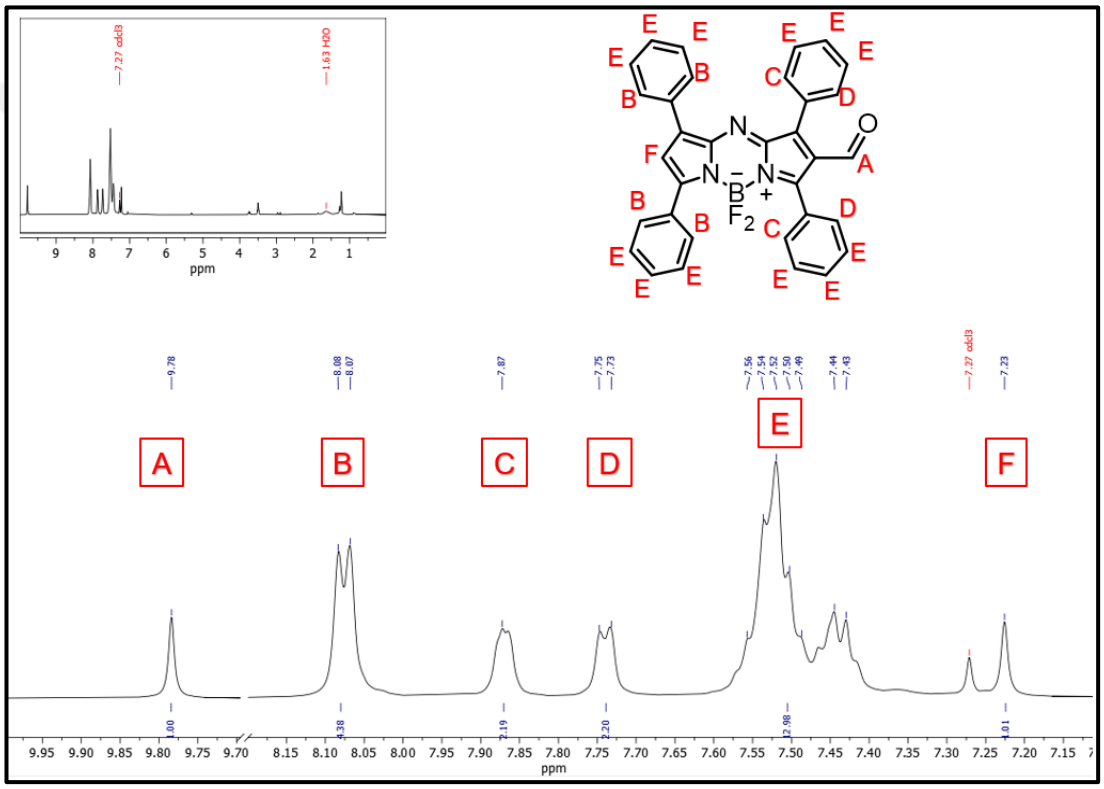

Figure 3.27 : (500 MHz, $CDCl_3$) ^{1}H – NMR of Compound 10.

3.3.5. Synthesis of Aza-BODIPY containing PGMA-*b*-OEGMA polymeric system

Aza-BODIPY carrier polymeric system was synthesized with RAFT polymerization system to control the PDI (Polydispersity Index) chain length. The synthesis of the polymeric system consists of three main parts.

1. Synthesis stage of PGMA macro-CTA

2. Synthesis of PGMA-*b*-OEGMA

3. Attachment of Aza-BODIPY (Compound 4) molecule to the obtained PGMA-*b*-OEGMA polymer by epoxy opening reaction

3.3.5.1. Synthesis of PGMA macro-CTA (11)

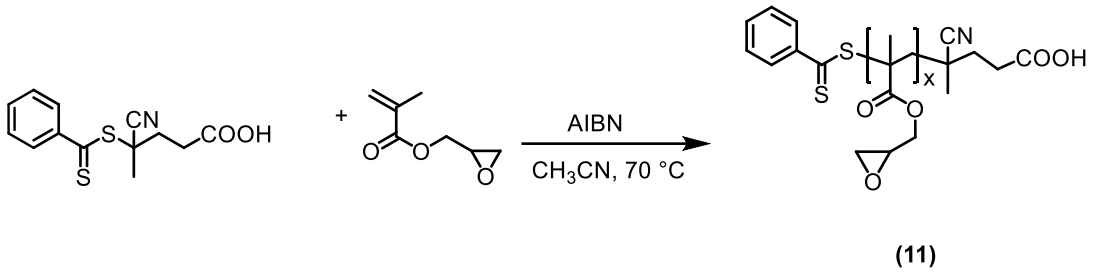

(11)

Figure 3.28 : Synthesis of PGMA macro-CTA (11).

Glycidyl methacrylate (GMA) which was first purified to remove the inhibitor it contained, For this purpose, aluminum oxide 90 active neutral was used, azobisisobutyronitrile (AIBN), cyano-4-(phenylcarbothiolthio)pentanoic acid (CPADB) and acetonitrile (ACN) were used for the synthesis of PGMA macro-CTA. In this process, GMA served as monomer, CPADB as RAFT agent and AIBN as polymerization initiator, while ACN was used as solvent. Excluding solvent, the GMA:CTA:AIBN molar ratio was determined as 1:0.02:0.0025. For synthesis, 2.85 g GMA (0.02 mol), 0.112 g CPADB (0.0004 mol) and 0.0082 g AIBN (0.00005 mol) were dissolved in 25 mL acetonitrile (ACN) in a bottom flask. The mixture was dissolved under N_2 gas and purged from ambient air by nitrogen flow in an ice bath for 30 min. Then, the reaction medium was completely filled with N_2 gas and the bottom flask was sealed. The reaction was started at 70 °C and continued for 8 h. At the end of the period, the reaction medium was suddenly cooled and the obtained polymer was precipitated in a mixture of petroleum ether and diethyl ether (total 100 mL) at a 1:1 volume/volume ratio. Finally, the product was purified by drying under vacuum (Karagoz et al., 2014). The reaction scheme of synthesis of PGMA macro-CTA is given in Figure 3.28.

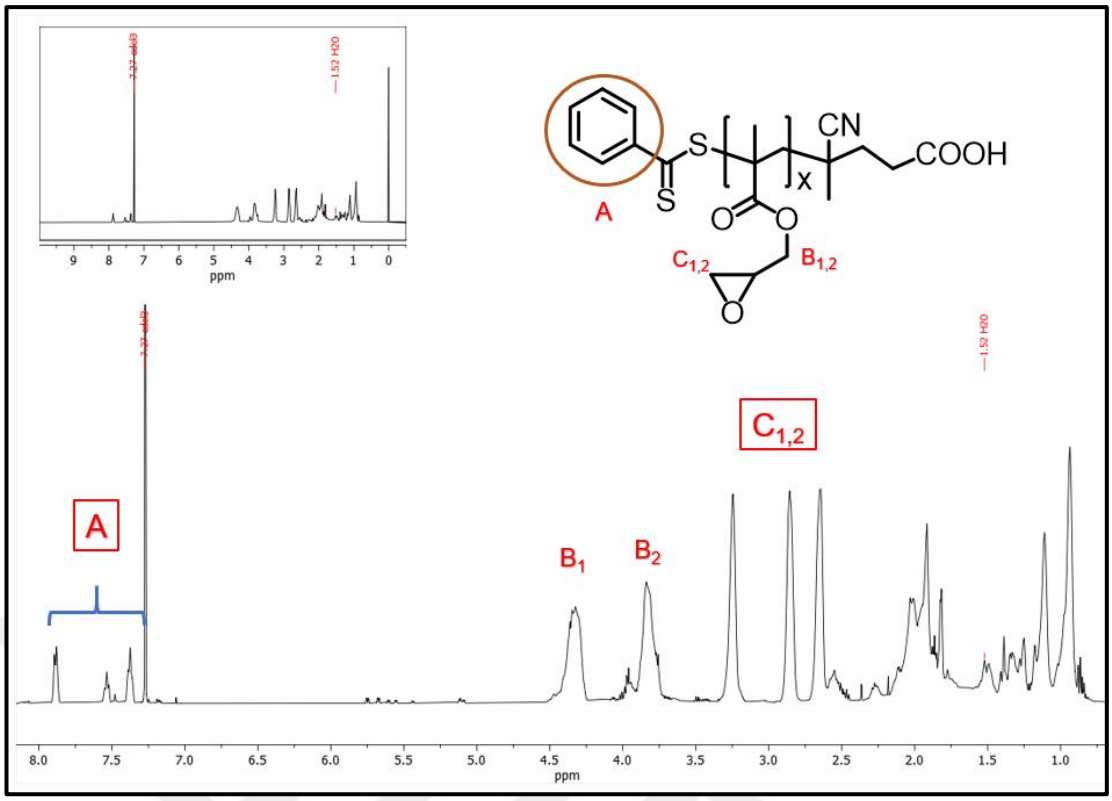

Figure 3.29 : (500 MHz, $CDCl_3$) ^1H – NMR of Compound 11.

3.3.5.2. Synthesis of PGMA-*b*-OEGMA (12)

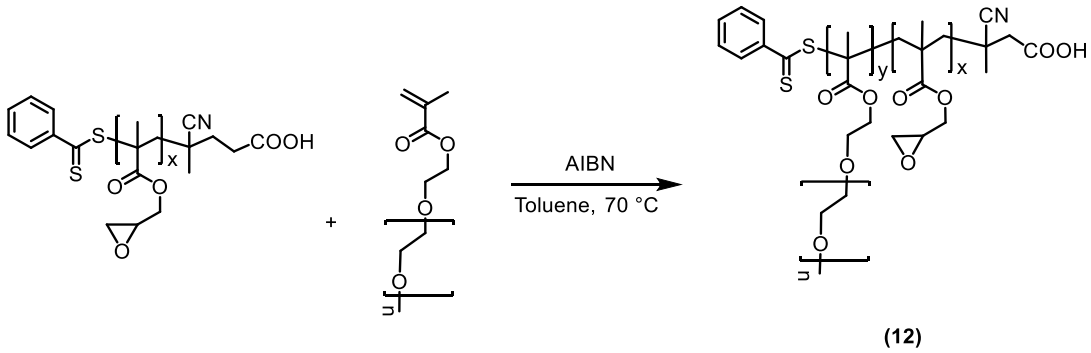

Figure 3.30 : Synthesis of PGMA-*b*-OEGMA (12).

Oligo(ethylene glycol) methacrylate (OEGMA) was used for synthesis of PGMA-*b*-OEGMA. PGMA-*b*-OEGMA was synthesized by RAFT polymerization. GMA CTA:OEGMA:AIBN = 1:20:2:0.4 ratio was preferred for the synthesis. For synthesis, 1.235 g PGMA CTA (10×10^{-5}mol), 0.288 g OEGMA (2×10^{-3} mol) and 0.0066 g AIBN (4×10^{-5} mol) were dissolved in 5 mL toluene in a bottom flask. The mixture was dissolved under N_2 gas and purged from ambient air by nitrogen flow in an ice bath

for 30 min. Then, the reaction medium was completely filled with N_2 gas and the bottom flask was sealed. The reaction was started at 70 °C and continued for overnight. At the end of the period, the reaction medium was suddenly cooled and the obtained polymer was precipitated in a mixture of petroleum ether and hexane (total 10 mL) at a 1:1 volume/volume ratio. Finally, the product was purified by drying under vacuum. The reaction scheme of synthesis of PGMA-*b*-OEGMA is given in Figure 3.30.

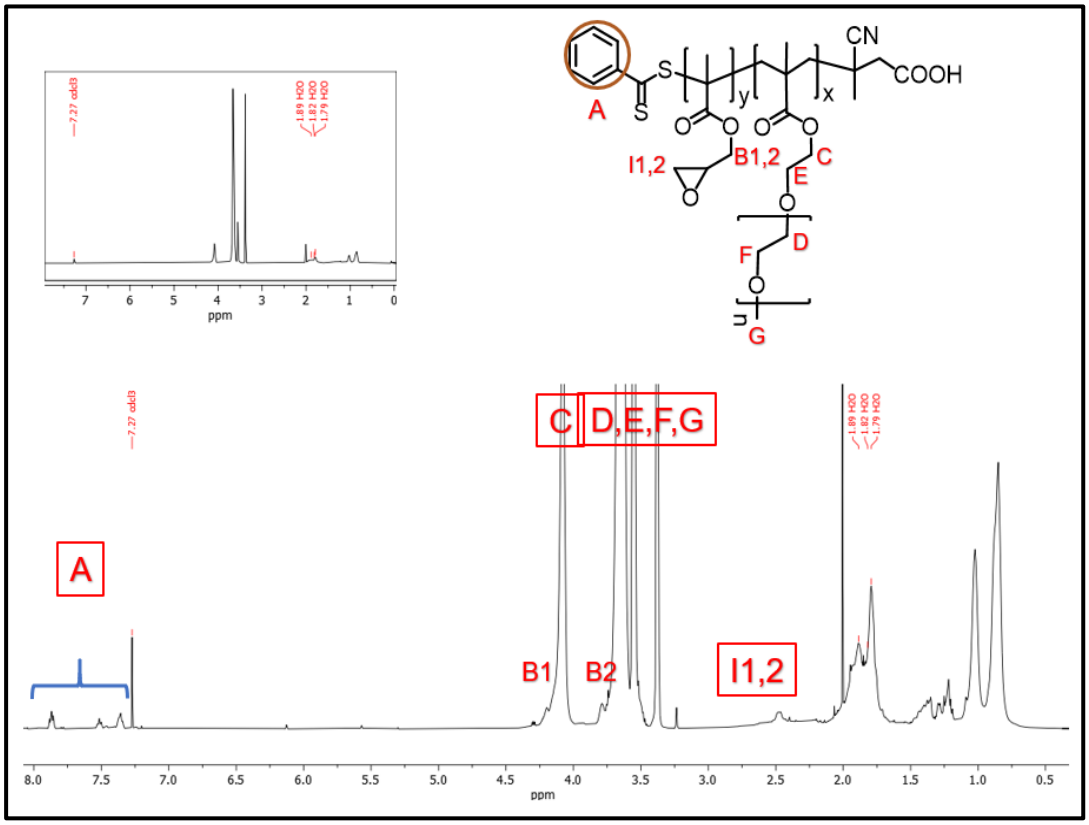

Figure 3.31 : (500 MHz, $CDCl_3$) ^1H – NMR of Compound 12.

3.3.5.3. Synthesis of PGMA-*b*-OEGMA_Aza-BODIPY (13)

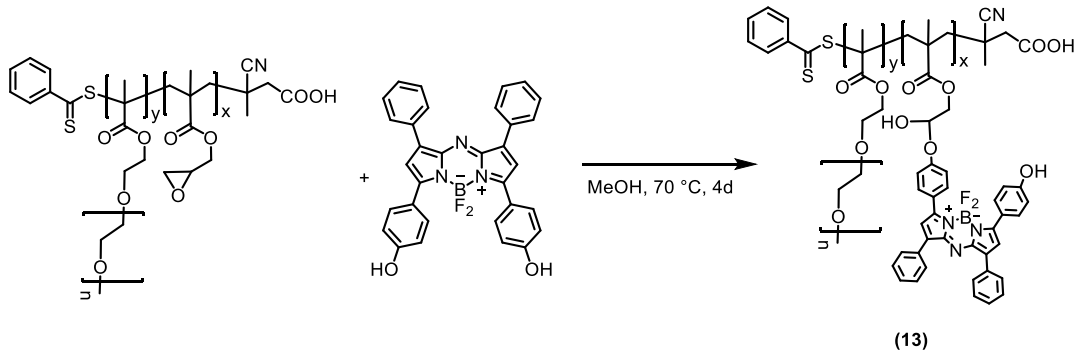

Figure 3.32 : Synthesis of PGMA-*b*-OEGMA_Aza-BODIPY (13).

Synthesis of PGMA-*b*-OEGMA_Aza-BODIPY polymer PGMA-*b*-OEGMA:Aza-BODIPY = 1:20. For this, 0.912 g (6×10^{-5} mol) of PGMA-*b*-OEGMA polymer and 6.3 g (12×10^{-4} mol) of Compound 4 were taken and stirred in MeOH for 4 days. After cooling, the reaction mixture was dried in a freeze dryer and filtered with distilled water using a dialysis membrane with a 1000 cut-off (Chung et al., 2015). The reaction scheme of synthesis of PGMA-*b*-OEGMA_Aza-BODIPY is given in Figure 3.32.

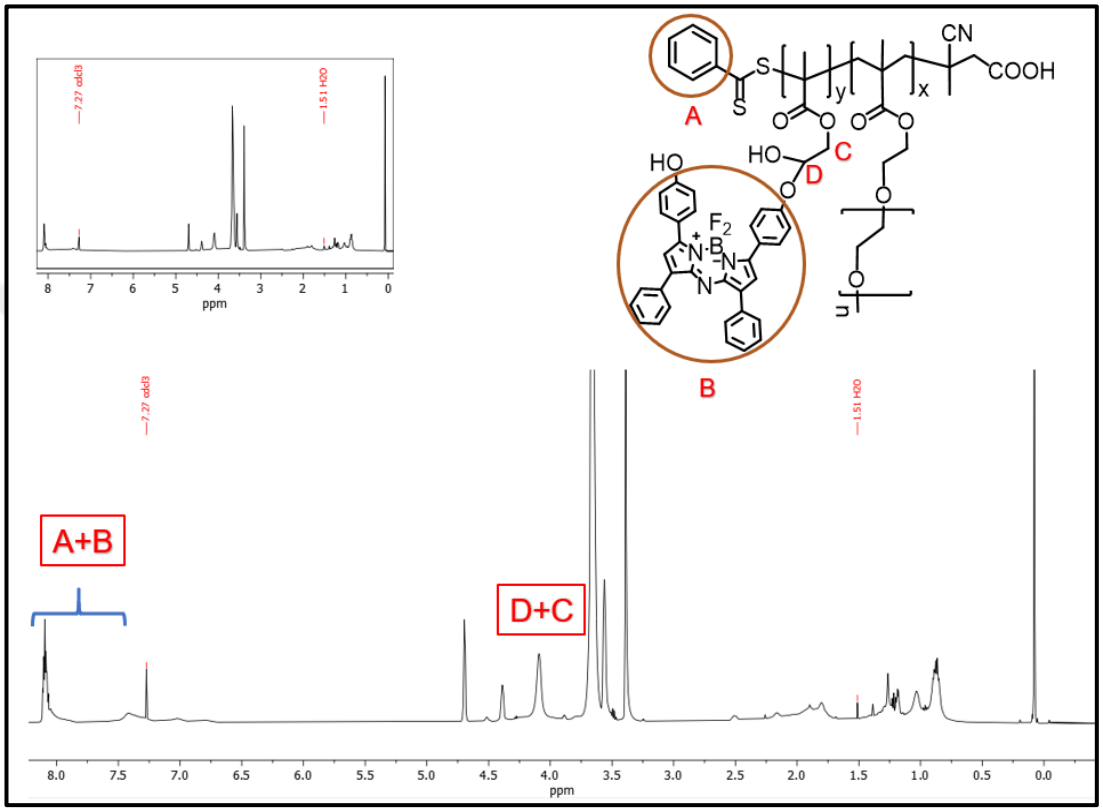

Figure 3.33 : (500 MHz, $CDCl_3$) ^1H – NMR of Compound 13.

3.3.6. Synthesis of Aza-BODIPY-C4P Molecule

3.3.6.1. Synthesis of compound 4 TBA salt (14)

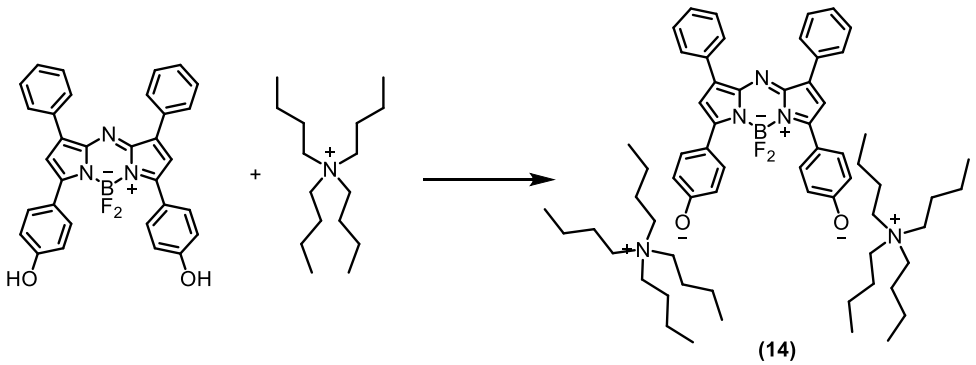

Figure 3.34 : Synthesis of Compound 4 TBA Salt (14).

A 0.6 mmol MeOH solution of Compound 4 was prepared and reacted with tetrabutylammonium hydroxide in 1M MeOH at twice ratio. Following that, the reaction mixture was stirred for two hours at room temperature. Following methanol evaporation, the products were triturated in diethyl ether and vacuum-dried at 40 °C. The reaction scheme of synthesis of Compound 4 TBA Salt is given in Figure 3.34.

^{1}H – NMR (500 MHz, $CDCl_3$): δ = 9.01 (s, Pyrrole NH,); δ = 8.06 (dd, *J* = 14.3, 8.0 Hz, Aromatic H, 8H); δ = 7.46 (dt, *J* = 15.2, 7.3 Hz, 4H, Aromatic H); 7.08 – 6.91 (m, 8H, Aromatic H). (Figure 3.35)

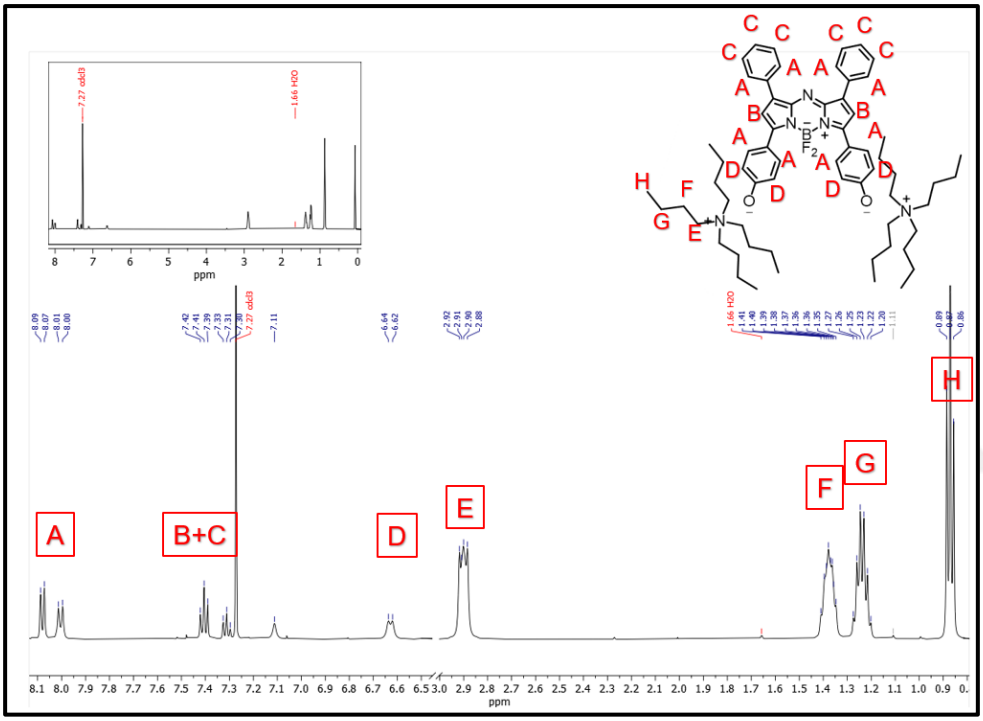

Figure 3.35 : (500 MHz, $CDCl_3$) ^{1}H – NMR of Compound 14.

3.3.6.2. Synthesis of Compound 4-Calix[4]pyrrole molecule (15)

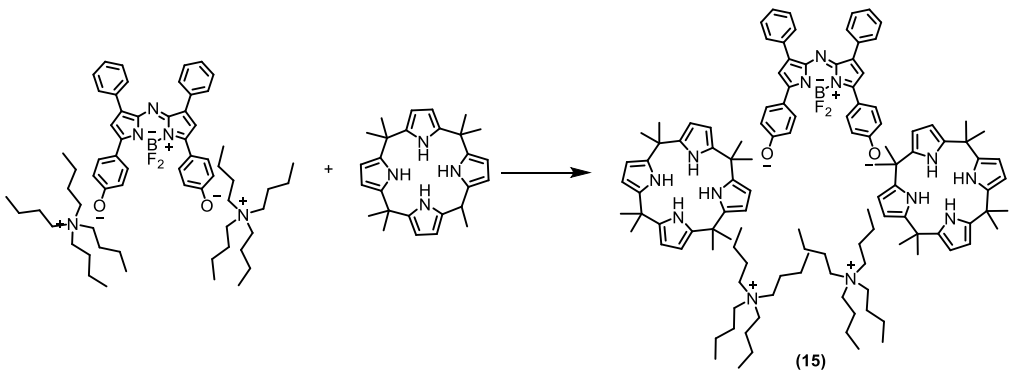

Figure 3.36 : Synthesis of Compound 4-Calix[4]pyrrole molecule (15).

Compound 4 TBA salt solution was prepared in 0.6 mmol water and twice this amount of equal amount of Calix[4]pyrrole was reacted. Following that, the reaction mixture was stirred for two hours at room temperature. Following methanol evaporation, the products were triturated in diethyl ether and vacuum-dried at 40 °C. (Figure 3.37)

^{1}H – NMR (500 MHz, $CDCl_3$): δ = 8.04 (dd, *J* = 37.8, 8.2 Hz, Aromatic H, 4H); δ = 7.36 (dt, *J* = 46.8, 7.5 Hz, Aromatic H, 8H); δ = 6.63 (d, *J* = 8.7 Hz, 4H, Aromatic H); δ = 2.94 – 2.87 (m, 8H, N-CH); δ = 1.43 – 1.33 (m, 8H, N-CH); δ = 1.24 (h, *J* = 7.2 Hz, 8H, N-CH); δ = 0.87 (t, *J* = 7.3 Hz, 8H, N-CH).

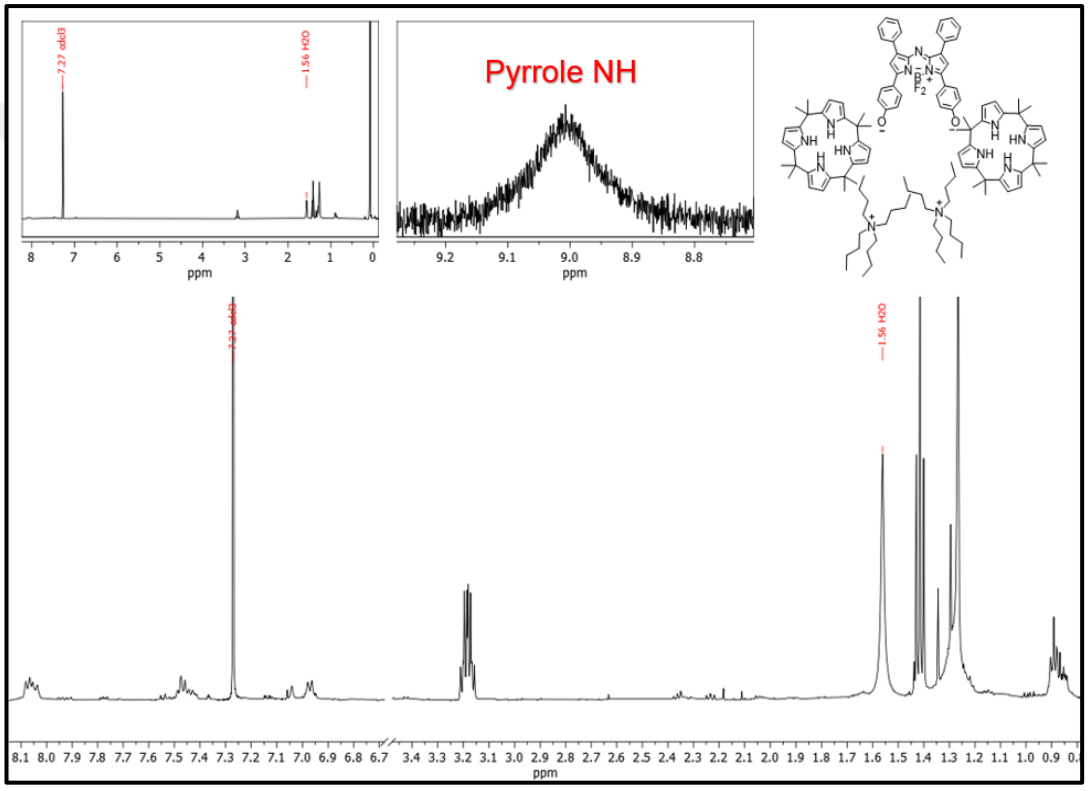

Figure 3.37 : (500 MHz, $CDCl_3$) ^{1}H – NMR of Compound 15.

4. RESULTS AND DISCUSSION

In this thesis, Aza-BODIPY compounds were synthesized and structurally modified to explore their potential in various application areas. The performance and behavior of each compound were evaluated within the scope of its specific use, and the results were interpreted accordingly, providing insight into the structure–property relationships influenced by different substituents.

4.1. Comparative Study of Hydroxy-, Bromo-, and Formyl-Substituted Aza-BODIPY Dyes for Detection of Nitroaromatic Compounds

Aza-BODIPY compounds are generally studied as sensors and their sensor properties against NACs have also been investigated in the literature (Sadikogullari et al., 2023). The unique part of this study is the investigation of the effect of EDG and EWG groups on this sensor application of Aza-BODIPY. For this purpose, Compounds 4, 9 and 10, which were synthesized and characterized within the scope of the thesis, were preferred for analysis. For the synthesis of Compound 4, firstly 4′ – hydroxy – *E* – chalcone was synthesized and the synthesis of the material was proven by NMR characterizations. (Figure 3.2, Figure 3.3) After that, Michael addition of to 4′ – hydroxy – E – chalcone has been done and the synthesis of the material was proven by NMR characterizations. (Figure 3.5, Figure 3.6) *p* – OH Substituted Aza-dipyrromethene was synthesized and its synthesis was proven by NMR characterizations. (Figure 3.8, Figure 3.9) Finally, the synthesis of Compound 4 was proven by NMR characterizations. (Figure 3.11, Figure 3.12, Figure 3.13) Before formylation and bromination processes, aza-BODIPY compound was synthesized. Synthesis of *E*-chalcone compound was proven by NMR technique. (Figure 3.15, Figure 3.16) Michael addition of NO_2 to *E*-chalcone compound was proven by NMR technique. (Figure 3.18, Figure 3.19) Then, synthesis of aza-dipyrromethene compound was proven by NMR characterization (Figure 3.21, Figure 3.22) and synthesis of Compound 8 was proven by NMR characterization. (Figure 3.24, Figure 3.25) Then, bromination synthesis of Compound 8 was made and Compound 9 was

synthesized and characterized by NMR. (Figure 3.27) Compound 8 was formylated and Compound 10 was synthesized. It was characterized by NMR technique. (Figure 3.29)

In order to compare the experimental results, each compound was prepared as 5 μM in DMSO and the analyte materials (Trinitrophenol, Trinitrotoluene, Dinitrotoluene, Mononitrotoluene, Nitrobenzene, Nitromethane, Nitroethane and Nitropropane) were prepared as 500 μM and gradually added to the solution in 2.5 μL aliquots per application. Also, TNP was prepared as 500 μM in water and used in titration. All fluorescence measurements were taken at room temperature, and the maximum wavelength was found to be 746 nm for Compound 4, 677 nm for Compound 9, and 662 nm for Compound 10. In order to study the optical detection of nitro compounds using fluorescence quenching of Aza-BODIPY, fluorescence titrations were performed at least three times. In order to determine LOD, the standard deviation (σ_{10}) was computed from the intensity of the naked sensor (I_0) in many fluorescence measurements.

Initially, Compound 4 was tested against, five different nitroaromatic compounds. According to results, when commercially available nitroaromatic molecules (TNT, DNT and MNT) were examined, similar K_{sv} results were obtained around $1\times10^5\ M^{-1}$. This similarity can be attributed to Compound 4 being highly electron-rich due to the presence of hydroxyl groups, enabling strong interactions with electron-deficient nitroaromatic compounds, such that the degree of electron deficiency among these nitroaromatics becomes negligible in determining the interaction strength. Interestingly, binding constant toward nitroalifatics observed to be higher than any nitroaromatic compound which can be rationalized by hydrogen bonding. The phenolic hydroxyl groups in Compound 4 enable hydrogen bonding with the acidic proton of the nitroaliphatic molecule, thereby potentially facilitating fluorescence quenching. When all the results are considered, addition of hydroxy group increasses affinity to nitroaromatic compounds but also decreases of the selectivity towards nitroaromatics. It was observed that Compound 4 gave the highest K_{sv} value to TNP dissolved in water, which can be attributed to reasons mentioned above. TNP has a more acidic structure than other nitroaromatics due to its phenolic hydroxyl group. This situation caused Compound 4, which has an electron-rich structure in particular, to exhibit strong π–π stacking and acid-base interaction. The –OH group of TNP can act as a hydrogen bond donor and the hydroxyl groups of Compound 4 increased the

binding constant. When, quenching efficiencies are considered 60-80% quenching was observed in all tested nitro compounds, indicating low selectivity except for TNP which shows total quenching when prepared in water. This situation is thought to result from the low water solubility of Aza-BODIPY molecules, which may have affected the aqueous quenching efficiency; however, this difference was not considered significant. (Figure 4.1, Figure 4.2, Figure 4.3 and Table 4.1)

Table 4.1 : K_{sv} and QE (quencher efficiency) results obtained by titration of Compound 4 (5 μM) with 500 μM nitro compounds.

Nitro Compound (in solvent)	**K_{sv} (M^{-1})**	**QE**
TNP (in water)	2.0×10^6; 7.8×10^6	97%
TNP (in DMSO)	4.1×10^5	66%
TNT (in DMSO)	7.8×10^5; 2.8×10^5	79%
DNT (in DMSO)	1.3×10^5	52%
MNT (in DMSO)	2.3×10^5	64%
NB (in DMSO)	1.8×10^5	59%
NM (in DMSO)	2.4×10^5	67%
NE (in DMSO)	5.4×10^5	81%

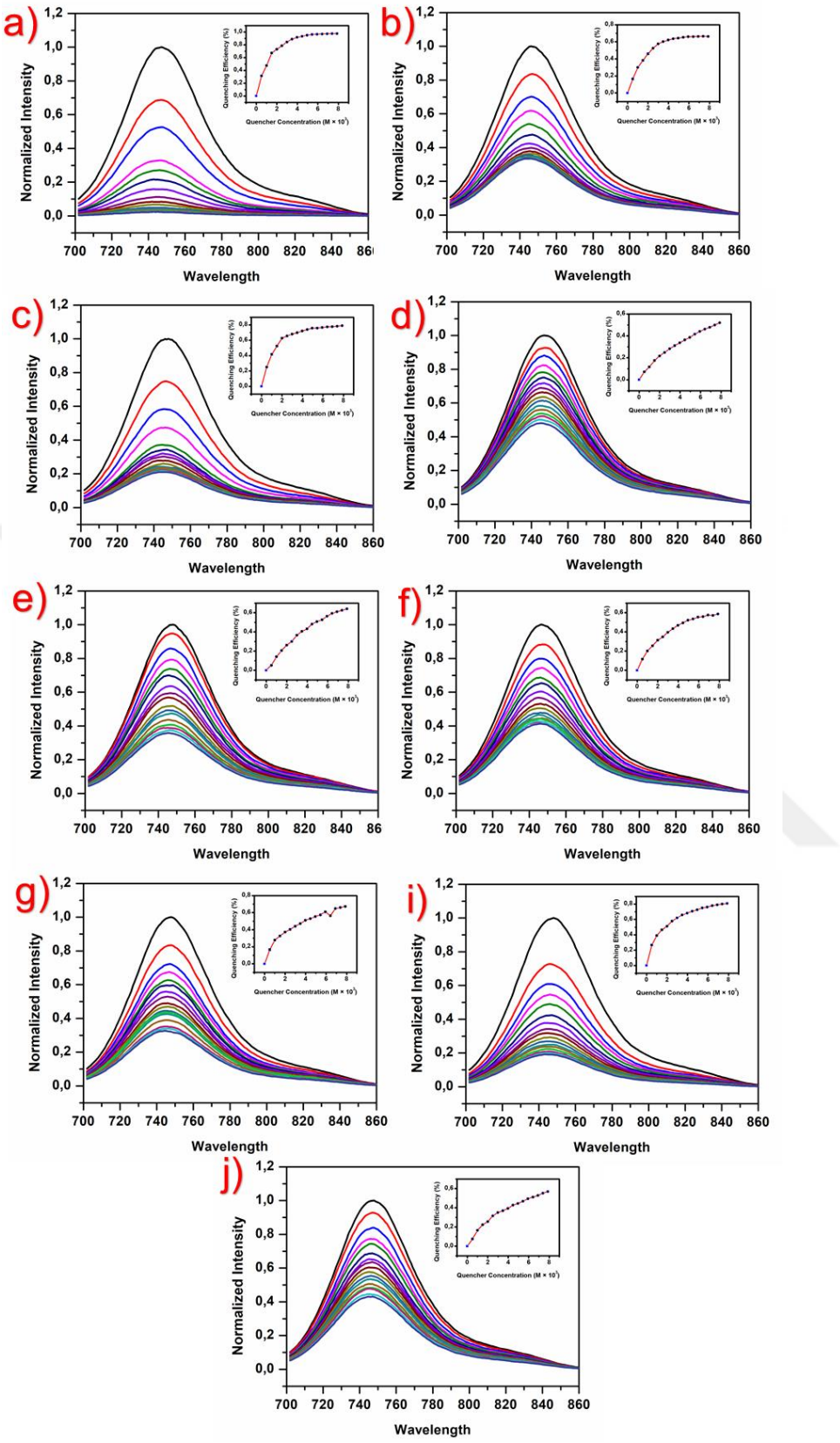

Figure 4.1 : Fluorescence quenching spectra of Compound 4 titrations in DMSO using TNP in water (a), TNP in DMSO (b), TNT in DMSO (c), DNT in DMSO (d), MNT in DMSO (e), NB in DMSO (f), NE in DMSO (g), NM in DMSO (i) and NP in DMSO (j). Quencher efficiencies were also shown.

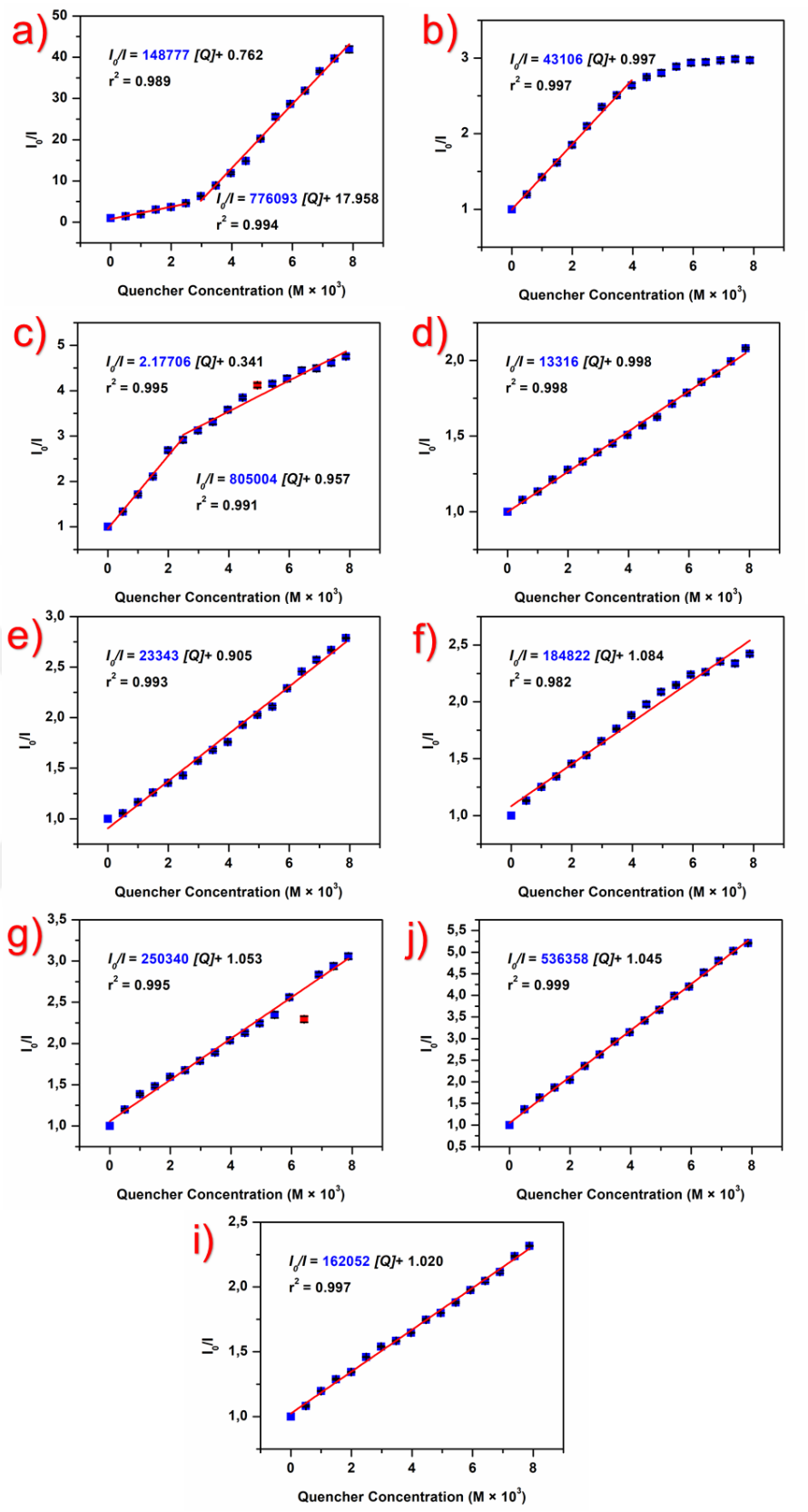

Figure 4.2 : Stern−Volmer plots of Compound 4 titrations in DMSO using TNP in water (a), TNP in DMSO (b), TNT in DMSO (c), DNT in DMSO (d), MNT in DMSO (e), NB in DMSO (f), NE in DMSO (g), NM in DMSO (i) and NP in DMSO (j).

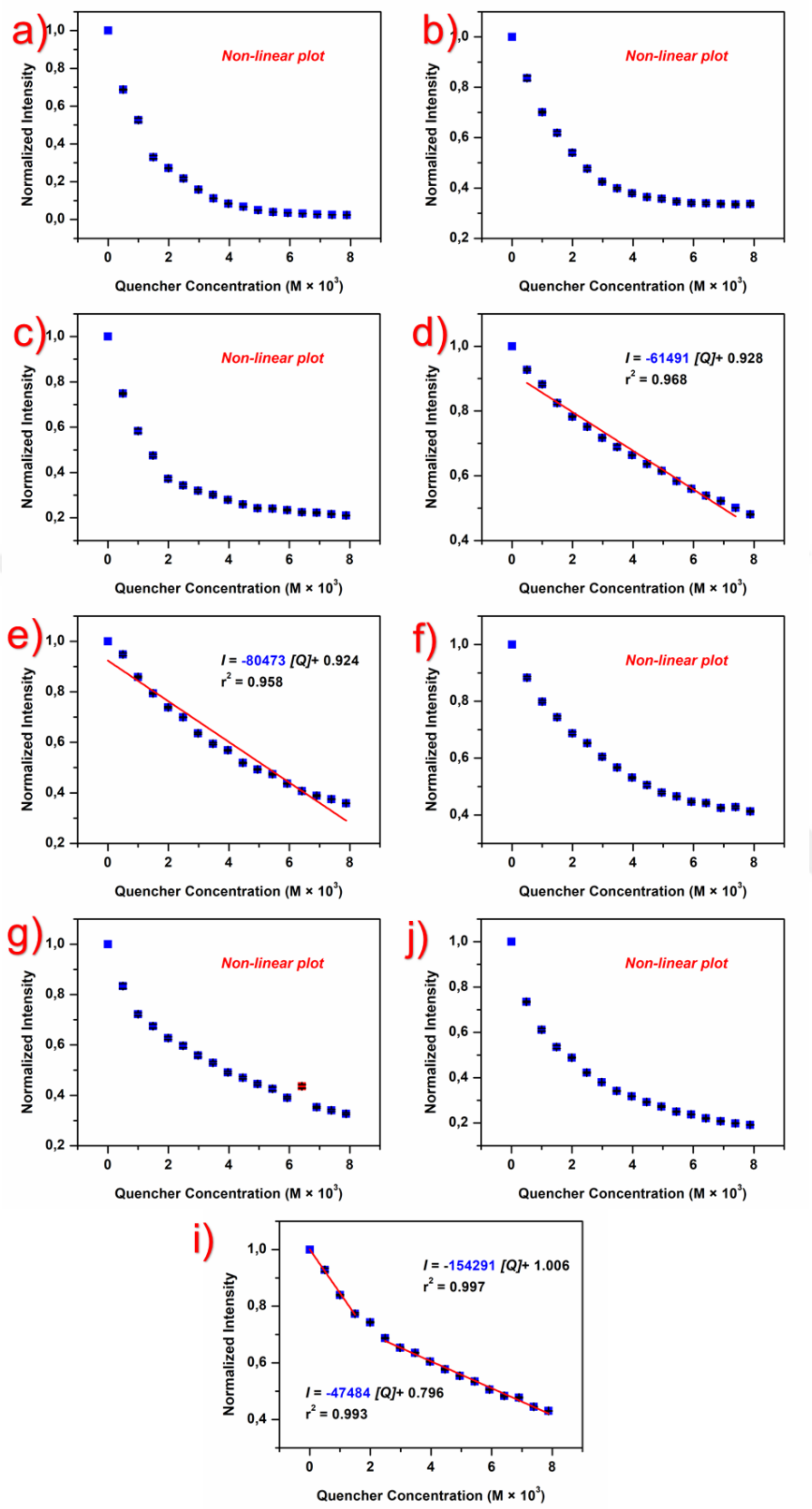

Figure 4.3 : Limit of detection spectra of Compound 4 titrations in DMSO using TNP in water (a), TNP in DMSO (b), TNT in DMSO (c), DNT in DMSO (d), MNT in DMSO (e), NB in DMSO (f), NE in DMSO (g), NM in DMSO (i) and NP in DMSO (j).

Compound 9 was first evaluated in comparison to five distinct nitroaromatic chemicals. Results showed that identical K_{sv} values of about 1×10^4 M^{-1} were achieved when commercially accessible nitroaromatic compounds (TNP, TNT, DNT and MNT) were investigated. Unlike Compound 4, one of the reasons why the results of the titrations with different nitro compounds in Compound 9 give similar Ksv values is that this compound does not contain a group such as hydroxy that can make hydrogen bonds. On the other hand, K_{sv} values were lower compared to the titrations performed with Compound 9. The hydroxyl groups of Compound 4 are EDG, which increased the electron richness of the Aza-BODIPY ring and had a fluorescence quenching with high K_{sv} with electron-poor nitro compounds. Bromine groups are EWGs and they reduced the electron density of the Aza-BODIPY ring and caused low K_{sv} values to be observed (Zhang et al., 2017). Interestingly, Compound 9 showed a similar response to nitroaromatics and nitroaliphatics. Aza-BODIPY usually contains an electron-rich π-system, which triggers the PET (photoinduced electron transfer) mechanism caused by nitro groups, and since Compound 9 and nitro compounds have similar electron acceptor capacities, the K_{sv}'s were observed at similar values of about 1×10^4. Bromine atom affected the quenching *via* phosphorescence or triplet state transfer by increasing the intersystem crossing (ISC) due to both electron-withdrawing (inductive) and heavy atom effect. When, quenching efficiencies are considered 8-20%, quenching was observed in all tested nitro compounds, indicating the addition of bromine group on the Aza-BODIPY molecule, decreases the electron-richness of the system. This situation caused because of the reducing interaction of Compound 9 with electron-poor nitro compounds. Considering all these results, it can be concluded that EWGs reduced the electron density on the ring and limited their selectivity in a nitroaromatic sensor application. (Figure 4.4, Figure 4.5, Figure 4.6 and Table 4.2)

Table 4.2: K_{sv} and QE (quencher efficiency) results obtained by titration of Compound 9 (5 μM) with 500 μM nitro compounds.

Nitro Compound (in solvent)	K_{sv} (M^{-1})	QE
TNP (in water)	3.3×10^4	21%
TNP (in DMSO)	1.0×10^4	8%
TNT (in DMSO)	2.7×10^4	18%
DNT (in DMSO)	2.6×10^4	18%
MNT (in DMSO)	1.9×10^4	13%
NB (in DMSO)	3.0×10^4	20%
NM (in DMSO)	1.8×10^4	12%
NE (in DMSO)	2.9×10^4	20%

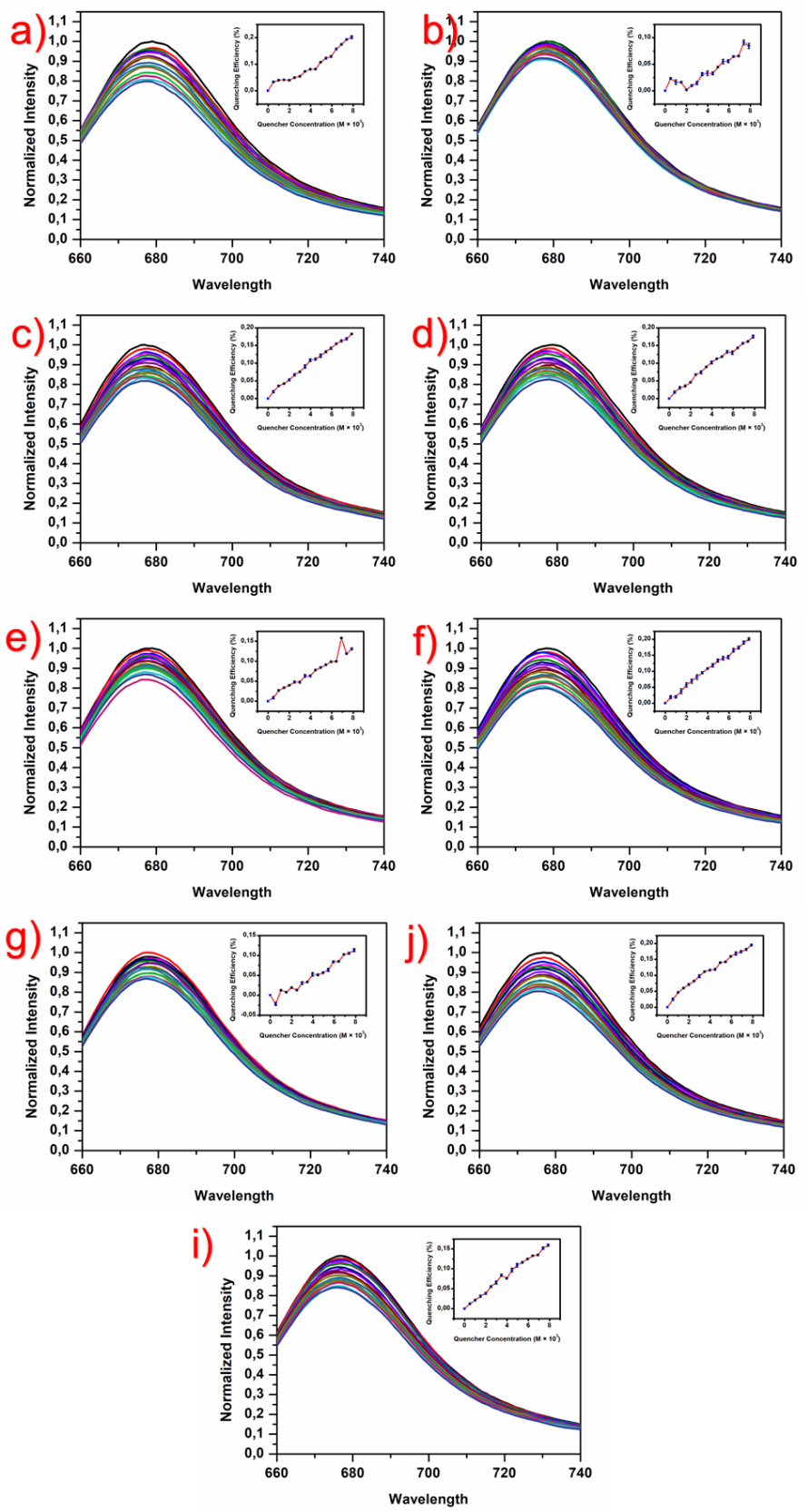

Figure 4.4 : Fluorescence quenching spectra of Compound 9 titrations in DMSO using TNP in water (a), TNP in DMSO (b), TNT in DMSO (c), DNT in DMSO (d), MNT in DMSO (e), NB in DMSO (f), NE in DMSO (g), NM in DMSO (i) and NP in DMSO (j). Quencher efficiencies were also shown.

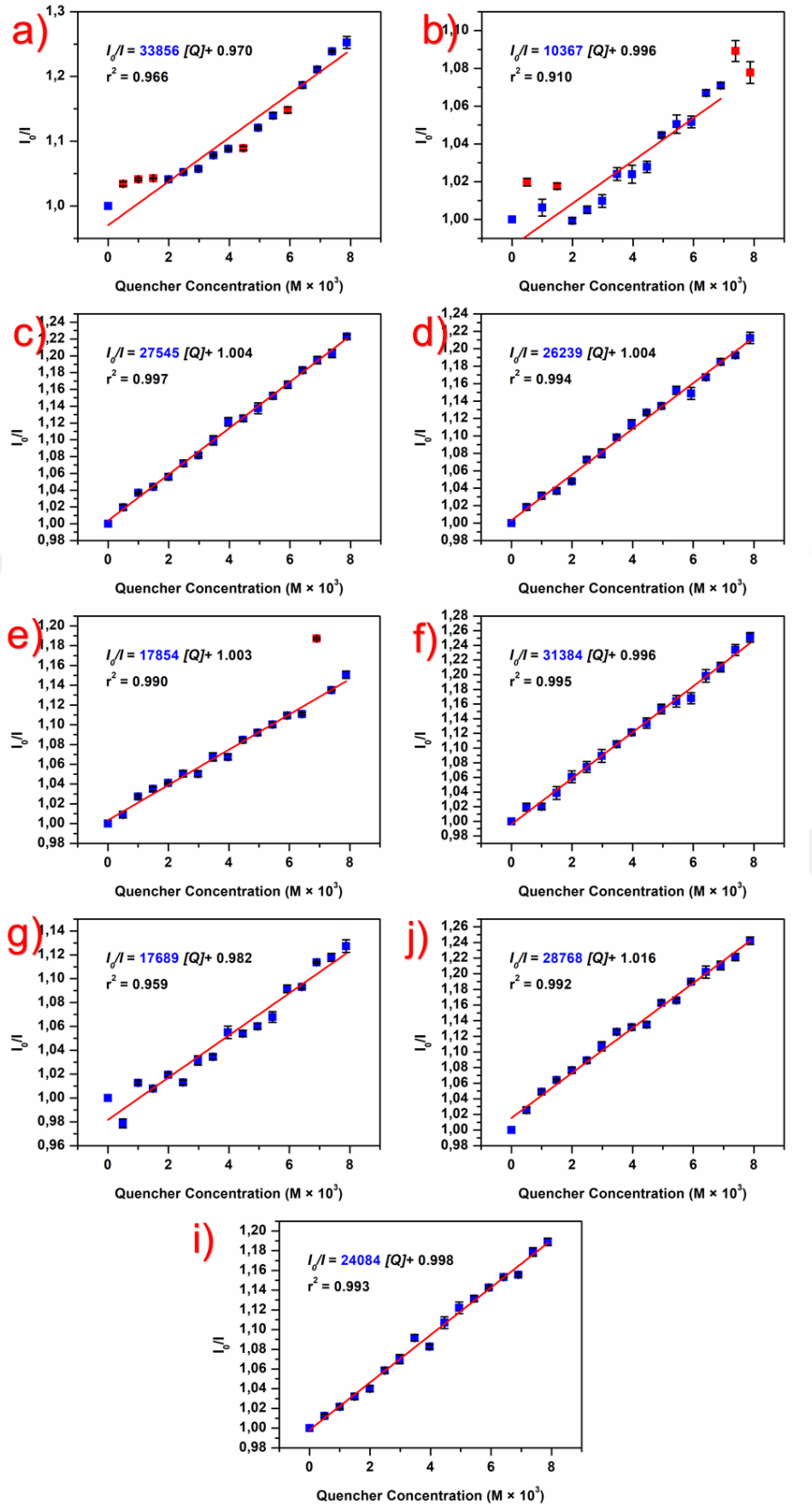

Figure 4.5 : Stern−Volmer plots of Compound 9 titrations in DMSO using TNP in water (a), TNP in DMSO (b), TNT in DMSO (c), DNT in DMSO (d), MNT in DMSO (e), NB in DMSO (f), NE in DMSO (g), NM in DMSO (i) and NP in DMSO (j).

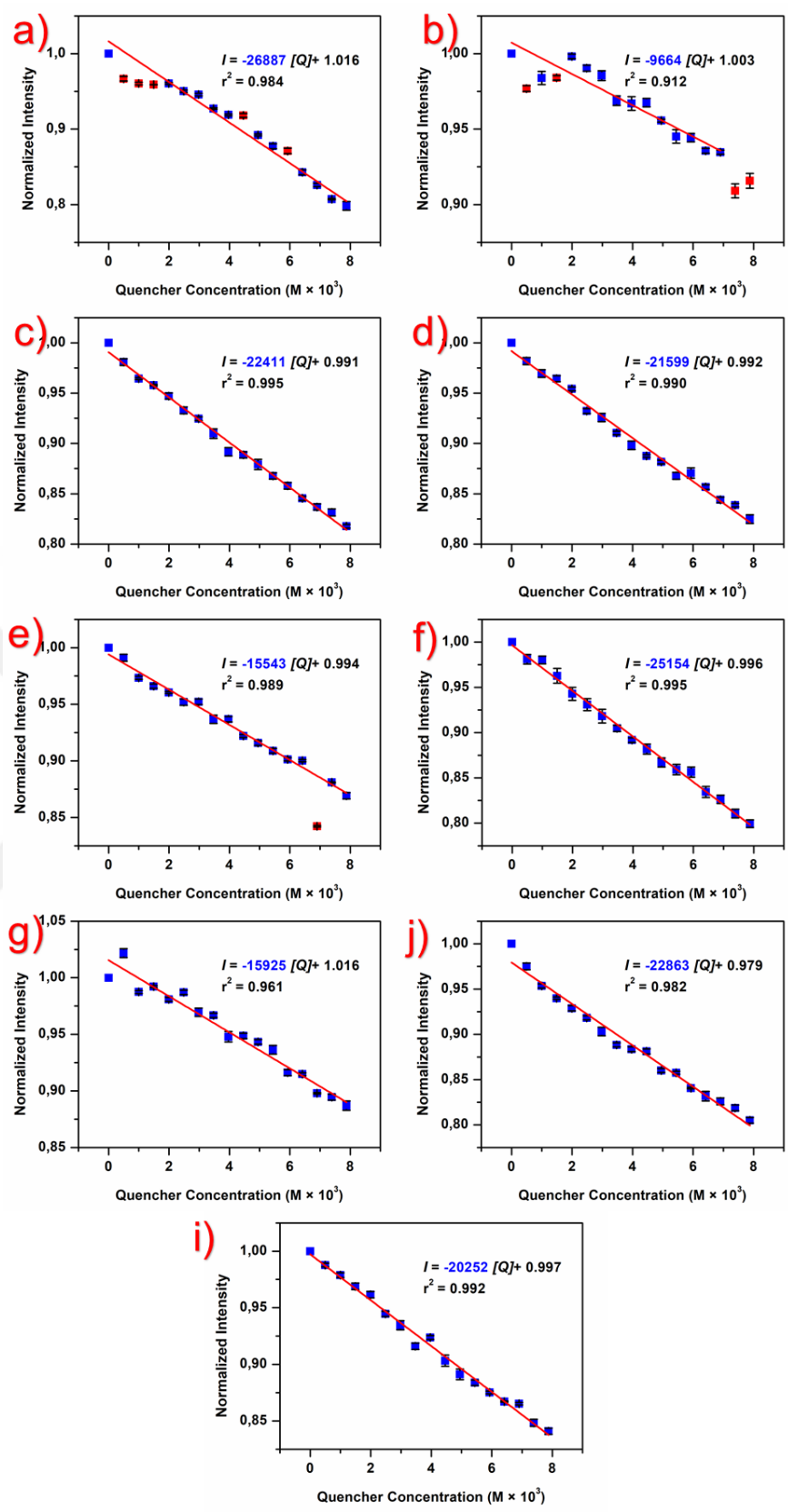

Figure 4.6 : Limit of detection spectra of Compound 9 titrations in DMSO using TNP in water (a), TNP in DMSO (b), TNT in DMSO (c), DNT in DMSO (d), MNT in DMSO (e), NB in DMSO (f), NE in DMSO (g), NM in DMSO (i) and NP in DMSO (j).

Finally, five distinct nitroaromatic compounds were used to evaluate Compound 10. Results showed that identical K_{sv} values of about 1×10^5 M^{-1} were found when commercially accessible nitroaromatic compounds (TNP, TNT, DNT, and MNT) were analyzed. When K_{sv} values were examined, similar values were obtained compared to an Aza-BODIPY (Compound 4) molecule having an EDG group. Although formyl group, known to be electron-withdrawing group, has a resonance effect while excited by light, the fluorophore group to which it is attached enters a high-energy electronic state (Szatylowicz et al., 2019). Thus, K_{sv} values at the level of 1×10^5 M^{-1} were obtained against electron-poor nitro compounds. Interestingly, the binding constant toward nitroalifatics was observed to be high as nitroaromatic compounds. The formyl group makes the sensor electron-poor. This situation causes Aza-BODIPY to be more sensitive to the PET (photoinduced electron transfer) mechanism in its excited state. The energy difference required for PET can be provided not only by aromatic but also by aliphatic nitro compounds. Because nitroaliphatics are also strong electron acceptors. The formyl group generally makes the Compound 10 sensitive to electrophilic species, but does not provide selectivity. In other words, Compound 10 showed a quenching response to both types of electron acceptors, regardless of whether they were nitroaromatic or nitroaliphatic. When looking at the quenching efficiencies, Compound 10 has values between 52-79% against nitro compounds. This shows that the formyl group does not increase the QE value as much as an EDG, but has higher QE values compared to Bromine due to the resonance effect. (Figure 4.7, Figure 4.8, Figure 4.9 and Table 4.3)

Table 4.3: K_{sv} and QE (quencher efficiency) results obtained by titration of Compound 10 (5 μM) with 500 μM nitro compounds.

Nitro Compound (in solvent)	K_{sv} (M^{-1})	QE
TNP (in water)	5.3×10^5	79%
TNP (in DMSO)	1.4×10^5	54%
TNT (in DMSO)	2.4×10^5	65%
DNT (in DMSO)	1.9×10^5	62%
MNT (in DMSO)	2.2×10^5	63%
NB (in DMSO)	2.6×10^5	66%
NM (in DMSO)	2.2×10^5	63%
NE (in DMSO)	1.8×10^5	58%

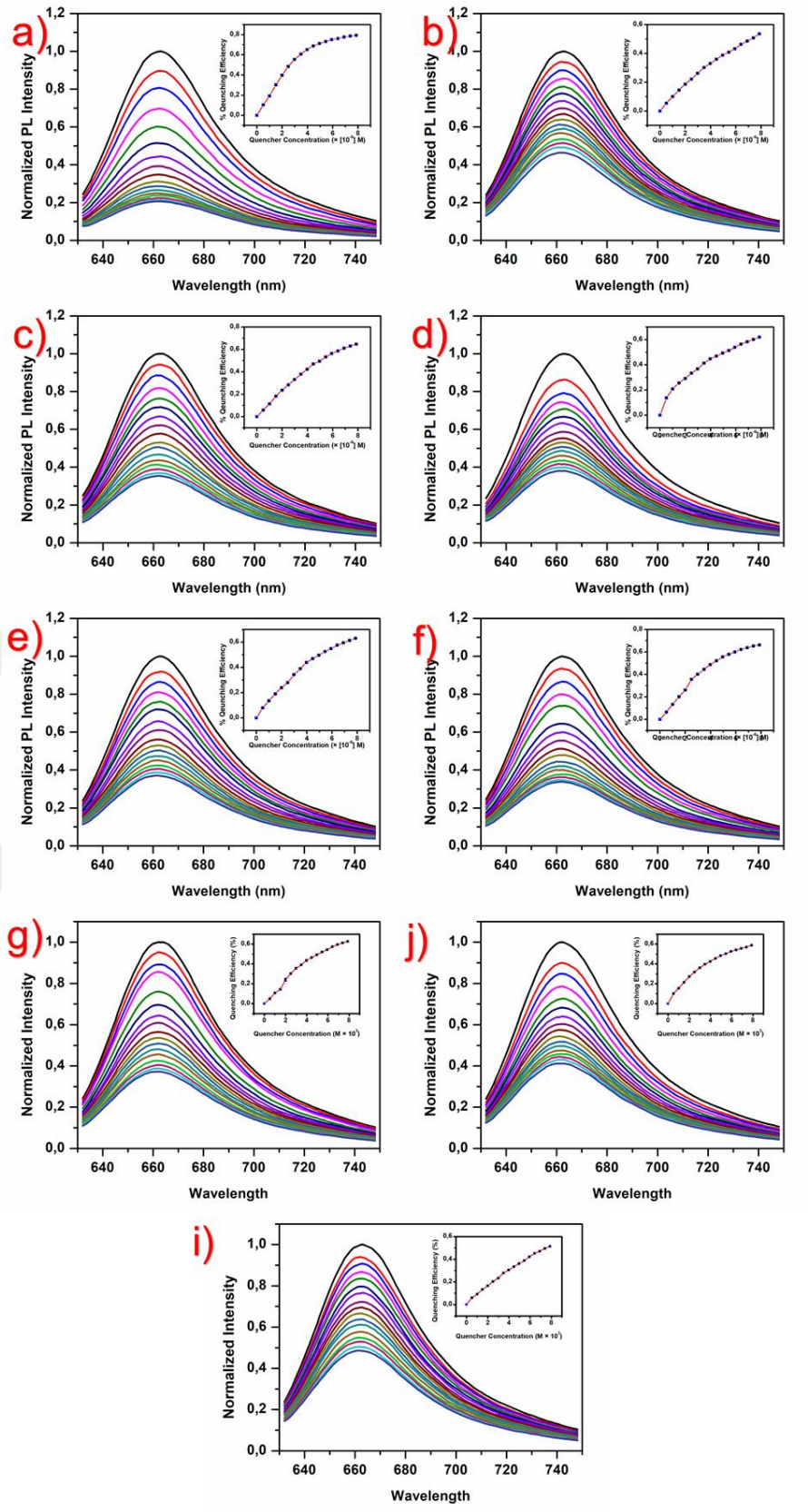

Figure 4.7 : Fluorescence quenching spectra of Compound 10 titrations in DMSO using TNP in water (a), TNP in DMSO (b), TNT in DMSO (c), DNT in DMSO (d), MNT in DMSO (e), NB in DMSO (f), NE in DMSO (g), NM in DMSO (i) and NP in DMSO (j). Quencher efficiencies were also shown.

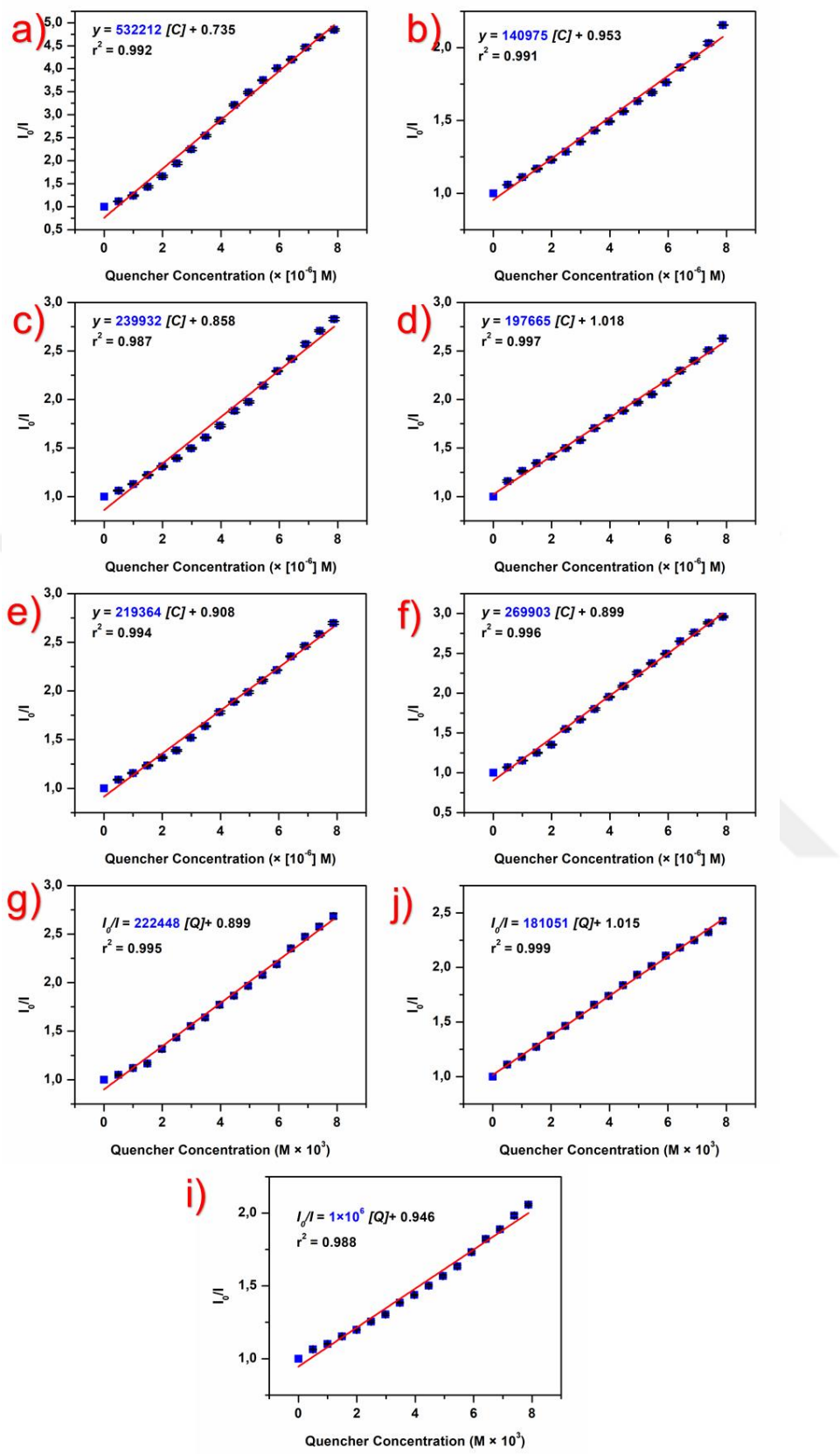

Figure 4.8 : Stern−Volmer plots of Compound 10 titrations in DMSO using TNP in water (a), TNP in DMSO (b), TNT in DMSO (c), DNT in DMSO (d), MNT in DMSO (e), NB in DMSO (f), NE in DMSO (g), NM in DMSO (i) and NP in DMSO (j).

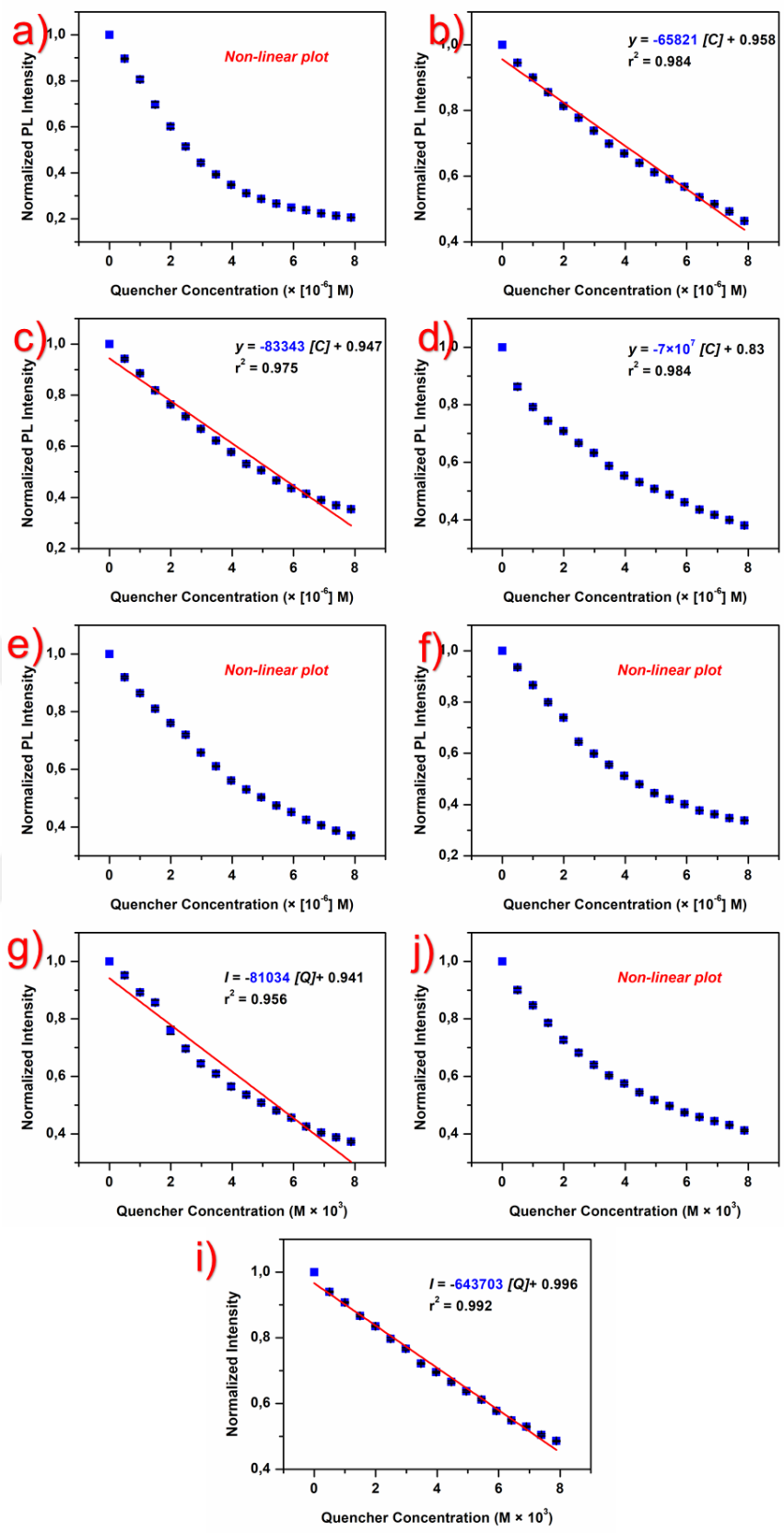

Figure 4.9 : Limit of detection spectra of Compound 10 titrations in DMSO using TNP in water (a), TNP in DMSO (b), TNT in DMSO (c), DNT in DMSO (d), MNT in DMSO (e), NB in DMSO (f), NE in DMSO (g), NM in DMSO (i) and NP in DMSO (j).

Figures 4,10 and 4.11 present a comparative analysis of the K_{sv} and quantum efficiency (QE) values, respectively, obtained from the titration experiments of Compound 4, Compound 9, and Compound 10 with various nitro compounds.

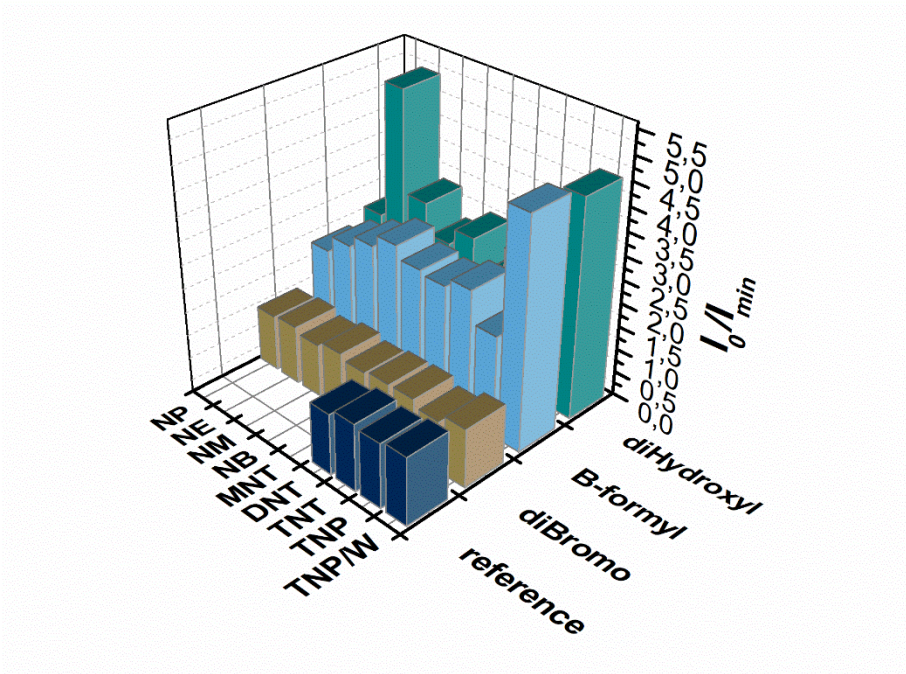

Figure 4.10 : Comparative K_{sv} values of Compound 4 (diHydroxyl), Compound 9 (diBromo) and Compound 10 (β-formyl) with the titration of nitrocompounds against reference Aza-BODIPY compound.

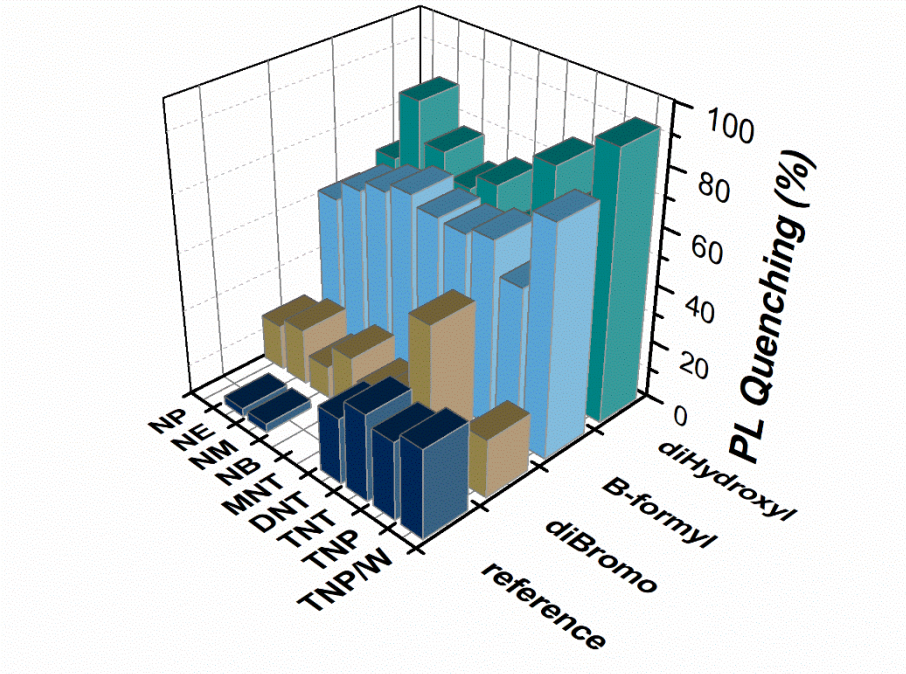

Figure 4.11 : Comparative quenching efficiencies of Compound 4 (diHydroxyl), Compound 9 (diBromo) and Compound 10 (β-formyl) with the titration of nitrocompounds against reference Aza-BODIPY compound.

When explosive sensors are examined in the literature, it is known that an electron-rich sensor molecule generally reacts with electron-poor NACs and this reaction occurs via π−π interaction (Liu et al., 2022). As a result of the analyses, it was observed that electron donor (EDG) and electron withdrawing (EWG) groups significantly affected the electronic density on the aromatic ring. In the comparative study conducted on three different compounds synthesized based on the Aza-BODIPY structure; Compound 4 contained a hydroxy group (EDG), Compound 9 a bromine group (EWG), and Compound 10 a formyl group (EWG). The effects of these functional groups were evaluated through the photophysical responses (K_{sv} and QE values) of the compounds with nitro compounds. Since nitro compounds, as known, have strong electron acceptor (electron-poor) properties, the PET (photoinduced electron transfer) mechanism plays an active role in the interactions with electron-rich sensor molecules. In this context, it is expected that Compound 4, which carries a hydroxy group, will show the strongest interaction, and the experimental data also confirmed this. The hydroxy group, which increases the electron density on the ring thanks to its electron donor property, has created a more effective quenching mechanism with nitro compounds. On the other hand, in Compound 9 carrying a bromine group, fluorescence quantum yield was suppressed due to the electron-withdrawing character as well as the 'heavy atom effect' and the interaction with nitro compounds was weakened. Surprisingly, a stronger interaction was observed for Compound 10 carrying a formyl group, contrary to expectations. This situation can be explained by the resonance effect of the formyl group, which increases the energy levels after photoexcitation in the Aza-BODIPY structure, allowing a more effective PET interaction with nitro compounds. In other words, the formyl group made the excited state of the system more reactive. In comparisons made with the literature, it was observed that all the synthesized compounds responded more strongly to nitro compounds than classical Aza-BODIPY derivatives (Sadikogullari et al., 2023). However, the fact that they responded to certain levels not only to nitroaromatic compounds but also to nitroaliphatic compounds reveals that these sensors have low selectivity levels. The loss of selectivity reduces the usability of the sensors in specific applications, but still indicates significant potential in terms of general fluorescence sensitivity. In conclusion, in this study, the effects of three different groups (hydroxy, bromine and formyl) added to the Aza-BODIPY dye on the optoelectronic properties and interactions with target molecules were systematically evaluated and supported by

experimental data. The obtained results reveal the direct effect of the functional group selection on the sensor performance; at the same time, they shed light on the rational design of Aza-BODIPY derivatives to develop more selective and effective sensors.

4.2. Application of Aza-BODIPY Compound (Compound 4) in Live-Cell Imaging

Due to the low solubility of Aza-BODIPY compounds in water, it is necessary to increase the hydrophilic properties of the molecules in applications such as intracellular imaging. Therefore, Compound 4, which is intended to be used in intracellular imaging within the scope of the thesis, was desired to be integrated into a water-soluble polymeric system. Therefore, PGMA-*b*-OEGMA polymer was synthesized by RAFT method. First, PGMA macro-CTA was synthesized and characterized by NMR (Figure 3.29), then PGMA-*b*-OEGMA copolymer was synthesized and characterized by NMR (Figure 3.31). The hydroxyl groups of Compound 4 and the epoxy groups in the GMA monomer was ring-opened to obtain the target molecule, and Compound 4 was incorporated into the polymer and characterized using NMR. (Figure 3.33).

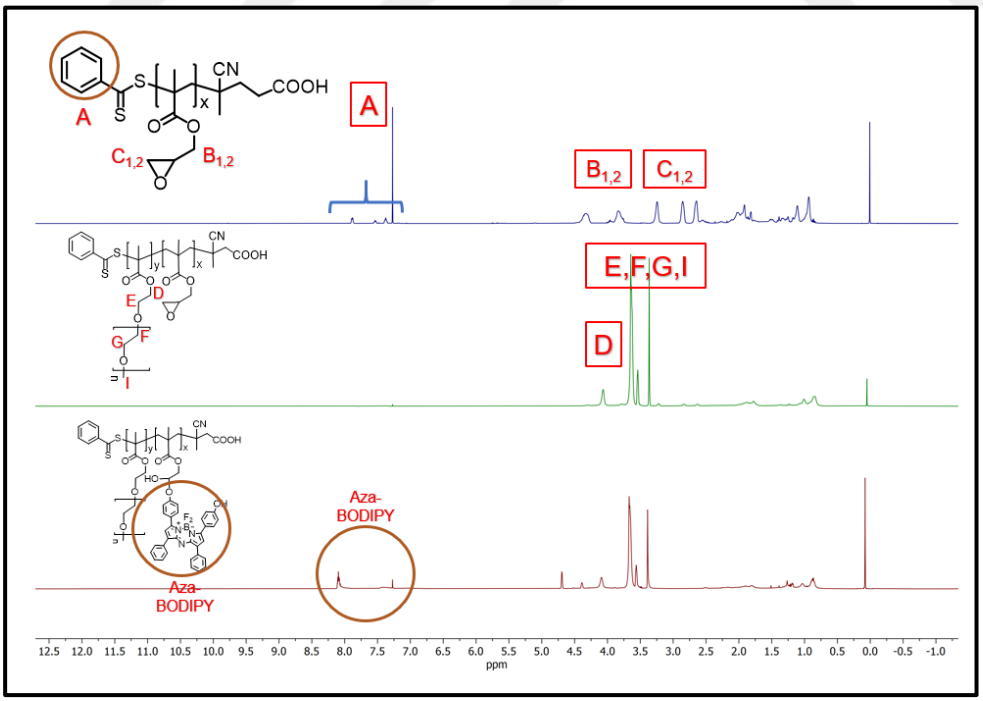

Figure 4.12 : ^{1}H-NMR spectra of PGMA macro-CTA (Compound 11), PGMA-*b*-OEGMA (Compound 12), and PGMA-*b*-OEGMA_Aza-BODIPY (Compound 13) in $CDCl_3$.

After the synthesis and characterization of PGMA macro-CTA, the PGMA-*b*-OEGMA polymer were synthesized. When the stacked NMRs of the two polymers are examined in Figure 4.12, OEGMA peaks (e, f, g and i) were appeared, and the a, $b_{1,2}$ and $c_{1,2}$ peaks belonging to PGMA macro-CTA are preserved. This shows that the PGMA-*b*-OEGMA polymer chain was successfully synthesized. After that, the obtained PGMA-*b*-OEGMA polymer was dissolved in methanol and Aza-BODIPY (Compound 4) integrated into the polymer chain by ring-opening of the epoxy. When the NMRs between the two polymers were examined at Figure 4.12, the peaks belonging to the epoxy (b_1, b_2, c_1, and c_2) disappeared and the peaks of Aza-BODIPY began to appear in the aromatic region. This showed that the polymer was successfully modified.

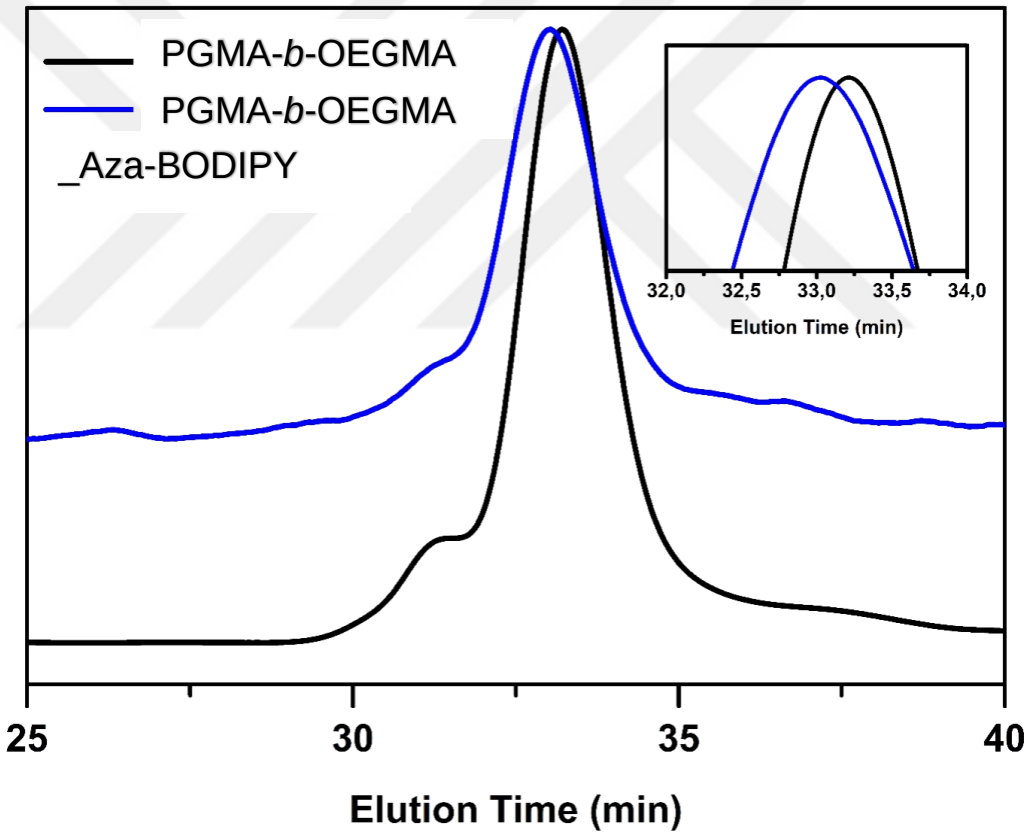

Figure 4.13 : Gel permeation chromatogram of PGMA-*b*-OEGMA and PGMA-*b*-OEGMA-co_Aza-BODIPY.

The GPC chromatograms exhibit a rightward shift in the peak, indicating an increase in the molecular weight of the polymer and suggesting successful integration of Compound 4 into the polymeric system. The PDI value of the two polymers was calculated as 1.09, which is an indication that controlled polymerization took place

and that the polymer was not damaged by the integration sequence of Compound 9. (Figure 4.13)

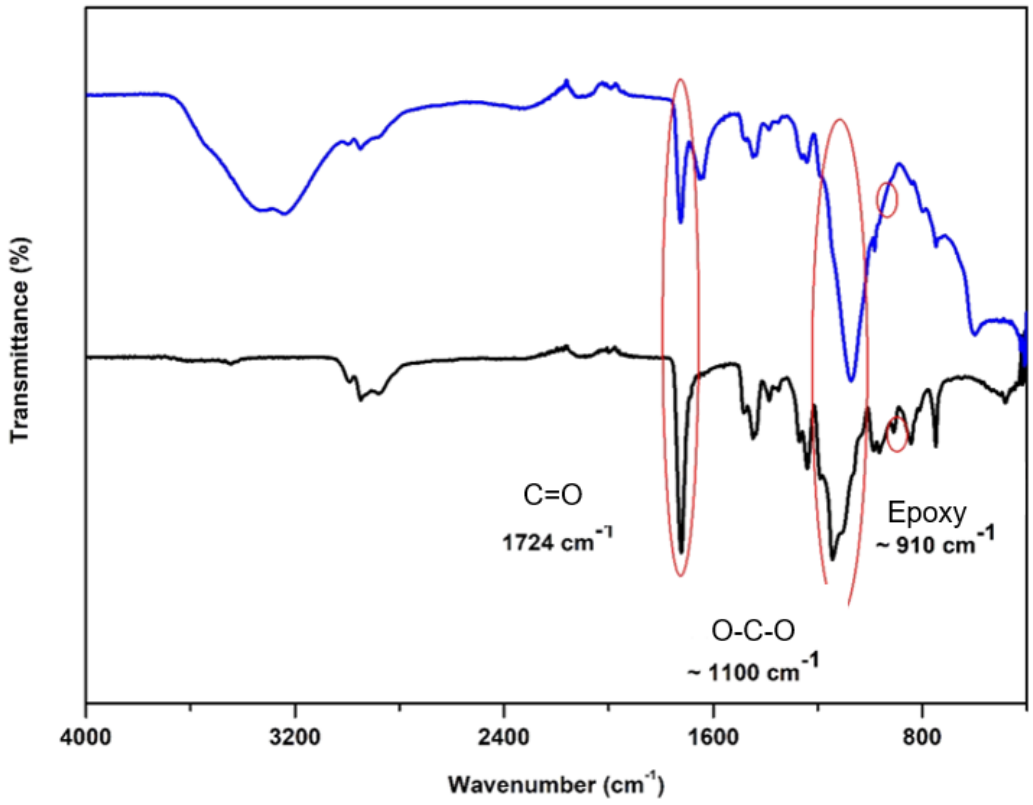

Figure 4.14 : FTIR spectra of PGMA-*b*-OEGMA and PGMA-*b*-OEGMA-co_Aza-BODIPY.

When looking at the FTIR spectra, the disappearance of the epoxy peak seen at 910 cm^{-1} is an indication that the integration of Compound 4 was successful. In addition, the preservation of the C-O-C stretching vibration seen at 1100 cm^{-1} and the carbonyl peak seen at 1724 cm^{-1} show that the polymer is not damaged. In light of all these results, the polymeric system to be used in intracellular imaging was successfully synthesized. (Figure 4.14) Intracellular imaging studies of the obtained polymer will be continued. In addition, PGMA-*b*-Fructose polymer will be synthesized within the scope of the study and integrated into Compound 4 polymer by opening the epoxy. This new polymer will also be used in intracellular studies. While the PGMA-*b*-OEGMA polymer system was designed to evaluate the ability to cellular uptake, the PGMA-*b*-Fructose system was developed to investigate the potential for specific targeting to cancer cells.

4.3. Application of Aza-BODIPY Compound as an IDA Sensor Against Fluorine Anion

Within the scope of the thesis, Aza-BODIPY molecule (Compound 4) was complexed with calix[4]pyrrole compound to be used as IDA sensor. For this purpose, Compound 4 was first reacted with TBA salt and turned into TBA salt and then TBA was replaced with calix[4]pyrrole. The synthesis of two molecules were characterized by NMR. (Figure 3.35, Figure 3.37)

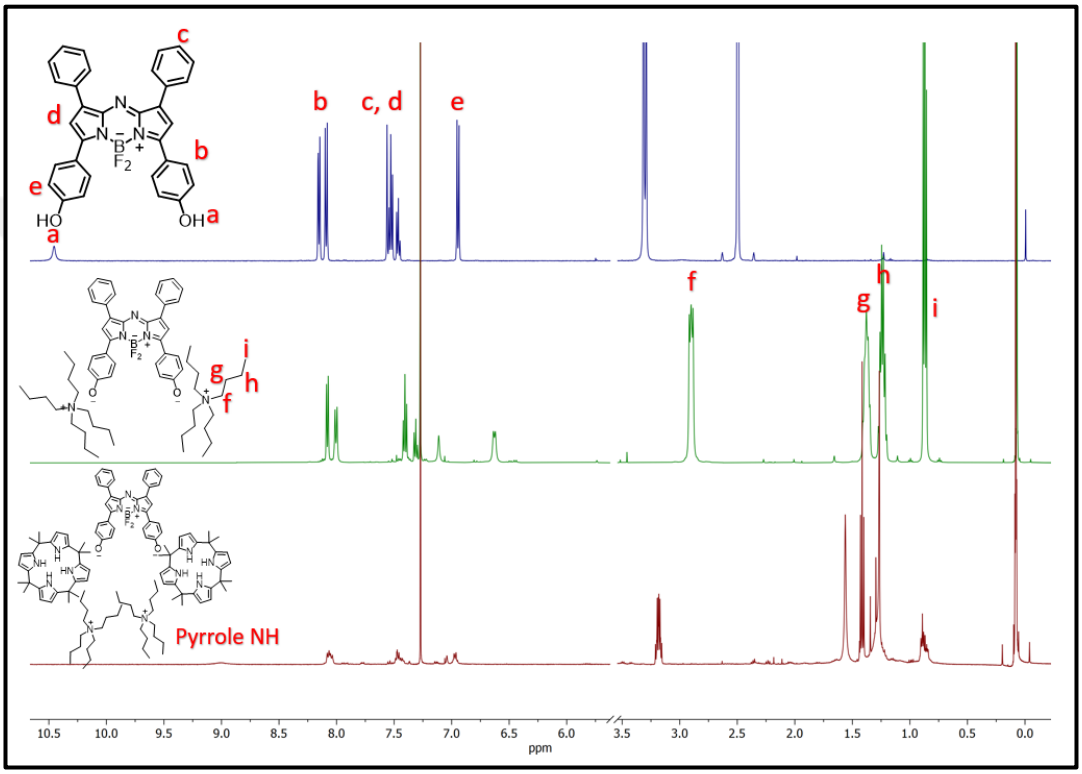

Figure 4.15 : ^{1}H-NMR spectra of Compound 4 (in d_6-DMSO), Compound 14 (in $CDCl_3$) and Compound 15 (in $CDCl_3$).

Following the synthesis and characterization of Compound 4, Compounds 14 and 15 were subsequently synthesized. As shown in the stacked NMR spectra of the three compounds (Figure 4.15), the characteristic peaks (a, b, c, d, and e) of Compound 4 are retained in all spectra, indicating structural continuity. Upon synthesis of Compound 14, additional peaks (f, g, h, and i), attributed to TBA, emerged in the NMR spectrum. In the final step, the appearance of the pyrrole NH signal in the spectrum of Compound 15 further supports the successful completion of the synthesis. Collectively, these spectral observations confirm the successful progression through each synthetic step.

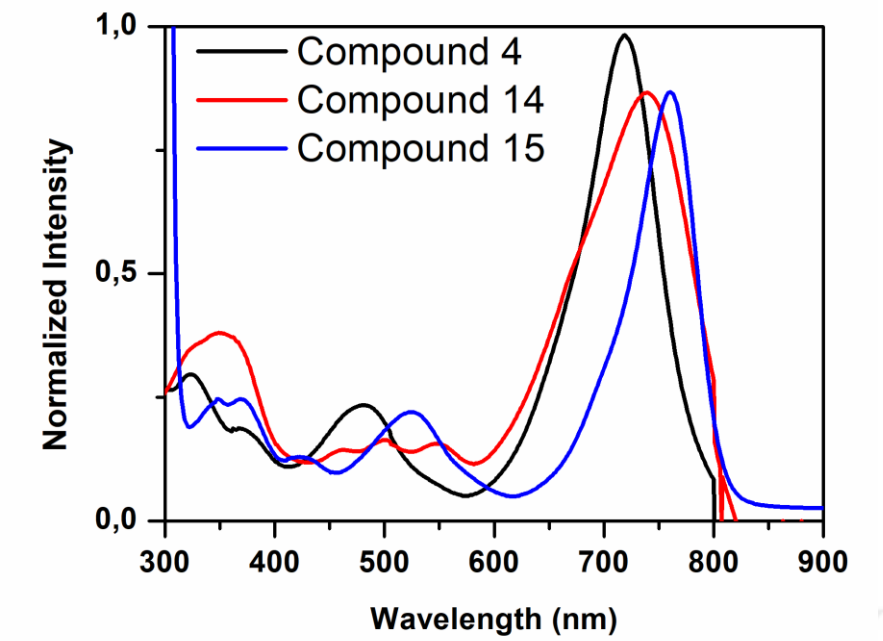

Figure 4.16 : UV-Vis spectra of Compound 4, Compound 14 and Compound 15.

Compound 4, Compound 14 and Compound 15 were dissolved in DMSO and Uv-Vis and fluorescence measurements were taken. UV-vis characterizations of the compounds were performed. All UV-Vis measurements were taken at room temperature and the UV-Vis spectra of Compound 4, Compound 14 and Compound 15 are given in Figure 4.16. Maximum wavelength was found to be 719 nm for Compound 4, 739 nm for Compound 14, and 710 nm for Compound 15.

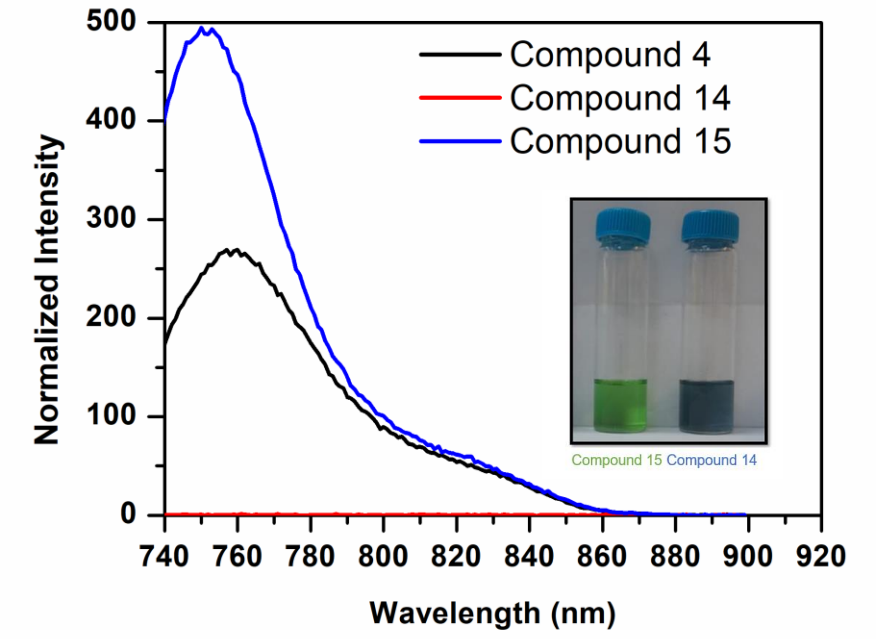

Figure 4.17 : Fluorescence spectra of Compound 4, Compound 14 and Compound 15.

Also, fluorescence characterizations of the compounds were performed. All fluorescence measurements were at room temperature and the fluorescence spectra of Compound 4, Compound 14 and Compound 15 are given in Figure 4.17. Maximum wavelength was found to be 760 nm for Compound 4 and 750 nm for Compound 15. But, Compound 14 shows no fluorescence emission. In light of this information, this system can be used as a selective IDA sensor for the fluoride ion, as in the examples in the literature.

5. CONCLUSIONS

Aza-BODIPY molecules attract great attention in various research areas due to their maximum emission wavelengths being tunable to the near-IR region, their high photostability and their ease of chemical modification. Thanks to these properties, they are suitable for use in many applications, especially in chemical sensors and biological imaging systems. Within the scope of this thesis, various Aza-BODIPY derivatives were synthesized, modified *via* functional groups and integrated into a polymeric system. The structural and functional properties of the obtained compounds were evaluated in detail over three different applications. Each application aims to reveal the effect of the groups added to the Aza-BODIPY structure on the molecular properties. In the first application area, the effect of different electron donor (EDG) and electron withdrawing (EWG) groups attached to the Aza-BODIPY core on the general electronic structure of the system was investigated. It was observed that compounds with EDG groups showed stronger interactions with nitro compounds by increasing the electron richness of the Aza-BODIPY structure. On the other hand, EWG groups generally reduce the electron density on the ring and limit the effectiveness of the PET (photoinduced electron transfer) mechanism, thus reducing sensor performance. However, some exceptions, such as the resonance effect of the formyl group, have caused such compounds to exhibit unexpectedly effective sensor behavior. These findings reveal that the selective sensing ability of Aza-BODIPY-based sensors is directly related to the functional group structure. In the second application, the Aza-BODIPY dye was integrated into a polymeric structure and made compatible with biological environments. This structure is currently being utilized in intracellular imaging studies. The third application was based on the conjugation of the Aza-BODIPY compound with the calix[4]pyrrole structure to create an IDA (Indicator Displacement Assay) sensor system selective for halogen ions (especially fluoride ions). Within the scope of the studies carried out in this thesis, the advantages (high photostability, wide wavelength tunability, structural flexibility, etc.) and some limitations (selectivity problems, solubility limitations, etc.) have been highlighted.

The obtained results clearly demonstrate the versatile usability of Aza-BODIPY-based systems and provide a platform that can be easily integrated into different areas.

REFERENCES

Akkoc, E., Karagoz, B. 2022. "One step synthesis of crosslinked fluorescent microspheres for the effective and selective sensing of explosives in aqueous media". *European Polymer Journal*, *172*, 111238.

Amharar, S., Aydogan, A. 2022. "Highly sensitive and cost-effective fluorescent turn-on sensors based on octamethylcalix[4]pyrrole receptor for the detection of fluoride anion". *Dyes and Pigments*, *197*(September 2021), 109918.

Austin, E., Geisler, A. N., Nguyen, J., Kohli, I., Hamzavi, I., Lim, H. W., Jagdeo, J. 2021. "Visible light. Part I: Properties and cutaneous effects of visible light.". *Journal of the American Academy of Dermatology*, *84*(5), 1219–1231.

Ayoob, S., and Gupta, A. K. 2006. "Fluoride in Drinking Water: A Review on the Status and Stress Effects". *Critical Reviews in Environmental Science and Technology*, *36*(6), 433–487.

Chansaenpak, K., Tanjindaprateep, S., Chaicharoenaudomrung, N., Weeranantanapan, O., Noisa, P., Kamkaew, A. 2018. "Aza-BODIPY based polymeric nanoparticles for cancer cell imaging". *RSC Advances*, *8*(69), 39248–39255.

Chen, X., Liu, Y.-C., Bai, J., Fang, H., Wu, F.-Y., Xiao, Q. 2021. "A “turn-on” fluorescent probe based on BODIPY dyes for highly selective detection of fluoride ions". *Dyes and Pigments*, *190*, 109347.

Chibani, S., Le Guennic, B., Charaf-Eddin, A., Maury, O., Andraud, C., Jacquemin, D. 2012. "On the Computation of Adiabatic Energies in Aza-Boron-Dipyrromethene Dyes.". *Journal of Chemical Theory and Computation*, *8*(9), 3303–3313.

Chung, F.-J., Liu, H.-Y., Jiang, B.-Y., He, G.-Y., Wang, shi-hao, Wu, W.-C., Liu, C.-L. 2015. "Random styrenic copolymers with pendant pyrene moieties: Synthesis and applications in organic field-effect transistor memory". *Journal of Polymer Science Part A: Polymer Chemistry*, *54*, n/a-n/a.

Gorman, A., Killoran, J., O’Shea, C., Kenna, T., Gallagher, W. M., O’Shea, D. F. 2004. "In Vitro Demonstration of the Heavy-Atom Effect for Photodynamic Therapy". *Journal of the American Chemical Society*, *126*(34), 10619–10631.

Gropp, C., Quigley, B. L., Diederich, F. 2018. "Molecular Recognition with Resorcin[4]arene Cavitands: Switching, Halogen-Bonded Capsules, and Enantioselective Complexation". *Journal of the American Chemical Society*, *140*(8), 2705–2717.

Gunturkun, D., Isci, R., Faraji, S., Sütay, B., Majewski, L. A., Ozturk, T. 2023. "Synthesis and characterization of naphthalenediimide-thienothiophene-conjugated polymers for OFET and OPT applications". *Journal of Materials Chemistry C*, *11*(38), 13129–13141.

Hall, M. J., McDonnell, S. O., Killoran, J., O'Shea, D. F. 2005. "A Modular Synthesis of Unsymmetrical Tetraarylazadipyrromethenes". *The Journal of Organic Chemistry*, *70*(14), 5571–5578.

He, G., Yan, N., Yang, J., Wang, H., Ding, L., Yin, S., Fang, Y. 2011. "Pyrene-Containing Conjugated Polymer-Based Fluorescent Films for Highly Sensitive and Selective Sensing of TNT in Aqueous Medium". *Macromolecules*, *44*(12), 4759–4766.

Isci, R., Can Sadikogullari, B., Sütay, B., Karagoz, B., Daut Ozdemir, A., Ozturk, T. 2025. "Thienothiophene based AIE-Active bulky materials for sensitive explosive detection". *Journal of Photochemistry and Photobiology A: Chemistry*, *459*, 116095.

Jiao, L., Yu, C., Li, J., Wang, Z., Wu, M., Hao, E. 2009. "Beta-formyl-BODIPYs from the Vilsmeier-Haack reaction.". *The Journal of Organic Chemistry*, *74*(19), 7525–7528.

Jing, Y.-N., Li, S.-S., Su, M., Bao, H., Wan, W.-M. 2019. "Barbier Hyperbranching Polymerization-Induced Emission toward Facile Fabrication of White Light-Emitting Diode and Light-Harvesting Film". *Journal of the American Chemical Society*, *141*(42), 16839–16848.

Karagoz, B., Esser, L., Duong, H. T., Basuki, J. S., Boyer, C., Davis, T. P. 2014. "Polymerization-Induced Self-Assembly (PISA) – control over the morphology of nanoparticles for drug delivery applications". *Polym. Chem.*, *5*(2), 350–355.

Kaur, M., Janaagal, A., Balsukuri, N., Gupta, I. 2024. "Evolution of Aza-BODIPY dyes-A hot topic". *Coordination Chemistry Reviews*, *498*, 215428.

Killoran, J., Allen, L., Gallagher, J. F., Gallagher, W. M., O′Shea, D. F. 2002. "Synthesis of BF2 chelates of tetraarylazadipyrromethenes and evidence for their photodynamic therapeutic behaviour". *Chem. Commun.*, (17), 1862–1863.

Killoran, J., McDonnell, S. O., Gallagher, J. F., O'Shea, D. F. 2008. "A substituted BF2-chelated tetraarylazadipyrromethene as an intrinsic dual chemosensor in the 650–850 nm spectral range". *New Journal of Chemistry*, *32*(3), 483–489.

Kim, D. S., Sessler, J. L. 2015. "Calix[4]pyrroles: Versatile molecular containers with ion transport, recognition, and molecular switching functions". *Chemical Society Reviews*, *44*(2), 532–546.

Koch, A., Ravikanth, M. 2019. "Monofunctionalized 1,3,5,7-TetraarylazaBODIPYs and Their Application in the Synthesis of AzaBODIPY Based Conjugates". *The Journal of Organic Chemistry*, *84*(17), 10775–10784.

Li, A., Wang, F., Li, Y., Peng, X., Liu, Y., Zhu, L., Chen, S. 2025. "Fluorination of Aza-BODIPY for Cancer Cell Plasma Membrane-Targeted Imaging and Therapy". *ACS Applied Materials & Interfaces*, *17*(2), 3013–3025.

Li, R., Du, Y., Guo, W., Su, Y., Meng, Y., Shan, Z., Meng, S. 2020. "Methotrexate coated AZA-BODIPY nanoparticles for chemotherapy, photothermal and photodynamic synergistic therapy". *Dyes and Pigments*, *179*, 108351.

Liu, L., Ding, R., Mao, Y., Sun, B. 2022. "Theoretical investigations on the nitro-explosive sensing process of a MOF sensor: Roles of hydrogen bond and π-π stacking". *Chemical Physics Letters*, *793*, 139393.

Lo, P. K., Wong, M. S. 2008. "Extended Calix[4]arene-Based Receptors for Molecular Recognition and Sensing". *Sensors*, *8*(9), 5313–5335.

Lv, W., Song, Y., Pei, H., Mo, Z. 2023. "Synthesis strategies and applications of metal–organic framework-quantum dot (MOF@QD) functional composites". *Journal of Industrial and Engineering Chemistry*, *128*, 17–54.

Murtagh, J., Frimannsson, D. O., O'Shea, D. F. 2009. "Azide Conjugatable and pH Responsive Near-Infrared Fluorescent Imaging Probes". *Organic Letters*, *11*(23), 5386–5389.

Nguyen, B. T., Anslyn, E. V. 2006. "Indicator–displacement assays". *Coordination Chemistry Reviews*, *250*(23), 3118–3127.

Qayyum, M., Bushra, T., Khan, Z. A., Gul, H., Majeed, S., Yu, C., Shahzad, S. A. 2021. "Synthesis and Tetraphenylethylene-Based Aggregation-Induced Emission Probe for Rapid Detection of Nitroaromatic Compounds in Aqueous Media". *ACS Omega*, *6*(39), 25447–25460.

Rogers, M. A. T. 1943. "Tetra-arylazadipyrromethines: A new class of synthetic colouring matter [5]". *Nature*, *151*(3835), 504.

Sadikogullari, B. C., Koramaz, I., Sütay, B., Karagoz, B., Özdemir, A. D. 2023. "Application of aza-BODIPY as a Nitroaromatic Sensor". *ACS Omega*, *8*(28), 25254–25261.

Sakai, E. M., Connolly, L. A., Klauck, J. A. 2005. "Inhalation Anesthesiology and Volatile Liquid Anesthetics: Focus on Isoflurane, Desflurane, and Sevoflurane". *Pharmacotherapy: The Journal of Human Pharmacology and Drug Therapy*, *25*(12), 1773–1788.

Sedgwick, A. C., Brewster, J. T., Wu, T., Feng, X., Bull, S. D., Qian, X., Sun, X. 2021. "Indicator displacement assays (IDAs): The past, present and future". *Chemical Society Reviews*, *50*(1), 9–38.

Selatnia, I., Sid, A., Benahmed, M., Dammene debbih, O., Ozturk, T., Gherraf, N. 2018. "Synthesis and Characterization of a Bis-Pyrazoline Derivative as Corrosion Inhibitor for A283 Carbon Steel in 1M HCl: Electrochemical, Surface, DFT and MD Simulation Studies". *Protection of Metals and Physical Chemistry of Surfaces*, *54*(6), 1182–1193.

Şen, F. B., Bener, M., Apak, R. 2021. "A Simple Determination of Trinitrotoluene (TNT) Based on Fluorescence Quenching of Rhodamine 110 with FRET Mechanism". *Journal of Fluorescence*, *31*(4), 989–997.

S**enthamizhan, A., Celebioglu, A., Bayir, S., Gorur, M., Doganci, E., Yilmaz, F., Uyar, T.** 2015. "Highly Fluorescent Pyrene-Functional Polystyrene Copolymer Nanofibers for Enhanced Sensing Performance of TNT". *ACS Applied Materials & Interfaces*, *7*(38), 21038–21046.

Shi, Z., Han, X., Hu, W., Bai, H., Peng, B., Ji, L., Huang, W. 2020. "Bioapplications of small molecule Aza-BODIPY: From rational structural design to: From vivo investigations". *Chemical Society Reviews*, *49*(21), 7533–7567.

Sun, X.-L., Liu, D.-M., Tian, D., Zhang, X. Y., Wu, W., Wan, W. M. 2017. "The introduction of the Barbier reaction into polymer chemistry". *Nature Communications*, *8*(1), 1210.

Sun, X., Liu, Y., Shaw, G., Carrier, A., Dey, S., Zhao, J., Lei, Y. 2015. "Fundamental Study of Electrospun Pyrene–Polyethersulfone Nanofibers Using Mixed Solvents for Sensitive and Selective Explosives Detection in Aqueous Solution". *ACS Applied Materials & Interfaces*, *7*(24), 13189–13197.

Swamy P, C. A., Priyanka, R. N., Mukherjee, S., Thilagar, P. 2015. "Panchromatic Borane–aza-BODIPY Conjugate: Synthesis, Intriguing Optical Properties, and Selective Fluorescent Sensing of Fluoride Anions". *European Journal of Inorganic Chemistry*, *2015*(13), 2338–2344.

Szatylowicz, H., Jezuita, A., Krygowski, T. M. 2019. "On the relations between aromaticity and substituent effect". *Structural Chemistry*, *30*(5), 1529–1548.

T**ian, R., Ma, H., Yang, Q., Wan, H., Zhu, S., Chandra, S., Chen, X.** 2019. "Rational design of a super-contrast NIR-II fluorophore affords high-performance NIR-II molecular imaging guided microsurgery". *Chemical Science*, *10*(1), 326–332.

Wu, D., Sedgwick, A. C., Gunnlaugsson, T., Akkaya, E. U., Yoon, J., James, T. D. 2017. "Fluorescent chemosensors: the past, present and future.". *Chemical Society Reviews*, *46*(23), 7105–7123.

Xu, Y., Li, C., Xu, R., Zhang, N., Wang, Z., Jing, X., Meng, L. 2020. "Tuning molecular aggregation to achieve highly bright AIE dots for NIR-II fluorescence imaging and NIR-I photoacoustic imaging". *Chem. Sci.*, *11*(31), 8157–8166.

Xue, H., Li, D. S., Cai, H.-W., Sun, X. L., Wan, W. M. 2023. "Radical Polymerization-Induced Nontraditional Intrinsic Luminescence of Triphenylmethyl Azide-Containing Polymers". *Macromolecules*, *56*(5), 1898–1906.

You, J. M., Jeong, H., Seo, H., Jeon, S. 2010. "A new fluoride ion colorimetric sensor based on dipyrrolemethanes". *Sensors and Actuators B: Chemical*, *146*(1), 160–164.

Zhang, C. Z., Li, T., Yuan, Y., Gu, C.-Y., Niu, M.-X., Cao, H. 2017. "Effect of bromine substituent on optical properties of aryl compounds". *Journal of Physical Organic Chemistry*, *30*(5), e3620.

Zhao, B., Liao, L., Zhu, Y., Hu, Z., Wu, F. 2023. "Near-infrared fluorescent Aza-BODIPY dyes: Rational structural design and biomedical imaging". *Journal of Luminescence*, *263*(June), 120099.

Zhu, L., Xie, W., Zhao, L., Zhang, Y., Chen, Z. 2017. "Tetraphenylethylene- and fluorene-functionalized near-infrared aza-BODIPY dyes for living cell imaging". *RSC Advances*, *7*(88), 55839–55845.

Zou, B., Liu, H., Mack, J., Wang, S., Tian, J., Lu, H., Shen, Z. 2014. "A new aza-BODIPY based NIR region colorimetric and fluorescent chemodosimeter for fluoride". *RSC Adv.*, *4*(96), 53864–53869.

CURRICULUM VITAE

Name Surname **:** Emre Can UYSAL

EDUCATION **:**

- **B.Sc.** **:** 2022, Istanbul Technical University, Faculty of Science and Letters, Department of Chemistry
- **B.Sc.** **:** 2024, Istanbul Technical University, Faculty of Science and Letters, Department of Molecular Biology and Genetics (Double Major)

PROFESSIONAL EXPERIENCE AND REWARDS:

- Research Assistant (2022-Current) - Istanbul Technical University, Chemistry Department

PUBLICATIONS AND PRESENTATIONS ON THE THESIS:

- **Uysal E.C.,** Memis D., Sadıkogulları B. C., Ozdemir A., Aydogan A., 2023, An Aza-BODIPY and Calix[4]pyrrole-Based IDA Sensor for Detection of Fluoride Anion in Aqueous Medium. 19th Asian Chemical Congress, July 8-14, 2023 Istanbul, Türkiye (Poster Presentation).